Sediment Provenance, Pathways and Sink Potential of the inner Gulf of Kachchh coast, Western India

Thesis Submitted To

The Maharaja Sayajirao University of Baroda

For the Degree of

Doctor of Philosophy in Geology

by

Siddharth Pravinbhai Prizomwala

Department of Geology
Faculty of Science
The Maharaja Sayajirao University of Baroda
Vadodara - 390002
India

2012

CERTIFICATE

This is to certify that the contents of this thesis comprise original research work of the candidate and have no time been submitted for any other degree. The candidate has fulfilled the requirements regarding attendance contained in O.Ph.D. 3(i).

(Siddharth Pravinbhai Prizomwala)
Candidate

(Dr. N.P. Bhatt)
Guiding Teacher

Head
Department of Geology

Dedicated to

My Guide Dr. Nilesh Bhatt

and

My Guru Prof. L. S. Chamyal

ACKNOWLEDGMENT

First and foremost I would like to convey my deep and sincere thank to my guide, Dr. Nilesh Bhatt for constant encouragement. He introduced me to coastal geomorphology / sedimentology and inspired me to work on this research issue. I want to thank him deeply for the faith and trust he showed in me. For every step I took, he supported and encouraged me. For all the silly questions I use to ask and to which he answered me patiently. For all the advices I sought academic/other than academic! I wouldn't have been able to be what I am today without his support and constant guidance. It is because of him that I believe that I have become a better researcher and more importantly a better human being today.

I am also deeply thankful to Prof. L.S. Chamyal, Head, Department of Geology, The M. S. University of Baroda, and co-ordinator of SSS (Science of Shallow Subsurface) programme of DST, New Delhi. He was a constant source of encouragement and inspiration for me throughout my study and will always remain. It was he who gave me sleepless nights by asking me the important questions like, "why I am pursuing this research issue?", "what is new that I am adding to current understanding?" and helped me whenever I needed. He changed my way of perceiving research and over all life in terms of being a good researcher and a good human being by helping others.

I would also like to thank Dr. D. M. Maurya for helping me understand various basic aspects of my study. I also want to thank him deeply for teaching me how to write a research paper.

I would also like to thank Prof. N. Basavaiah, Indian Institute of Geomagnetism Navi Mumbai for extending all his laboratory facilities and helping me in understanding and executing the mineral magnetic studies.

I would also like to thank Prof. Wilfried Winkler, ETH Zurich, Switzerland for hosting me at ETH under the Indo-Swiss Joint Research Programme, in which part of this work has been carried out. I would also like to convey my deep thanks towards Prof. A. M. Hirt and Prof. I. Hajdas for helping in mineral magnetic analysis and AMS ^{14}C dating of my samples. I would also like to thank Regula Schälchli and Katharina Fehr for all the support they gave me during my stay at ETH, Zurich.

I would like to specially thank Dr. Navin Juyal, Physical Research Laboratory, Ahmedabad, Dr. Satish Patel, Dr. Rachna Raj and Dr. Alpa Shridhar of The M. S. University of Baroda for their constant support and encouragement during my study. I would also like to thank Dr. B. K. Rastogi, Director General, Institute of Seismological Research for his encouragement and granting me leave for completion of my thesis.

I am very much grateful to Mr. Vikas Chowksey for taking the pain and going through all my manuscripts / presentations and (mercilessly) commenting on them to inspire me to ultimately improve the science in my papers. Sincere thanks are also due to Mr. Vishal Ukey for his unconditional help and support, especially in field works and department. Ms. Archana Das and Ms. Jaqulin Joseph are deeply thanked for sharing their lunches (and yeah! the coffee bills!) with me during my entire tenure at the MSU. Also, valuable discussions and critical comments by Archana Das, Jaqulin Joseph, Stephan Nagel, Shashi Shukla and Tathagath Ghosh were very much helpful during various stages of my study.

Thanks are due to non-teaching staff of the Department of Geology, Faculty of Science, The M.S. University of Baroda for the help provided by them, whenever and whatever required.

The study was funded by the Department of Science and Technology, New Delhi in the form of Project Fellowship / Junior Research Fellowship (Project No. SR/S4/ES-21/Kachchh Window/P6) since September 2008 to September 2011 and by Indo-Swiss Joint Research Programme in the form of Research Fellowship for visiting Geological Institute, ETH Zurich, Switzerland (Grant no. RF31) between October 2011 to June 2012. This very essential support is deeply acknowledged.

Last but not the least, I would like to thank my parents for their constant support, encouragement, love, blessings and faith in me. I would also like to thank Mr. Nisarg Makwana for being there with me, whenever I needed him.

Siddharth Prizomwala

Contents

Chapter 1

INTRODUCTION

1.1 Background

Coastline is one of the most dynamic environments in nature and its response to various external factors namely sediment supply, sea level rise, tectonic perturbations and climate change have always attracted researchers since decades. Around 40% of world population resides within 100 km of coastline, and hence it is of vital importance to better understand the processes acting along the coastline. Source to sink studies of sediment transit mechanism and dispersal system have recently gained considerable attention (Castelltort and Van Den Driessche, 2003; Kuehl et al., 2004; Allen, 2008; Jiang et al., 2011; Horng and Huh, 2011), as they help in better understanding and making the natural and human perturbations more predictable (Liquete et al., 2007). The source–to-sink studies typically envisages the fate of sediment as it is derived from the uplands (i.e. the source), its transport coupled with partial storage along the pathway and then ultimately its deposition into the ocean (i.e. the ultimate sink). The major aim employing a source-to-sink approach is that it helps to better understand the sediment dispersal system and stratigraphy. In a way the predictive capability of dispersal-system behavior has critical implications for understanding geochemical cycling (*e.g.*, carbon), ecosystem change (tied to global warming and sea-level rise), and resource management (*e.g.*, soils, wetlands, and groundwater). Also it helps in understanding how with time has the system evolved in response of changes in climate and sediment supply. The research with this regard has been focused upon mostly large river systems, their sediment delivery into the ocean and factors controlling it

(Goodbred, 2003; Wasson, 2003; Yang et al., 2009; Jiang et al., 2011). A few sites around the world have been studied in detail envisaging a source-to-sink approach starting the far uplands and tracing of sediments into the continental shelves (Waipaoa sedimentary system in New Zealand and the Papua New Guinea).

The Gulf of Kachchh has attracted many workers to study its offshore dynamics in this complex macrotidal regime. There are several papers published in terms of its current dynamics, suspended sediment transport, sediment character of sea floor and various sedimentation processes in this macrotidal regime (Hashimi et al., 1978; Nair et al., 1982; Vora et al., 1987; Chauhan, 1994; Shetye, 1999; Kunte et al., 2003; Chauhan et al., 2004; Babu et al., 2005; Vethamony et al., 2005; Chauhan et al., 2006; Ramaswamy et al., 2007; Vethamony et al., 2007). However, in general the understanding of coastline has remained '*terra incognita*', owing to a limited number of works published in terms of its geomorphology and textural attributes of the sediments (Kar, 1993; Maurya et al., 2008; Prizomwala et al., 2010; Shukla et al., 2010). The studies so far carried out with reference to the sediment provenance and sediment dispersion are indicative of the River Indus being the only major source of sediments to the Gulf of Kachchh, delivering about 59 x 10^6 tons of sediments annually (Milliman et al., 1987). Similar inference is drawn by some other workers using Suspended Sediment Concentration (SSC) and satellite imageries (Kunte et al., 2003; Chauhan et al., 2006; Ramaswamy et al., 2007). Some recent studies have pointed out the impact of small riverine systems supplying sediments to global oceans, which was underestimated so far (Syvitski et al., 2005). However, till date there is no published literature regarding the compositional attributes of the coastal sediments, their sources and probable pathways in the Gulf of Kachchh. With the presence of marine national park and

rapidly industrializing coastline, it is indeed necessary to generate a comprehensive understanding of processes acting in and along the Gulf of Kachchh coast.

1.2 Purpose and Scope

In light of the above mentioned background, understanding of the sediment dispersal system in the Gulf of Kachchh is of prime importance. The predictable nature of sediment pathways would better help coastal management experts in planning more sustainable development in balance with the environmental factors. The present study would outline the sediment nature, pathways of coastal sediments in Gulf of Kachchh and its accommodation potential in various geomorphic domains, specially the inner gulf mudflats. The proxies selected for the purpose included texture, environmental magnetism, clay mineralogy, sediment geochemistry and heavy minerals. The author has also tried to obtain AMS dates of some selected samples. The integration of the data generated could shed light on the evolution of the Gulf of Kachchh mudflats since Late Holocene.

1.3 Objective

In order to address above mentioned issues the following major objectives were identified for the present study.

1. To delineate the major sources of sediments contributing to the Gulf of Kachchh basin.
2. To study the pathways of these coastal sediments as a sediment dispersal system in this macrotidal regime.
3. To study the sink potential of these mudflats as an archive for studying climate change / sediment supply history at a high resolution.

1.4 Approach

In order to achieve the above mentioned objectives, the present author has followed the standard as well as some innovative methods that included the followings.

1. Literature survey to understand the geological constitution of the study area and also to identify probable end-members contributing sediments to the study area.
2. Characterize the end-members using a multiproxy approach for their provenance signatures and identify provenance discriminating characteristics for particular end-member.
3. Sample the entire coastline of Gulf of Kachchh and study it for various provenance discrimination proxies like grain size analysis, heavy mineral analysis, mineral magnetic analysis, sediment geochemistry and clay mineralogy.
4. Reconstruct and better understand the present day erosional engine i.e. the sediment dispersal system of the Gulf of Kachchh.
5. Study a shallow sequence from the mudflats of Gulf of Kachchh in terms of variations on a time line.

1.5 Kachchh and Gulf of Kachchh

The Gulf of Kachchh is situated in western most part of India, bounded by the Kachchh mainland and the Saurashtra peninsula in north, south and east (Figure 1.1). Kachchh is the largest district of India, and it falls under arid / extremely arid climatic regime with an annual rainfall of 50 cm or less (Chamyal et al., 2003).

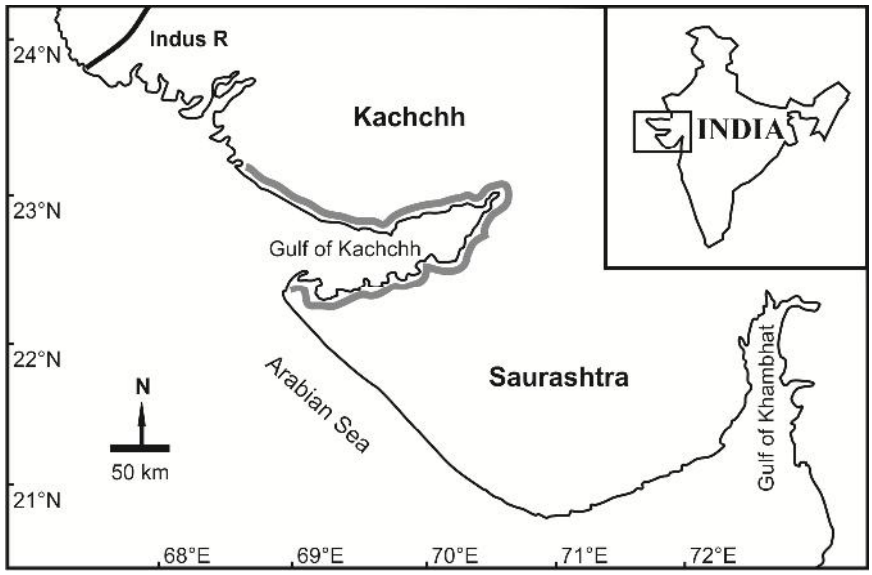

Figure 1.1: Location map showing study area (shaded gray line) and River Indus mouth in the upper left corner.

1.5.1 Physiography of Kachchh

Kachchh region can be divided into four major physiographic divisions which are described as under.

The Island belt

The Island belt comprises of an E-W trending linear series of four islands within the Great Rann located to the north of Wagad and Mainland Kachchh. These islands from west to east are the Pachchham, the Khadir, the Bela and the Chorar islands. Of these the Pachchham island is the largest and Chorar is the smallest in size. The highest elevation in the entire Kachchh is recorded in the Pachchham Island. All the islands display rugged hilly topography and exposed Mesozoic rocks with Tertiary rocks at the fringes of the Pachchham and Khadir islands. The northern margin of all the islands is marked by north facing escarpments which are the manifestation of the Island Belt Fault.

The Mainland Kachchh

The Mainland forms the largest geographic part in the Kachchh basin. It displays the most rugged and most well developed sequence of Mesozoic and Cenozoic rocks. The northern margin of the mainland is bounded by the Kachchh Mainland Fault (KMF) with the domal hilly region, the Northern Hill Range to its south. In the part, the Katrol Hill Fault (KHF) divides the Mainland Kachchh into southern mainland and northern mainland. The Vigodi Fault and the Naira River Fault are the other major faults located in the western and south western part of the Mainland. The Mainland outcrops a continuous succession from Bathonian to Santhonian. The oldest sequence from Bathonian to Callovian is exposed in the northernmost part of the Kachchh.

The Coastal zone of Kachchh

The coastal alluvial plain is a narrow gently sloping plain comprising unconsolidated Quaternary sediments to the south of the Katrol Hill Range. The change of topography is rather abrupt and sharply defined. The width of the alluvial plain varies from 10 - 25 km. The monotonous occurrence of alluvium is interrupted by the presence of Tertiary rocks between the Kharod and Kankawati rivers. The stretch of alluvial plain to the east of the Kharod river is termed as the eastern alluvial plain while to the one to the west of the Kankawati river is termed as the western alluvial plain by Maurya et al. (2008). The alluvial plain comprises one of the few cultivable areas in Kachchh. The alluvial plain in overlapped by the coastal sediments near the shoreline which is sandy in western end and mostly muddy in eastern part (Prizomwala et al., 2010).

The Great Rann of Kachchh and the Banni plain

The flat terrain of the Great Rann and Banni plain together comprise a vast barren landscape that is hostile and almost non-navigable (Glennie and Evans, 1976). These contiguous terrains occur a few meters above sea level and are believed to be part of a former gulf occupying an E-W trending tectonic depression. The Ranns, which constitute a flat terrain with no surface exposures, are the product of marine deposition (Biswas, 1974; Glennie and Evans, 1976). The evolution of the Great Rann of Kachchh has been linked to tectonic activity in recent times. The basin was filled up by sediments supplied from the Indus drainage basin while the surface has been smoothened by the frequent earthquakes. The Ranns are therefore the most promising areas of the Kachchh for neotectonic and palaeoseismic investigations. These unique geomorphic features occupy eastern and northern parts and have a total area of 22,000 sq km. The Great Rann of Kachchh has been the site of the 1819 AD earthquake which produced surface rupture known as the 'Allah Bund' resulting in the upliftment of the northern part of the Rann. The Little Rann is an extension of the Gulf of Kachchh when the sea level was high during the Holocene. This vast wasteland is about 4 m above high water line. The Great Rann and Little Rann comprise unique examples of Holocene sedimentation (Biswas and Deshpande, 1970). The two Ranns mark the site of sediment accumulation in a shallow gulf that was marked by a fluctuating strandline since the beginning of the Holocene. Because of extensive salinity and long dry spells, the Rann sediments show poor development of organic life (Glennie and Evans, 1976). The plain of Banni is regarded as a raised mudflat between the Mainland Kachchh and the Great Rann. It occurs 3 - 10 m above the level of the Great Rann. It is more or less flat and almost gradient less saline grassland covering an area of about 3000 sq km. The Banni plain is only flooded by the rivers from the south and monsoon precipitation (Glennie and Evans, 1976). The presence of gullies and incised fluvial channels on the elevated eastern part of the Banni

plain are indicative of the latest phase of uplift (Biswas, 1974). Extensive liquefaction occurs in the Rann area during the large magnitude earthquakes that have occurred several times in the past.

1.5.2 The Gulf of Kachchh

The Gulf of Kachchh is one of the largest macrotidal regimes in Asia, with a tidal range of 4 m at its mouth and 11 m in its intrinsic creeks. The reason for this tidal amplification in the Gulf of Kachchh is attributed to its funnel shaped geometry, orientation, bathymetry and its coastal configuration. The Gulf of Kachchh is around 70 km wide in its western part and reduces to 10 km in its eastern end. The bottom topography is also quite complex with maximum depth of 60 m in its western mouth which reduces to 15 m at Kandla and gets as low as 3 m in intrinsic creeks eastwards. Also, the western mouth and central part of the Gulf of Kachchh hosts several shoals namely Lushington, Ranwara, Gurur, Bobby, etc. which exhibits strong control on the residual current in the gulf. The Gulf of Kachchh was considered to be a well mixed system; however, some recent studies have shown that only the central gulf is well mixed. The temperature-salinity variations, horizontally as well as vertically show that in eastern gulf the cold and highly saline tongue is advecting along the subsurface layers (Vethamony et al., 2007). The spatial variability in salinity of the Gulf of Kachchh exhibits a characteristic feature of an "inverse estuary", with values of 36.60 psu in its western mouth and 41.00 psu in its eastern part (Vethamony et al., 2007).

According to the present understanding the currents enter in to the gulf from the western end and travels predominantly along the (i.e. via alongshore currents) northern coast of Gulf of Kachchh till it reaches the central part. As the width of the central part of gulf reduces and the

orientation changes, the currents get deflected towards north from here after. They continue travelling along

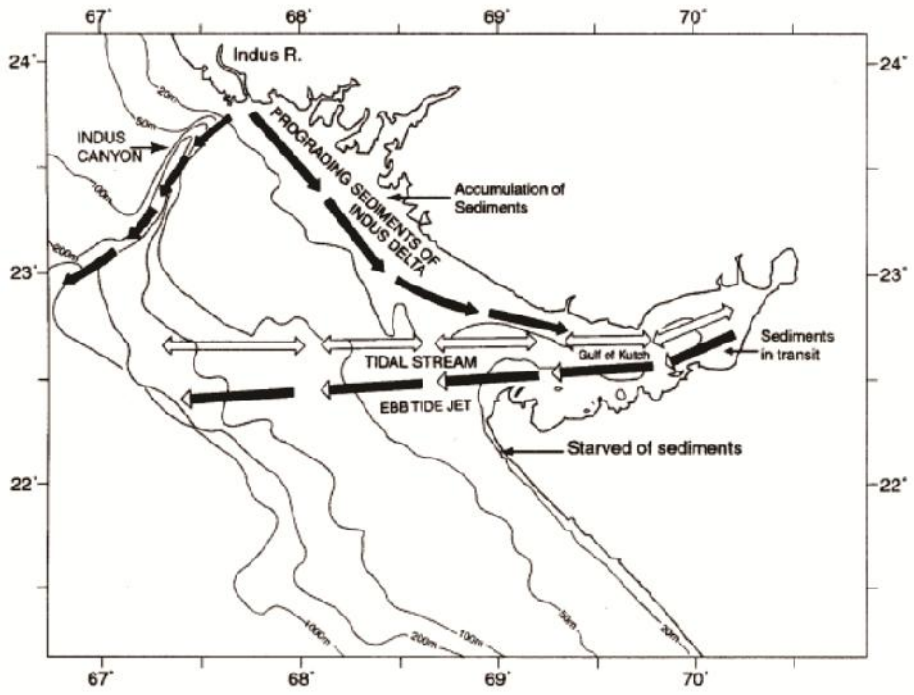

Figure 1.2: Present day current dynamics in the Gulf of Kachchh (After Nair et al., 1982, Chauhan, 1994, Kunte et al., 2003, Chauhan et al., 2006).

the coast and the currents gets reversed from the head of gulf. From here the current travel along the southern coast of the Gulf of Kachchh and exits the mouth of Gulf of Kachchh at Okha (Nair et al., 1982, Chauhan, 1994, Kunte et al., 2003, Chauhan et al., 2006) (Figure 1.2). A small portion of it is transported southward along the Saurashtra coast.

1.5.3 Geology

The geological setup of Kachchh is very well documented (Biswas, 1993). The Mesozoic age sandstones and shales are outcropping in the northern mountain ranges, which are fringed by the Deccan Trap intrusive (Figure 1.3). The Deccan Trap Formation is overlain by friable

sandstones, shales and limestones of the Tertiary age (Figure 1.3). The Quaternary deposits cover the rest of Kachchh mainland topography (Figure 1.3). These Quaternary sediments were deposited into structural lows formed by the movement of dissected basement blocks in the Gulf of Kachchh half graben (Biswas, 1993). The Great Rann of Kachchh in north and the Little Rann of Kachchh in east are believed to be mostly Late Quaternary deposits. The coastal deposits comprise of a series of sandy beach-ridge-dune complexes and with wide intertidal mudflats towards the east (Prizomwala et al., 2010). These coastal deposits are considered to be mostly Holocene in age.

On the other hand Saurashtra peninsula host magmatic rocks like granophyres, feldspar porphyries and basalts of the Deccan Trap Formation (Figure 1.3). Most of the fluvial systems draining into the Gulf of Kachchh from Saurashtra originate from the Barda hills which is a magmatic intrusive. These volcanic rocks are overlain by limestone of Dwarka Formation and clay beds of Gaj Formation of Tertiary age near the coastline of the Gulf of Kachchh (Figure 1.3).

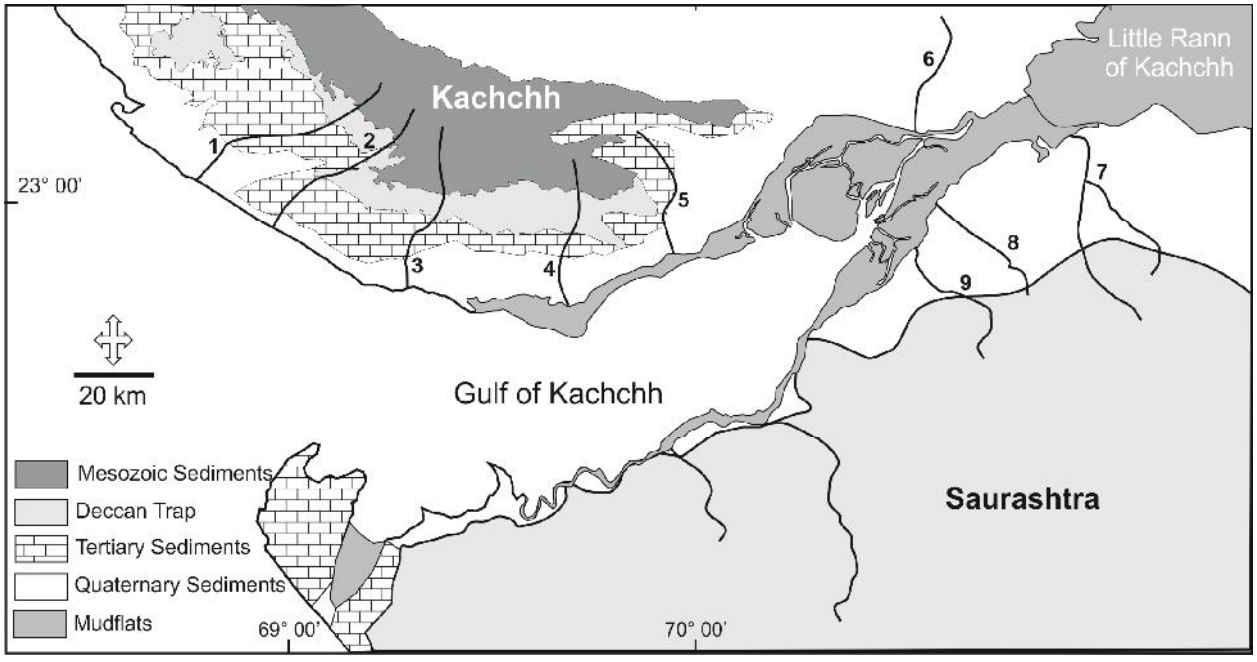

Figure 1.3: Geological map of the area around Gulf of Kachchh and coastal fluvial system. 1- Naira, 2- Kankawati, 3- Rukmawati, 4- Bhukhi, 5- Nagwati, 6- Adhoi, 7- Macchu, 8- Demi and 9- Aji

1.5.3.1 Stratigraphic framework of Kachchh

The Middle Jurassic to Lower Cretaceous rocks are exposed in the highlands of the Kachchh mainland, while the Upper Cretaceous sediments have been encountered only in the offshore wells in Kachchh continental shelf, about 35km from the coast. The early Middle Jurassic strata are exposed in the northern island chain (i.e. The Island Belt), whereas a complete and thicker succession ranging from Middle Jurassic to Lower Cretaceous is exposed in the Kachchh Mainland which has been the depocenter region. Strata of intermediate age are seen in Wagad highland. Except in the south where the Mesozoic rocks are covered by 1000 m thick Deccan Trap lava flows, these rocks are overlain by the Tertiary and Quaternary deposits.

Mesozoic Record

Table 1.1 : Mesozoic lithostratigraphy of Kachchh (after Biswas, 1977).

AGE	MAINLAND			PATCHAM			E. KUTCH (KHADIR-BELA-WAGAD)		
	Formation	Member	Litho	Formation	Member	Litho	Formation	Member	Litho
NEOCOMIAN TO ALBIAN	**BHUJ**	Upper +260m	X-bedded sst, clay-stone.						
		Ukra +30m	Sst, Sh, Fossilifer						
		Ghuneri 325m	Sst- sh, Plant, fossils				**WAGAD SS**	Gamdu + 165 m	Felds-sst, sh, red iron-stone plant fossil
	JHURA	Katesar 190m	X-bedded sst,fossils						
KIMMERI-DGIAN		Upper 300m	Thin-bedded calc sst,					Kanthkot	(Upper) Sst-sh

TO TITHO-NIAN	**N**	Middle 160m	Shales				**T**	200m	(Middle) X-sst
		Lower 120m	Shale / sst Fossils						(Lower) Silt-sh
OXFOR-DIAN	**JUMARA**	Dhosa Oolite 113m	Shales oolitic- lst bands				**WASTHAWA**	Bamanka Shales 160 m	Sh, fossils
CALLO-VIAN		Middle 75m	Sst - Lst, Golden Oolite	**GORADONGAR**	Modar Hill			Gadhada 189m	Sh and sst
		Lower 89m	Green shales		Raimalro			Hadibhadang 280m	(Upper) Lst and cherty
	JHURIO	Upper 70m	Bedded limestone		Gadaputa		**KHADIR**		(Middle) Sst
BATHO-NIAN		Middle 85m	Shales with Golden Oolite		Flagstone				(Lower) Shales Fossils
		Lower 139m	Lst-Sh, interbed--ded	**KALA DONGAR**	Kala Dongar Sand-stones			Cheriyabet 25m	Pegmatic Granite-Cobble-Conglo. and arkose
					Kuar Bet				
								Precambrian	Granitic basement

Wynne (1872) was the first to suggest a two-fold sub-division of the Mesozoic rocks of Kachchh based on general lithological characteristics after extensive mapping of the entire basin. Later on Biswas (1977) proposed a new lithostratigraphic classification which is widely in use (Table 1.1).

The lithostratigraphic sequence of the Mainland Kachchh is divided into four formations named as the Jhurio (Jhura), Jumara, Jhuran and Bhuj Formations in ascending order. The Bhuj Formation is disconformably overlain by the basalt flows of the Deccan Trap Formation on the south while the base of the Jhurio Formation is unexposed. In Pachchham island stratigraphic sequences are divided in two formations namely, Goradongar and Kaladongar Formations

whereas remaining island belt (Khadir and Bela) and wagad has been marked with Wagad, Wasthawa and Khadir Formations.

Cenozoic Record

The geological record pertaining to the Cenozoic age is restricted to the northwest, west and south areas of Kachchh, mostly comprising its coastal region. It is important for its Eocene-Oligocene boundary and also for a thick Miocene-Pliocene sequence. However, the Pleistocene record is relatively patchy, although an important unit Miliolite Formation is present in the form of locally occurring obstacle dune deposits and reworked sheets on river banks. Mata-no-madh Formation, Naredi Formation, Harudi Formation, Fulra Limestone Formation, Maniyara Fort Formation, Khari nadi Formation, Chhasra Formation and Sandhan formation are part of this Cenozoic record (Table 1.2).

Table 1.2: Tertiary lithostratigraphy of Kachchh (after Biswas, 1971).

Age	**Formation**	**Members**
Pliocene	Sandhan	
Lower Miocene (Burdigalian)	Chhasra	Siltstone
		Claystone
Lower Miocene (Late Aquitanian)	Khari Nadi	

Oligocene	Maniyara Fort	Bermoti Coral Limestone Lumpy clay Basal member
Late Middle Eocene	Fulra Limestone	
Middle Eocene	Harudi	
Late Paleocene	Naredi	Ferr. Claystone Assilina Limestone Gypseous Shale
Upper Paleocene	Matanomadh	
Cretaceous–Lower Plaeocene	Deccan Trap	

1.5.3.2 Stratigraphic framework of Saurashtra

The northern coastal stretch of Saurashtra region consists of rocks belonging to Mesozoic and Cenozoic Era. Stratigraphically the sequence begins with Juro-Cretaceous sedimentary

formations which are nonconformably overlain by the upper Cretaceous volcanic igneous rocks followed by the Mio-Pliocene and Quaternary sedimentary sequences. (Table 1.3).

Table 1.3: Lithostratigraphy of Saurashtra region (Shrivastava, 1963, Mathur and Mehra, 1975 and Bhatt, 2000).

Era	**Period**	**Formation**	**Age**
Cenozoic	Quaternary	Unclassified Holocene deposit	Holocene
		Chaya	Late Pleistocene
		Miliolite	Middle to Late Pleistocene
	Tertiary	Dwarka	Lower Pliocene to Middle Miocene
		Gaj	Lower to Middle Miocene
Mesozoic	Juro-Cretaceous	Deccan Trap	Upper cretaceous to Eocene
		Wadhwan	Middle Cretaceous
		Dhrangadhra	Upper Jurassic to Lower Cretaceous

1.5.4 Tectonic framework

The structure, basin architecture and evolution of Kachchh region has been discussed in a series of publications by Biswas (1980; 1987; 2005). The major faults like Kachchh Mainland

Fault (KMF), Katrol Hill Fault (KHF), Island Belt Fault (IBF), Allahband Fault, etc. have always been discussed by many while describing the tectonic framework of Kachchh basin (Fig. 1.4). The basin is peri-cratonic embayment through a marginal graben between Nagar Parkar and Saurashtra uplifts, respectively to the north and south. To the east, the basin is limited by the Radhanpur arch. The regional slope of the basin is towards WSW and the depositional axis passes close to the Saurashtra uplift to the south. Basinal hinge zone is marked by a first order basement high (Median high) across the middle of the embayment. This hinge zone is the extension of the Indus shelf hinge perpendicular to the depositional axis (Biswas, 1987). The basin is featured by residual basement ridge along primordial faults parallel to the major Precambrian trends (Biswas, 1982). These ridges were passive highs within the basin, but later rejuvenated by reactivation of the faults. They are manifested in subparallel uplifts with narrow flexures along the master faults (Biswas, 1980). Mesozoic rocks are exposed mainly in these uplift areas surrounded by "residual depression" (Beloussov, 1962) which are occupied by vast mud and salt flats of the Great and the Little Ranns of Kachchh and the Banni Plains. The culmination along the marginal flexures formed domal structures which expose older Mesozoic strata.

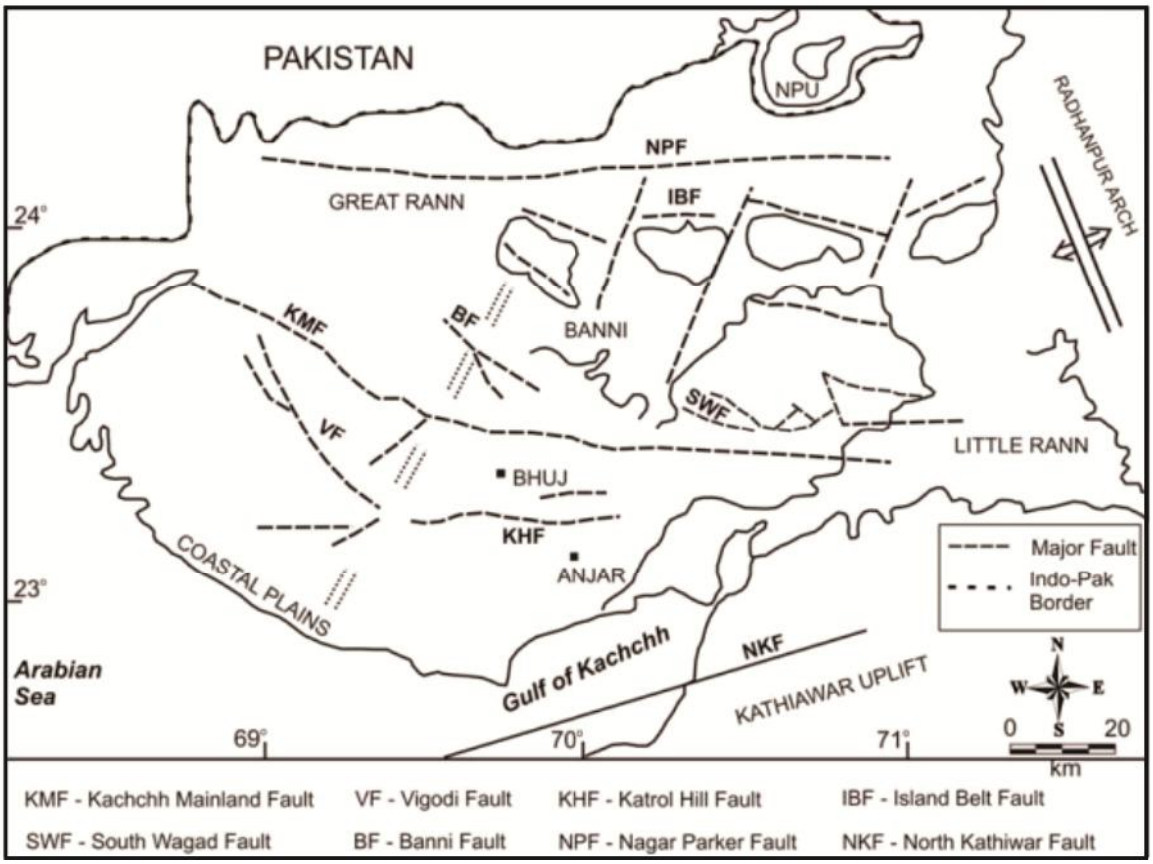

Figure 1.4: Tectonic map of Kachchh (after Biswas and Khattri, 2002).

Chapter 2

GRANULOMETRIC ANALYSIS

2.1 Significance

It is well known that the spatial changes in grain size characteristics essentially result from sediment transport processes and possibly mixing of sediments from various sources (Swift et al., 1982). Initial studies (Pettijohn and Ridge, 1932) have suggested that the mean grain size decreases in the direction of transport (especially in fluvial environments). However, sometimes coarsening is also observed specially in beach environments where spatial changes in grain size are longshore currents dependent. Hence, the grain size trend analysis has been used by many in ascertaining the residual sediment transport direction and the sediment pathways in intertidal and near shore (Van Lancker et al., 2004; Hequette et al., 2008), fluvial (Radoane, et al., 2007; Frings, 2008), estuarine (Gao and Collins, 1994) and beach environments (Pedreros et al., 1996).

Gulf of Kachchh coastline consists of both, sand dominating landforms in the west, and the mud dominating landforms in the eastern ends. The geomorphic setup of western segment of the Kachchh coastline shows presence of tidal flats, beaches, berm plain, foreshore and backshore dunes. Therefore sampling was carried out from intertidal microenvironment from all along coastline. Shore normal transects were also selected to sample berm, berm plain and dunes in the northern sandy segment. Figure 2.1 shows schematic diagram of various microenvironments along northern sandy segment of the Kachchh coast.

2.2 Methodology

As the coastline had both, sandy and muddy sediments, the grain size analysis was performed on sandy sediments using a mechanical sieving technique, while the muddy sediments were studied following pipette analysis technique which are described below in detail.

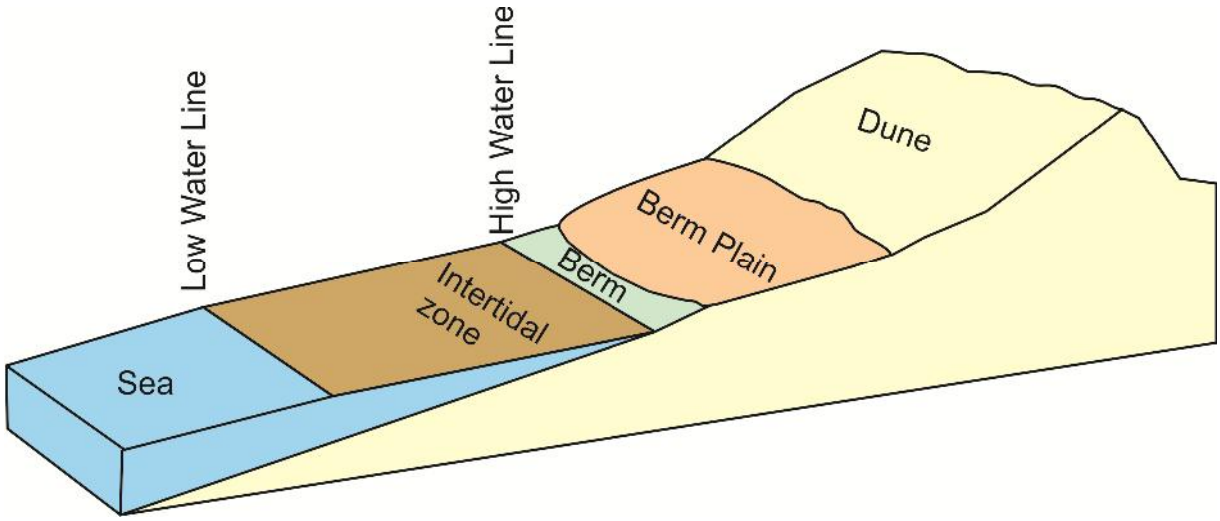

Figure 2.1: Schematic diagram of various microenvironments sampled along the northern Gulf of Kachchh coast.

2.2.1 Mechanical sieving

About 50 gm of sample was initially weighed for the mechanical sieving after homogenization of the sample collected from field. The homogenization of sample was performed following 'coning and quartering' method. Thereafter the sample was put in standard ASTM sieve set ranging from 10 ASTM (> 2 mm) to 230 ASTM (< 0.063 mm). The sieves were arranged on mechanical sieve shaker in decreasing sieve size from top to bottom with a pan at the base. The mechanical sieving was carried out for 20 minutes for each sample and then the weight retained in each sieve was measured using digital weighing machine. The analysis was done with half phi size interval. Different statistical parameters like Mean, Median, Standard Deviation, Skewness, and Kurtosis were calculated following Folk (1974).

2.2.2 Pipette Analysis

This technique relies on the fact that in a dilute suspension, particles settle through a column of water at velocities which are dependent upon their size. If a material behaves according to Stokes' Law then, by repeatedly sampling at a fixed depth below the surface progressively finer and finer sediments are present at the sampling depth. Temporal variations of solid concentrations at that level indicate the relative abundance of particles whose diameters may be calculated. The sample was initially sun dried for few days till it gets completely dry. The dried sample was weighed to about 10 gm of weight and taken in a 1 liter borosil glass beaker which was filled up with distilled water and kept undisturbed for 24 hours. After the settling of sample at bottom, the beaker was emptied to half of its volume carefully, without disturbing the sample which is settled at bottom. Same procedure was followed another day by filling up the beaker by distilled water and keeping it for again next 24hrs. Next day the water was drained to a maximum possible level, while taking care that the sample is still remaining in the beaker. About 5ml of 30%W/V H_2O_2 (Hydrogen peroxide) was added to the sample for removal of organic matter and again the beaker was kept undisturbed for about 24hrs. Clay has cohesive properties and hence, it forms aggregates when saturated, therefore 10ml of known concentration (44gm/100ml) sodium hexa-meta-phosphate solution was added as a dispersant. After adding the dispersant the sample was again kept for 24hrs. The concentration of dispersant solution should be known to obtain the weight correction factor to finally estimate the clay %. Next day the sample was passed through 230 ASTM sieve and collected in a cylinder of 1 liter capacity. The sample retained in the sieve was dried and weighed to estimate the sand fraction whereas, sample collected in the cylinder represents silt and clay fractions. The cylinder was then filled up with distilled water till 1 liter mark and agitated vigorously till the entire amount of sample comes in suspension. A fixed temperature of 27 ºC is maintained as the settling of

particles in temperature dependant. Using a pipette 10 ml of volume of solution was withdrawn from the top 10 cm depth of cylinder after six hours and thirty minutes and taken in a dry (pre-weighed) petridish. It was kept for drying in electric oven for 24 hrs at 50 ºC. As the viscosity of medium is temperature dependent and settling velocity is viscosity dependent, temperature at which the pipette analysis is done decides the time of the withdrawal of clay solution by pipette after its homogenization in the cylinder. The calculation of clay fraction percentage was done using the following equation.

Clay Percentage = (A - B) x KD

Where, A = weight in grams of dried pipette fraction

B = weight correction for dispersing agent

K = 1000/(volume contained in pipette)

D = 100/(initial oven dry weight of sample)

Now subtracting the weight percentages of sand and clay fraction from 100 would give the silt percentage in the sample.

2.3 Results

2.3.1 Jakhau to Modwa Segment

Granulometric analysis (Table 2.1) summaries that intertidal and dune microenvironments have the finer grain size compared to berm and berm plain microenvironment, wherein berm plain has the most coarse grain sediments. The mean grain size class ranges between 0.5 Φ and 2.5 Φ. The site Pingleshwar (P) in the extreme west has medium sand (0.5 Φ - 1.0 Φ) as dominant grain size which is fining in eastward direction to attain 1.0 Φ - 2.0 Φ value of mean size at site Rawal Pir (R) in all the microenvironments (Figure 2.2). Intertidal is the most active microenvironment in a coastal configuration for sediment transport and sediment supply.

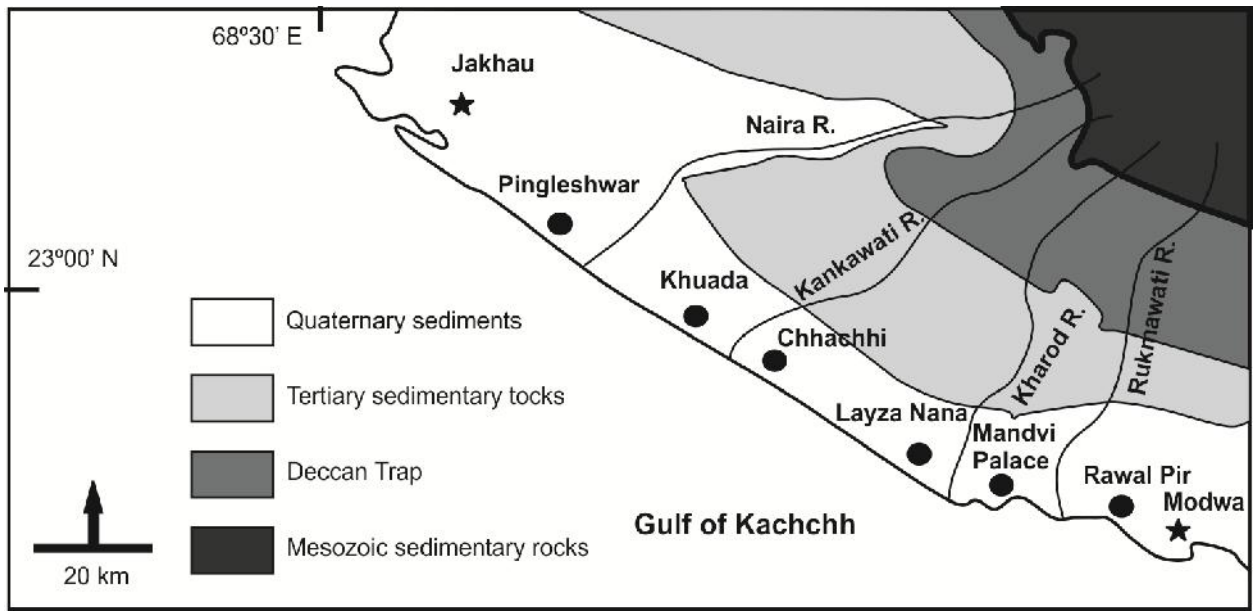

Figure 2.2: Sampling locations for shore normal profiles along northern Gulf of Kachchh coast.

The accretion of sediments in berm plain is mostly caused due to spring high tides or storms which deposit large amount of sediments in supratidal regions, whereas the dunes get sediment supply from aeolian action ultimately from the intertidal, berm and berm plain. The dominant coarse size class in berm plain is indicative of frequent high energy events (i.e. storms), which is also evident by other parameters like high standard deviation values owing to less sorting. The dunes on the other hand show fine grained assemblage with low standard deviation values. From west to east the kurtosis values increase whereas the skewness values become more negative.

Table 2.1: Grain size parameters of coastal sediments of the southwest Kachchh. (P - Pingleshwar, K - Khuada, C - Chhachhi, L - Layza Nana, M - Mandvi Palace, and R - Rawal Pir)

	Location	Mean	Standard Deviation	Skewness	Kurtosis
Dune	P	0.79	0.6	0.2	1.06
	K	1.86	0.55	0.14	0.94
	C	0.97	0.8	0.31	1.03
	L	2.44	0.46	-0.08	1.38
	M	1.96	0.58	-0.07	0.91
	R	1.35	0.83	0.1	0.81

Berm Plain	P	0.73	0.76	0.05	1.16
	K	1.84	0.56	0.13	0.95
	C	0.51	0.64	0.05	1.47
	L	1.51	0.95	-0.04	0.71
	M	1.14	1.19	0.33	0.92
	R	1.14	0.8	0.26	0.89
Berm	P	0.75	0.66	0.18	1.16
	K	1.84	0.56	0.13	0.95
	C	1.37	0.67	0	1.07
	L	2.54	0.32	0.11	1.22
	M	1.9	0.61	0	0.93
	R	0.62	1.04	0.22	1.11
Intertidal	P	0.9	0.68	-0.05	0.98
	K	1.04	0.57	0.04	0.91
	C	1.01	0.71	-0.15	1
	L	1.93	0.76	-0.25	1.11
	M	2.01	0.81	-0.44	1.26
	R	1.69	0.91	-0.27	0.66

Geomorphologically, this stretch consists of two major zones; the straight and sandy segment between Pingleshwar to Layza nana, and the transition zone from Layza nana to Rawal Pir (Prizomwala et al., 2010). Figure 2.3 shows the fining of sediments towards east. The result of granulometric analysis shows the fining in sediments from west to east and increase in standard deviation. The kurtosis values decrease from west to east, indicating increased bimodality in grain size distribution, which is due to mixing of varied sediment size transported in long-shore currents and supplied by coastal rivers like Kankawati, Kharod and Rukmawati.

The more negative skewness values in intertidal microenvironment are indicative of strong wave action leading to washing away of the fine sediments. The increase in standard deviation values from Layza Nana towards east and presence of both, sandy as well as muddy landforms between Layza Nana and Mundra indicates of this zone being a ‘transition zone’ for sediment transport processes. The granulometric characteristics of dune, berm plain, berm and

intertidal microenvironments are indicative of near-shore mixing and subordinate sorting of sediments supplied from two distinct sources viz., distal Indus River mouth and proximal Kachchh mainland.

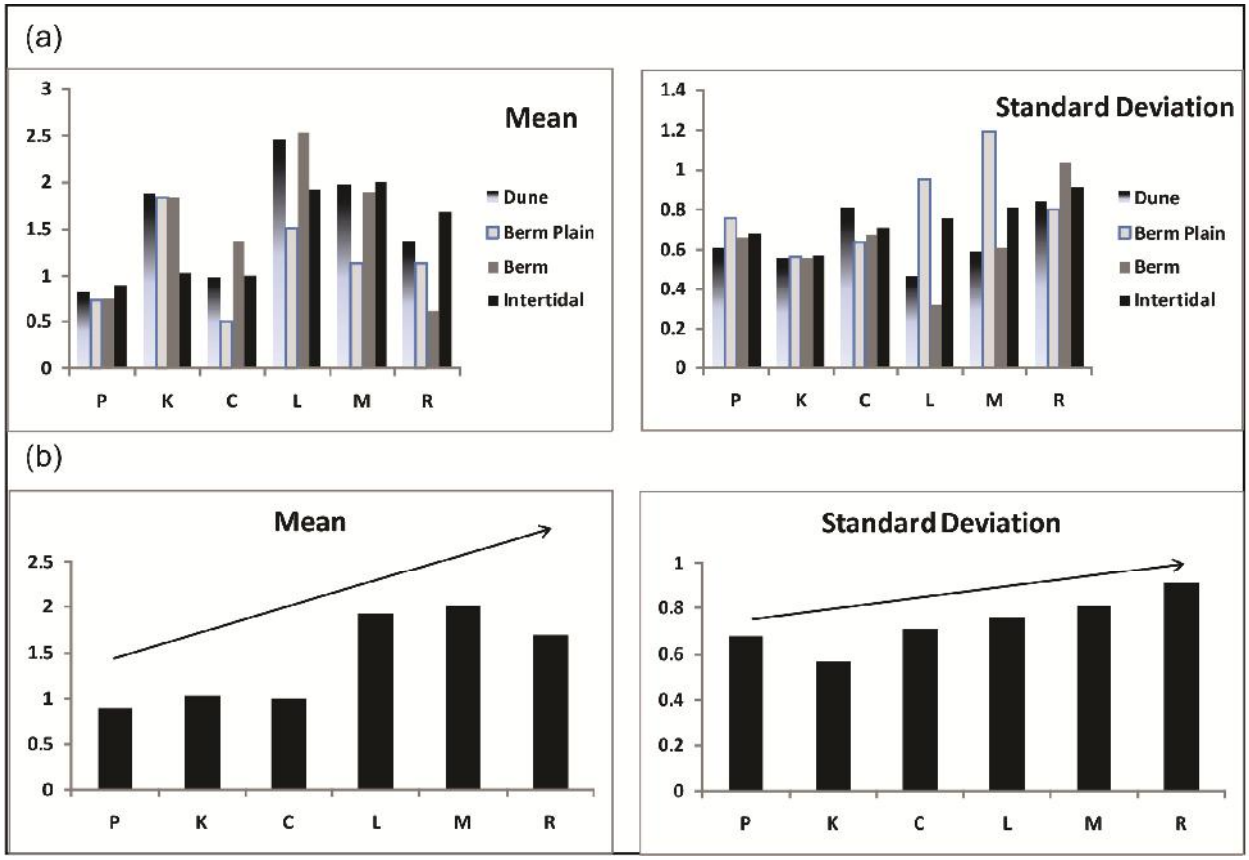

Figure 2.3: (a) Plots of mean and standard deviation within various microenvironments from different locations, (b) Plots of mean and standard deviation in intertidal sediments along the coast (P - Pingleshwar, K - Khuada, C - Chhachhi, L - Layza Nana, M - Mandvi Palace, and R - Rawal Pir).

2.3.2 Modwa to Okha Segment

The mudflat bearing coast starts from the Modwa and mudflats get wider and wider eastwards. The inner Gulf of Kachchh coast has wide mudflats and has variable sand concentration from 2 – 20 % (Figure 2.4). The mudflats are mostly silty but, in extreme inner gulf the clay content increases to more than 50 % (i.e. at Samakhyali). The increase in sand content along southern coast of inner Gulf of Kachchh is due to the presence of few ephemeral

rivers like Aji, Machchhu, Demi etc, which bring in ample amount of sand to the coastline owing to their ephemeral nature. The southern mouth of Gulf of Kachchh shows increase in silt content with decrease in amount of clay at its western most part a significant increase in amount of sand could be seen (i.e. at Okha and Pindara). This can again be attributed to higher energy condition near the mouth as compared to the head area of the gulf.

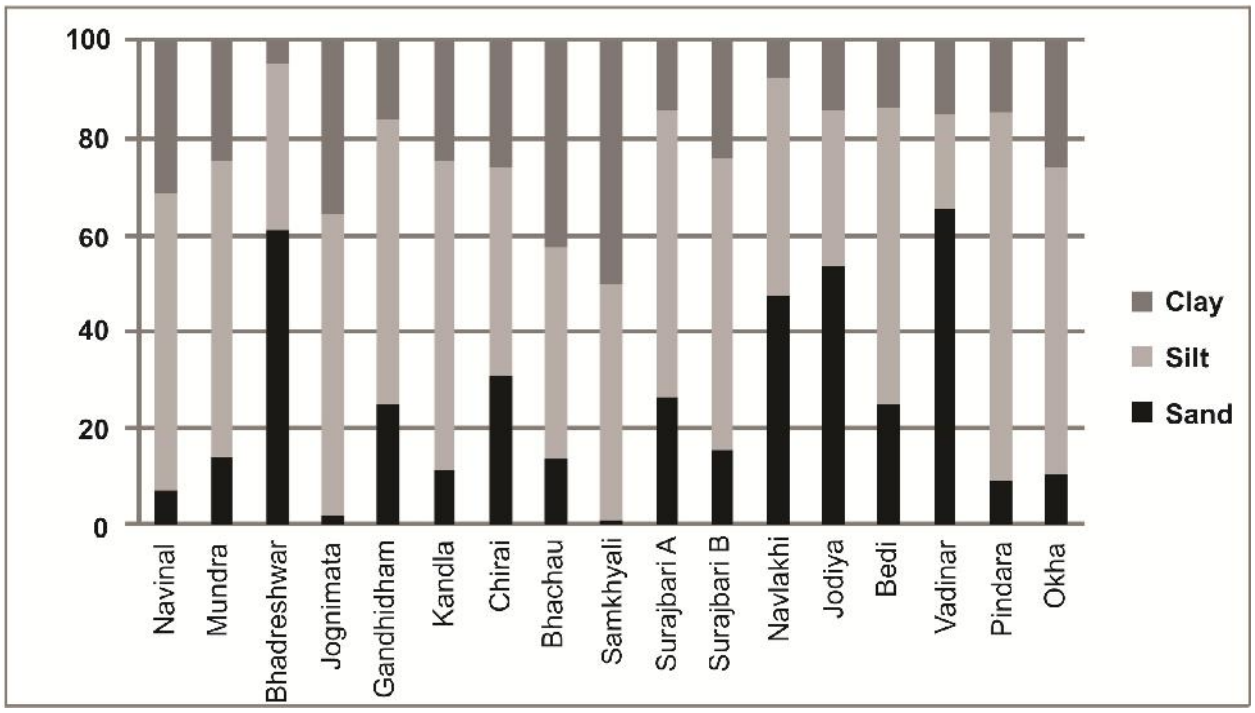

Figure 2.4: Grain size distribution in intertidal sediments form the segment between Modwa and Okha.

In general, the grain size distribution along the Gulf of Kachchh coastline showed significant role of energy of tidal currents and coastal fluvial systems, which controls the sediment transport pathways and geomorphic assemblages along the gulf coastline. The characteristic grain size distribution pattern of the western and eastern segments of gulf also corroborated the wave dominated and tide dominated landforms along the Gulf of Kachchh coastline.

Chapter 3

Mineral Magnetic Analysis

3.1 Principle & Techniques

Sediment finger printing technique for source ascription has been employed using various conventional proxies like mineralogy, geochemistry, radionuclide and isotopic concentrations. However, these techniques are enormously time consuming and expensive. Hence, there is a vital need for a technique which is more or equally robust, fast and less expensive. Mineral magnetic analysis is a non-destructive modern technique often used to study the concentration, grain size and mineralogy of magnetic minerals in natural samples. Many types of studies that are now classified as 'environmental magnetism' have been in existence for some time. However, the first explicit description of environmental magnetism as a distinct field did not appear until 1980. In a landmark article in Science (vol. 207 pp. 481 - 486), Thompson et al. (1980) showed how mineral magnetic parameters can be used in a wide range of environmental studies. The publication of 'Environmental Magnetism' by Thompson and Oldfield (1986) brought this field to the attention of a wider audience and remained instrumental for a rapid expansion in the use of mineral magnetic techniques to solve a variety of environmental problems in recent time. Study of various mineral magnetic properties has been successfully employed to various depositional environments like fluvial (Oldfield et al, 1985; Walden et al, 1997), marine (Lepland and Stevens, 1996; Schmidt et al, 1999; Ellwood et al, 2006; Liu et al, 2010; Horng and Huh, 2011; Prizomwala et al, in press) and marine - fluvial interactions (Maher et al, 2009). Mineral magnetic measurements have been identified as a suitable tool for determining sediment

provenance (Oldfield and Yu, 1994; Booth, 2002; Liu et al, 2010) and sediment transport pathways (Lepland and Stevens, 1996; Maher et al, 2009; Wang et al, 2010). The magnetic properties of sediments normally vary as per the characteristic magnetic minerals they contain with their respective mineralogy, concentration and magnetic domain state. The most commonly occurring magnetic minerals are Magnetite, Maghemite, Hematite and Goethite. These magnetic minerals occur in minor and even in trace amount in a sample, but they carry important information as they differ characteristically depending upon their source and depositional history (Maher et al., 2009).

For the present study the surface samples were collected from the entire Gulf of Kachchh coastline (n=105), however, special emphasis was given to the sandy Kachchh coast between Jakhau and Rawal Pir from where intertidal, berm, berm plain and foreshore dunes were sampled. The samples were packed in plastic bags to avoid contamination. They were then dried at 40° C and packed into 10 cc Perspex bottles using thin foils. Mineral magnetic measurements viz, magnetic susceptibility (χ), frequency dependent susceptibility (χ_{fd}%), anhysteretic remanent magnetization (ARM) and isothermal remanent magnetization (IRM) were carried out on all separated fractions. Magnetic susceptibility was measured using MFK1-FA multifunction frequency Kappabridge with a sensitivity of 10^{-6} SI. Frequency dependent susceptibility (χ_{fd}%) was calculated using the expression (χ_{LF} - χ_{HF})/ χ_{LF} x 100, where χ_{LF} is magnetic susceptibility at low frequency (976 Hz) and χ_{HF} is susceptibility at high frequency (15,616 Hz). ARM was imparted in a steady 0.05 mT field superimposed over decreasing alternating field (AF) up to 100 mT using a Molspin AF demagnetizer. ARM is expressed as ARM per unit steady field, χ_{arm}. All remnant magnetization of ARMs and IRMs were measured using Molspin spinner magnetometer. IRM measurements were carried out at forward fields (mT) of 20 and 1000 and

backward fields (mT) of 20, 40, 60, 100 and 300 using Molspin pulse magnetizer. IRM imparted at 1 T forward field is considered as SIRM as all magnetic particles would be saturated at this signal. The S-ratio, simplified here as ratio of $IRM_{-0.3T}$/SIRM, is used as indicator of relative contributions of magnetic mineralogy in terms of ferrimagnetic and antiferromagnetic components.

Oldfield et al. (1994) identified that low frequency magnetic susceptibility measurement can be used to infer presence of coarse multi-domain magnetite in sand and silts. The measure of χ_{arm} is approximately proportional to concentration of ferromagnetic grains in stable single domain (0.03-0.05μm) size range (Maher, 1988), while χ_{fd} indicates presence of fine viscous grains near super paramagnetic and stable single domain boundary (Maher, 1988; Oldfield and Yu, 1994). SIRM is proportional to concentration of only remanence carrying magnetic matter in single and multi-domain grains (Thompson et al., 1980). The ratio parameters like χ_{arm}/SIRM reflects variations in ferromagnetic grain size with values peaking in SD range (Maher, 1988) and are used as grain size indicators of magnetic minerals (Banerjee et al., 1981; Maher, 1988). Table 3.1 shows mass specific magnetic measurements and their interpretations used in this study based on the available literature (Thompson et al., 1980; Banerjee et al., 1981; Thompson and Oldfield, 1986; Maher, 1988; Oldfield and Yu, 1994; Jenkins et al., 2002; Basavaiah and Khadkikar, 2004; Booth et al., 2005 and Maher et al., 2009).

Table 3.1: Mass specific magnetic parameters and their interpretations.

Parameters	**Interpretation**
χ	Initial low field mass specific magnetic susceptibility. Its value is roughly proportional to concentration of magnetic minerals in a sample.

χ_{fd} **(%)**	Frequency dependent susceptibility. It is calculated as X_{fd}=(100x(X_{LF}-X_{HF}))/ $X_{LF.}$ It indicates the presence of viscous grains lying at stable single domain/super paramagnetic boundary.
χ_{arm}	Anhysteretic remnant magnetization was induced in sample in this study by combining peak AC field of 100mT with a small DC biasing field. The value is roughly proportional to concentration of ferrimagnetic grains in 0.03-0.05μ m (stable single domain) range
SIRM	Saturated isothermal remnant magnetization is the highest amount of magnetic remanence that can be produced in a sample by applying a large external field. Field of 1T was considered to be 'saturated' for this samples, however it might not saturate some minerals (e.g. Goethite). SIRM is concentration of all remanence carrying minerals in a sample but is also dependent on mineral type and its grain size.
S-ratio	In this study S-ratio = $_{-0.3T}$IRM/SIRM. It is indicator of dominant mineral type, and is very good in discriminating ferrimagnetic minerals and antiferromagnetic minerals. Values reaching "1" indicate dominant ferrimagnetic mineral assemblage, where as values reaching "0.5" have dominant antiferromagnetic mineral assemblage.
χ_{arm}**/SIRM**	It is a dimensionless ratio indicating ferrimagnetic grain size. Higher values indicate finer (stable single domain) grain size. Low X_{arm}/SIRM denote large multi-domain (magnetite) component in sample.

3.2 Results

3.2.1 Shore normal profile samples

Six sites were selected from the northern coast of Gulf of Kachchh which hosts more sandy landforms. Samples were collected from different microenvironments along the segment between Jakhau to Modwa, namely Pingleshwar (P), Khuada (K), Chhachhi (C), Layza Nana (N), Mandvi Palace (M) and Rawal Pir (R). Sampling was done at these selected locations from both, east and west of various river mouths to infer the effect of longshore currents that was expected to be from west towards east (Nair et al, 1982, Prizomwala et al, 2012) during the sampling period of May-June 2009. Five samples from intertidal microenvironment at each location were collected and a part of which was homogenized. Also, transects across the coast were taken to study the representative surface samples from each microenvironments like intertidal, berm, berm plain and dune. A total of 48 samples were collected from this segment of the coastline.

Table 3.2 shows the selected mineral magnetic parameters used for evaluation of magnetic mineral concentration, mineralogy and grain size. As observed at all the sites, the concentration dependent parameters of χ, SIRM and χ_{arm} show that the enrichment of magnetic minerals is mostly in berm, berm plain and dune microenvironments and to a lesser extent in intertidal microenvironment. This may be due to the sediment sorting processes involved in these microenvironment. Being heavy minerals (specific gravity >2.89), most of the magnetic minerals are found more in the berm and berm plain environment which gets accreted during high energy events (e.g. storms). The site Chhachhi shows maximum enrichment of magnetic minerals due to considerable detrital flux from the rivers draining from the Kachchh Mainland, whereas site

Pingleshwar shows minimum concentration due to absence of any Kachchh mainland drained river debouching west of it.

Table 3.2 : Results of mineral magnetic measurements on shore normal samples.

Locations	Magnetic Concentration			Magnetic Grain size			Magnetic Composition			Micro-environments
	χ_{lf} 10^{-8} m^3kg^{-1}	SIRM 10^{-6} Am^2kg^{-1} (10^3)	χ_{arm} 10^{-6} Am^2kg^{-1}	χ_{fd} %	ARM/SIRM 10^{-3}	χ_{arm}/χ_{lf} 10^3	Soft IRM 10^{-6} Am^2kg^{-1} (10^3)	Hard IRM 10^{-6} Am^2kg^{-1} (10^3)	S-Ratio ($IRM_{0.3T}$/SIRM)	
P	6.52	1.14	0.15	5.03	5.31	19.40	0.86	0.44	0.58	Intertidal
K	9.25	1.56	0.23	3.11	5.82	8.46	1.44	0.15	0.90	
C	86.85	15.26	2.39	2.46	6.24	0.71	13.33	0.63	0.96	
L	40.91	6.68	1.10	2.02	6.52	1.24	6.01	0.13	1.00	
M	59.08	10.09	1.59	2.43	6.28	1.03	9.46	0.19	0.99	
R	60.44	10.70	1.55	2.08	5.88	0.86	9.15	0.32	0.96	
P	25.72	3.61	0.44	3.51	4.83	3.43	3.01	1.09	0.70	Berm
K	33.86	5.14	0.20	3.11	5.74	2.31	0.60	4.00	0.95	
C	250.00	60.00	13.95	1.95	9.25	0.20	55.00	0.65	0.99	
L	157.70	29.25	3.08	1.13	4.19	0.18	26.42	2.42	0.92	
M	202.78	35.32	4.40	1.50	4.95	0.19	30.84	0.71	0.99	
R	61.74	10.16	1.44	2.09	5.65	0.85	7.79	0.37	1.00	

Continued

P	20.36	2.83	0.32	4.98	4.43	6.15	2.19	0.98	0.65	Berm Plain
K	33.86	5.14	0.69	3.11	5.36	2.31	4.95	0.24	0.95	
C	199.75	32.86	4.86	2.34	5.88	0.29	27.91	1.26	1.00	
L	107.22	18.66	2.33	1.61	4.96	0.38	16.23	0.76	0.96	
M	141.99	56.94	2.85	1.85	1.99	0.33	51.75	5.00	0.40	
R	116.15	21.69	2.81	1.61	5.15	0.35	18.65	0.72	1.00	
P	29.62	4.48	0.59	3.90	5.20	3.31	3.31	1.69	0.62	Dune
K	42.34	6.49	0.83	3.76	5.11	2.23	6.23	0.32	0.95	
C	164.52	28.00	3.68	2.20	5.23	0.34	23.89	0.12	1.00	
L	76.87	13.65	1.73	1.77	5.04	0.58	12.83	0.02	1.00	
M	49.74	9.68	1.43	1.74	5.87	0.88	9.02	0.35	0.96	
R	97.45	20.36	2.36	0.93	4.62	0.24	18.40	1.44	0.93	

The magnetic grain size as indicated by χ_{fd}%, ARM/SIRM and χ_{arm}/χ_{lf} shows that the intertidal microenvironment has dominant fine magnetic grains i.e. SSD, whereas berm, berm plain and dune microenvironments have dominant coarser size range i.e. MD. However, this is true for all locations barring Pingleshwar and Khuada, where all microenvironments show finer (SSD) size range as depicted by the χ_{arm}/χ_{lf} values (Figure 3.1).

The coercivity dependent parameters of Soft IRM, Hard IRM and S-ratio show that magnetic mineralogy is location specific and is consistent throughout all microenvironments. The site P shows contrastingly different magnetic assemblage with higher Hard IRM values and S-ratio dropping to 0.57, indicating dominant high coercivity antiferromagnetic minerals (i.e. hematite). The other locations have high Soft IRM values with S-ratio mostly remaining >0.92, indicating dominant low coercivity ferrimagnetic mineral assemblages (i.e. magnetite).

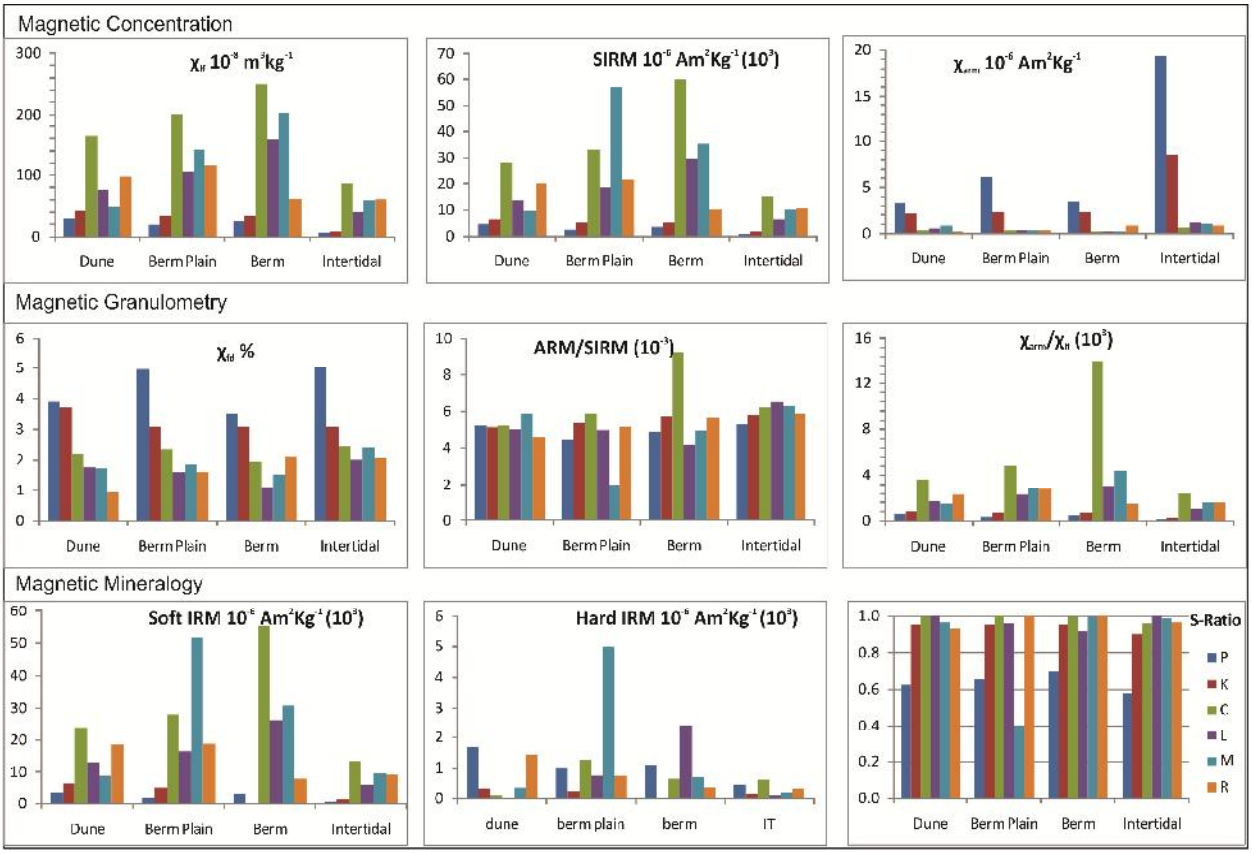

Figure 3.1: Mass specific mineral magnetic parameters from shore normal profiles.

The relative higher contribution of low coercivity magnetic mineral phases may be attributed to the contribution from Deccan basalt lithology of the Kachchh mainland.

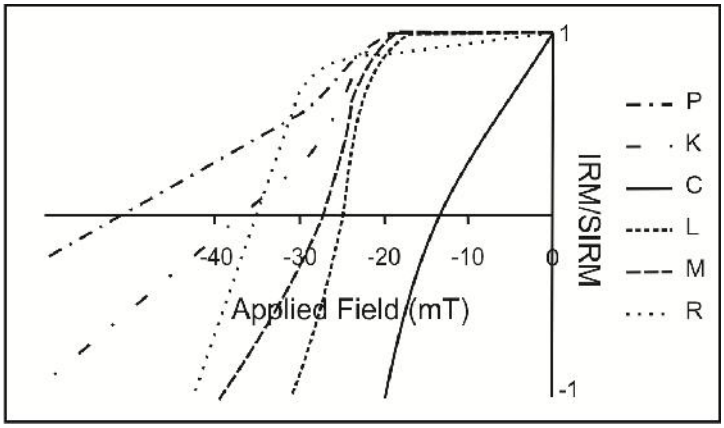

Figure 3.2: Plot of normalized IRM with applied field.

Figure 3.2 shows contribution from low coercivity minerals with H_{cr} values ranging from 20 to 35 mT for all the locations east of P (i.e. K, C, L, M and R), whereas western end (i.e. P) is characterized by higher coercivity mineral contribution with H_{cr} values >50 mT.

3.2.2 The intertidal samples along the entire Gulf of Kachchh coastline

Figure 3.3 shows the sampling location for the complete stretch of the Gulf of Kachchh coast, i.e. Jakhau (a), Pingleshwar (b), Khuada (c), Chhachhi (d), Layza Nana (e), Mandvi Palace (f), Mandvi (g), Rawal Pir (h), Navinal (i), Mundra (j), Bhadreshwar (k), Jogni mata (l), Kandla, (m), Gandhidham (n), Chirai (o), Bhachau (p), Samakhyali (q), Surajbari-a (r), Surajbari-b (s), Navlakhi (t), Jodiya (u), Bedi (v), Vadinar (w), Pindara (x) and Okha (y). Sampling was restricted to intertidal microenvironment only as the major aim was to study variations in mineral magnetic properties along the coastline. From each site around 3 samples were collected (n = 75) and separated into > 63 micron fraction and < 63 micron fraction for further analysis.

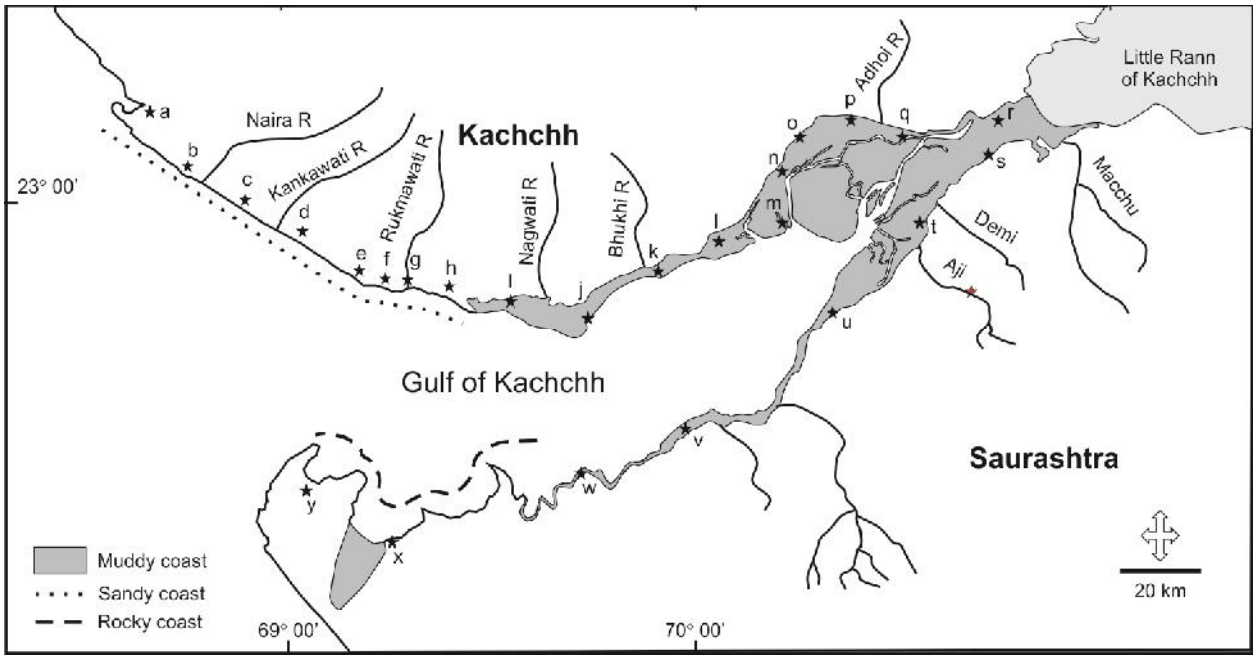

Figure 3.3: Sampling locations for entire Gulf of Kachchh coastline.

Mineral magnetic analysis of >63micron fraction

The samples drawn from the area near Jakhau of the Gulf of Kachchh has lesser concentrations of magnetic minerals (65 x 10^{-7} m^3kg^{-1} to 300 x 10^{-7} m^3kg^{-1}), but the magnetic concentration increases from Chachhi towards east, owing to the sediment input from several coastal rivers draining through Kachchh mainland and debouching in to the Gulf of Kachchh (Table 3.3). The segment between Chachhi and Mundra (i.e. transition zone) has intermediate amount of magnetic mineral concentration (400 x 10^{-7} m^3kg^{-1} to 1100 x 10^{-7} m^3kg^{-1}), barring the station Mandvi (2400 x 10^{-7} m^3kg^{-1}). Interestingly the sand fraction in mudflats of the northern coast of the inner Gulf of Kachchh has low to intermediate magnetic mineral concentration (280 x 10^{-7} m^3kg^{-1} to 2700 x 10^{-7} m^3kg^{-1}) while an enormous increase has been seen in southern coast of the inner Gulf of Kachchh (3100 x 10^{-7} m^3kg^{-1} to 7500 x 10^{-7} m^3kg^{-1}). Near the mouth of the Gulf of Kachchh i.e southern coast, shows anomalously lower concentration of magnetic minerals at Okha (57 x 10^{-7} m^3kg^{-1} to 70 x 10^{-7} m^3kg^{-1}).

Table 3.3: Results of mineral magnetic measurements on >63 micron fraction of intertidal sediments.

Locations	Magnetic Concentration		Magnetic Grain size		Magnetic Mineralogy		
	χ_{lf}	χ_{arm}	χ_{fd}	χ_{arm}/χ_{lf}	Soft IRM	Hard IRM	S-Ratio
	10^{-7} m^3kg^{-1}	10^{-5} Am^2kg^{-1}	%	10^3	10^{-5} Am^2kg^{-1} (10^3)	10^{-5} Am^2 kg^{-1} (10^3)	($IRM_{0.3T}$/SIRM)
a	395.23	0.10	4.78	0.26	214.15	36.16	0.90
b	65.24	1.26	5.03	3	86.47	44.40	0.57

c	92.49	0.78	3.11	1.5	143.74	15.34	0.89
d	868.52	0.61	2.46	0.71	1333.04	63.47	0.95
e	409.08	0.50	2.01	1.24	601.29	12.73	1
f	590.80	0.60	2.42	1.03	945.72	19.42	0.98
g	2383.06	1.72	2.94	0.72	1025	26	0.96
h	1085.82	0.52	2.68	0.48	915.18	31.82	0.96
i	445.39	0.11	4.07	0.26	917.31	24.20	0.97
j	475.39	0.14	2.77	0.30	1805	38.45	1
k	1790.2	0.49	3.13	0.27	2280.91	48.56	1
l	1111.11	0.36	3	0.32	1803.51	16.50	1
m	492.41	0.13	2.94	0.28	484.53	50.73	0.91
n	435.47	0.10	6.06	0.24	424.01	21.20	0.95
o	282.89	0.06	4	0.22	297.63	50.81	0.84
p	2733.72	0.56	3.56	0.20	5583.74	610.42	0.89
r	493.51	0.11	2.91	0.22	1062.81	53.29	0.95
s	359.63	0.08	2.44	0.22	1312.34	231.94	0.83
t	6740.27	2.31	3.48	0.34	5300.14	423.74	0.95

u	1785.29	0.44	3.37	0.24	2143.87	267.05	0.88
v	7684.84	1.26	2.07	0.16	10095.41	374.50	0.96
w	3129.06	0.63	3.66	0.20	5994.54	596.35	0.91
x	57.63	0.04	5.89	0.77	46.59	2.18	0.95
y	69.28	0.04	3.66	0.58	73.56	21.21	0.75

χ_{arm} values are higher in the sandy segment of northern coast of Gulf of Kachchh (0.5 x 10^{-5} Am^2kg^{-1} to 1.7 x 10^{-5} Am^2kg^{-1}), and are very low in mudflat bearing segment (0.05 x 10^{-5} Am^2kg^{-1} to 0.5 x 10^{-5} Am^2kg^{-1}). However, on the southern coast of inner Gulf of Kachchh, where it shows abrupt increase from 0.5 x 10^{-5} Am^2kg^{-1} to 2.3 x 10^{-5} Am^2kg^{-1}. At the Okha site on southern mouth of Gulf of Kachchh is again low concentration of χ_{arm} values (0.04 x 10^{-5} Am^2kg^{-1}) were noticed. χ_{fd}% for all the stations was below 5%, except the stations like Pingleshwar, Kandla and Okha, indicating negligible contribution from super-paramagnetic grains. The sites at the mouth of northern and southern coast of Gulf of Kachchh showed higher ratio of χ_{arm} / χ_{lf} indicating more stable single domain size range of magnetic grains compared to the inner Gulf of Kachchh. The S-ratio which depicts the dominant magnetic mineralogy remained >0.90 for entire coastline, but sites Pingleshwar and Khuada in northern sandy segment, and sites Chirai and Surajbari on inner gulf coast values dipped to 0.85. However the S-ratio values remained identical ~ 0.72 for the sites like Jakhau and Okha on northern and southern mouth of the gulf respectively (Figure 3.4).

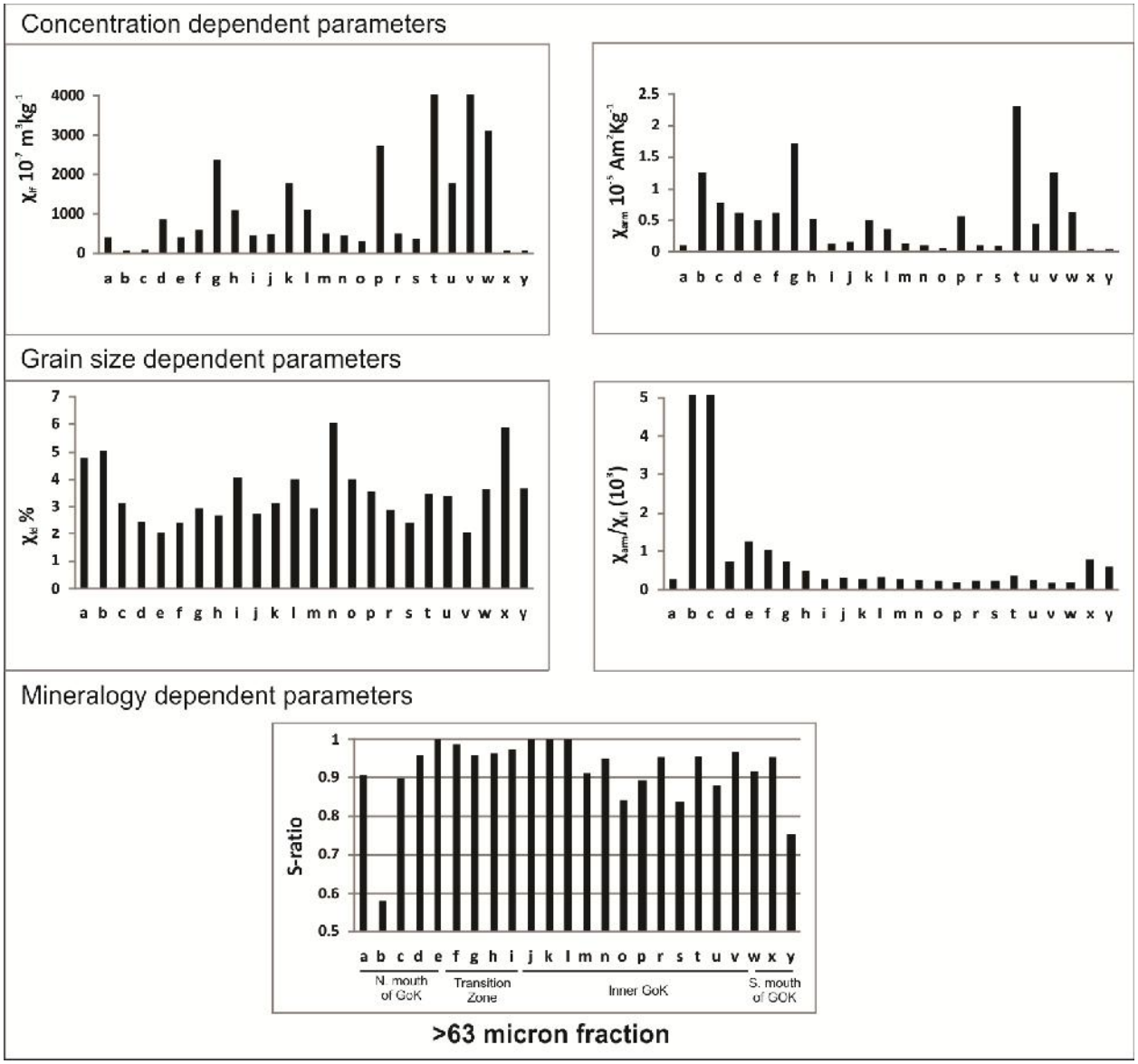

Figure 3.4: Mass specific mineral magnetic parameters from intertidal sediments of the Gulf of Kachchh coast.

Mineral magnetic analysis of <63micron fraction

The sites Pingleshwar (b), Khuada (c), Chhachhi (d), Layza Nana (e), Mandvi Palace (f), Mandvi (g) and Rawal Pir (h), hosts beaches as dominant landforms and hence had negligible amounts of <63 micron fraction which was not suitable for analysis therefore this sites are not studied for <63 micron fraction.

Table 3.4: Results of mineral magnetic measurements on <63 micron fraction of intertidal sediments.

Locations	Magnetic Concentration		Magnetic Grain size		Magnetic Mineralogy		
	χ_{lf}	χ_{arm}	χ_{fd}	χ_{arm}/χ_{lf}	Soft IRM	Hard IRM	S-Ratio
	10^{-7} m^3kg^{-1}	10^{-5} Am^2kg^{-1}	%	10^3	10^{-5} Am^2kg^{-1} (10^3)	10^{-5} Am^2 kg^{-1} (10^3)	($IRM_{0.3T}$/SIRM)
a	575.82	0.28	5.38	2.68	510.70	62.84	0.89
g	4538.69	1.96	2.92	1.43	1486	52	0.96
i	2333.63	0.70	3.29	1.20	2051.03	59.30	0.97
j	1120.69	0.28	2.64	1.00	2506.84	42.84	1
k	2339.55	0.59	3.12	1.01	2918.60	28.69	0.99
l	945.89	0.42	3.24	1.76	940.75	15.01	0.98
m	964.6	0.29	2.90	1.22	1033.58	78.12	0.92
n	1017	0.36	3.23	1.42	1006.54	95.28	0.90
o	972.26	0.34	3.09	1.41	930.00	79.45	0.92
p	968.14	0.48	3.45	1.97	835.09	10.88	0.98
r	1109.26	0.22	2.65	0.81	535.28	59.97	0.89
s	1285.37	0.28	2.78	0.89	365.13	54.30	0.86

t	2861.36	0.77	3.78	1.07	2181.81	109.95	0.95
u	3155.55	0.96	3.37	1.21	3282.53	243.05	0.93
v	4723.45	1.03	2.39	0.86	5508.89	256.29	0.96
w	2197.21	0.59	3.87	1.08	3680.42	483.98	0.90
x	438.23	0.39	3.69	3.54	364.80	47.41	0.88
y	221.35	0.12	4.13	2.28	163.03	43.37	0.78

The magnetic mineral concentration in <63 micron fraction of sediments (Table 3.4) showed enrichment of magnetic minerals in the segment between Mundra (1120 x 10^{-7} m^3kg^{-1}) and Navinal (2300 x 10^{-7} m^3kg^{-1}) whereas, it remained intermediate in the inner Gulf of Kachchh mudflats (900 x 10^{-7} m^3kg^{-1} to 1200 x 10^{-7} m^3kg^{-1}) and further shows a sharp increases along the southern coast (2100 x 10^{-7} m^3kg^{-1} to 4700 x 10^{-7} m^3kg^{-1}). At the mouth of southern coast a sharp decrease in magnetic mineral concentrations (220 x 10^{-7} m^3kg^{-1} to 430 x 10^{-7} m^3kg^{-1}) was noticed. χ_{arm} values are intermediate (0.5 to 2) and shows similar trend as magnetic susceptibility. χ_{arm} /χ_{lf} shows similar trend as in >63 micron fraction and has higher values at the mouth of northern and southern coasts, indicating more stable single domain magnetic grain size at the western end. The χ_{fd}% remains less than 5% and hence contribution from the superparamagnetic grains is believed to be negligible. S-ratio values are mostly >0.90 for all sites barring western most sites at the mouth of Gulf of Kachchh and at Surajbari (Figure 3.5).

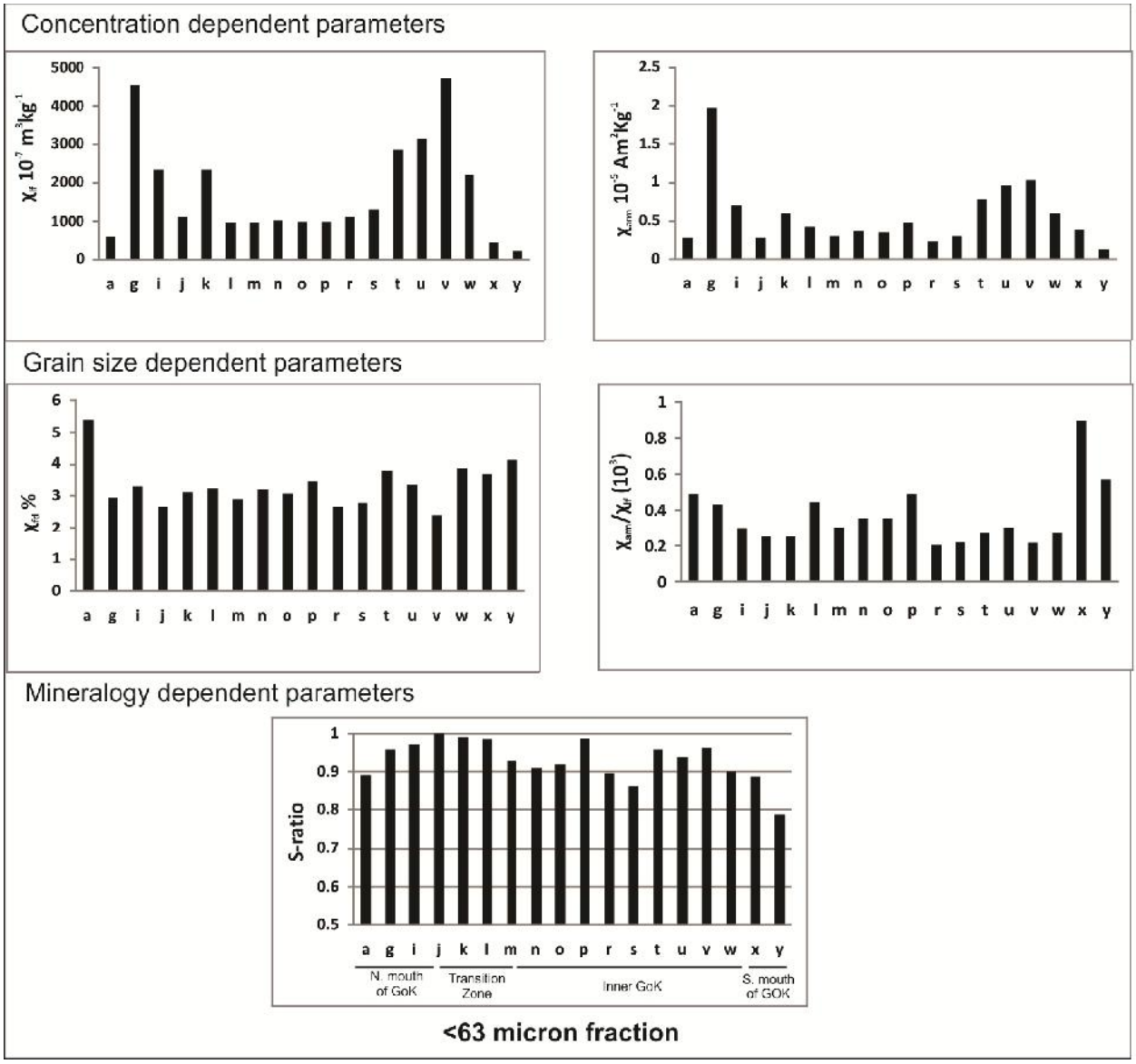

Figure 3.5: Mass specific mineral magnetic parameters from intertidal sediments of the Gulf of Kachchh coast.

Chapter 4

Clay Mineralogy and Sediment Geochemistry

4.1 Clay Mineralogy

4.1.1 Significance & Methodology

The fine grained composition and relative abundance of clay minerals are mainly controlled by the source rocks and the weathering conditions present therein. The composition of clay minerals largely depends on climate, geology and topography of the region (Singer, 1984; Chamley, 1989). The nature and composition of clay mineral provides valuable information regarding the type and intensity of weathering on land. Owing to this fact and presence of characteristically different weathering and climatic conditions in hinterland, this technique is well proven in the Arabian Sea region (Konta, 1975; Kolla et al., 1976, 1981; Chauhan, 1994; Rao and Rao, 1995; Thamban et al., 2002; Kessarkar et al., 2003; Thamban and Rao, 2005; Chanhan et al., 2006; Ramaswamy et al., 2007). Based on clay mineral distribution of the surface sediments along the western continental margin of India, Rao and Rao (1995) pointed out three different sources from north to south viz., (1) Himalayan source in the north characterized by high illite and chlorite that are mainly transported by the River Indus and its influence decreases from north to south; (2) Deccan Trap Formation source in the central region characterized by high smectite which are the erosion products of basic volcanic rocks of the Central India; (3) Gneissic province characterized by high kaolinite and gibbsite that are the weathering products

of Precambrian gneissic rocks of the southern India. Later on these results were supplemented by further clay mineral and isotopic studies (Kessarkar et al., 2003; Chauhan et al., 2006; Thamban et al., 2002; 2005).

In the present study the samples (n = 40) were first treated with 5 ml acetic acid and 10 ml hydrogen peroxide so as to make them free of carbonate and organic matter. The aliquots were then washed several times with de-ionized water to remove the excess reagents and decanted. Oriented clay slides were then prepared at the M.S. University of Baroda, Vadodara using <2 micron fraction following Stoke's law, for XRD analysis. Each specimen was run between 2° and 30° 2Θ on a Philips X-ray diffractometer using nickel-filtered Cu K alpha radiation and basic three runs were made of each specimen (1) dry run, (2) specimens were exposed to glycolation treatment (using ethylene glycol) for 24 hrs and (3) specimens were heated up to 550 °C for 1 hr and then scanned. The clay mineral identification was done using basal reflection peaks (Biscaye, 1965, Petschick et al., 1996). Relative percentages of different clay minerals like kaolinite (K), chlorite (C), illite (I) and smectite (S) were estimated by weighting the integrated peak areas of basal reflections in the glycolated X-ray diffractograms, following the semi-quantitative method of Biscaye (1965). Accordingly, the peak areas of 17 Å peak of smectite was multiplied by 1, 10 Å peak of illite by 4 and 7 Å of kaolinite and chlorite by 2. The kaolinite (3.54 Å) and chlorite (3.58 Å) peak areas were used to obtain the individual percentages. All samples were scanned from 24° to 26° 2Θ at l/2° 2Θ min^{-1} speed to differentiate kaolinite and chlorite. The reproducibility of the clay mineral analyses was estimated from X-ray diffractograms obtained independently on the prepared duplicate slides of few selected samples. The relative error associated with clay mineral quantification was within ± 5%.

4.1.2 Spatial Distribution of Clay Minerals

The clay mineralogy of the <2 micron fraction showed that the dominant mineral assemblages were illite-chlorite and smectite-kaolinite (Table 4.1). The concentration of Illite varied from 25-52%, whereas chlorite varied from 10-22%. The illite-chlorite assemblage shows a clear trend of higher concentration along northwestern coast (i.e. a to j in Fig.--) and subsequently reduces eastwards. The smectite concentration varies from 7-54%, whereas kaolinite is found in small concentrations varying from 5-25%. The smectite-kaolinite assemblage dominates along southern coast of the inner Gulf of Kachchh which hosts the mudflats. illite-chlorite are major weathering products of Himalayan rivers (in this case the Indus River) owing to predominant physical weathering in cold and arid climate (Kolla et al, 1976; Ramaswamy et al, 2007). Whereas, smectite is a major weathering product of the Deccan Trap basalts, which is mostly produced in dry and warm climates and kaolinite is a weathering product of warm and humid climate. The landmasses of Kachchh and Saurashtra experiences warm and dry climate and have the Deccan Trap basalts as major lithology in their hinterland which acts as a major source of smectite. Kaolinite is mostly derived from reworking of the Mesozoic sediments of Kachchh and Little Rann which have their primary source in the Aravallis which are known to have considerable proportion of kaolinite (Fursich et al., 2005). The author has employed the (illite + chlorite) / (smectite + kaolinite) ratio which in present study would act as a tool to decipher the sediment source provinces in the study area. The higher values of this ratio would point out dominantly the River Indus source, whereas values less than 1.0 would point out dominance of the hinterland sources (i.e. Kachchh and Saurashtra mainland).

Table 4.1 Spatial distribution of major clay minerals along the Gulf of Kachchh coast.

Locations	**Illite (%)**	**Chlorite (%)**	**Smectite (%)**	**Kaolinite (%)**
a	45.1	21	11.5	22.4
g	46.2	20.6	7.7	25.5
i	41.8	18.7	26.5	13
j	44.8	16.6	28.5	10.1
k	32.6	11	48.2	8.2
l	34.7	18.8	42	4.5
m	44.2	20.4	30.4	5
n	38	18.4	34.8	8.8
o	38.6	14.6	40.4	6.4
p	32.9	14.5	44.6	8
r	26.8	10.2	54.6	8.4
s	25.2	10.4	52.8	11.6
t	26.4	16.2	48.6	8.8
u	24.8	18.1	42.8	14.3
v	22.4	15.4	44	18.2

w	51.3	12.4	26.4	9.9
x	52.4	18.6	22.6	6.4
y	50.6	20.4	18.6	10.4

4.2 Sediment Geochemistry

4.2.1 Significance & Methodology

Chemical characteristics of marine sediments are strongly influenced by several factors namely, source area composition of adjacent landmasses, climate, length and energy of sediment transport, redox conditions in the depositional environments, etc. (Bhatia and Cook, 1986; Fralick and Kronberg, 1997). Due to the socioeconomic and environmental relevance the geochemical studies on the coastal marine systems focuses on the abundance and distribution of sedimentary components to assess local human impacts, to determine sedimentary sources and/or to understand patterns of exchange of major and trace elements at the land–sea interface (Cho et al., 1999; Kim et al., 1999; Aloupi and Angelidis, 2001; Shumilin et al., 2001). The concentration of different major and trace elements in the sediments are due to a variety of mineral assemblages present therein, energy of sediment transport processes and climate. Hence, their study would give a better understanding of the processes acting and provenance of source end members contributing to the basin (Spagnoli et al., 2008, Singh, 2010).

The sampling for this purpose was restricted to intertidal microenvironment as it is considered most active microenvironment in coastal setting for sediment transport (Pethick, 2000). Around 75 samples were collected from 25 different sites and packed in plastic bags. This samples were dried at 40 °C and 1gm of homogenized <63 micron fraction was utilized for this purpose and measured using XRF (SPECTRO XEPOS) at the Indian Institute of Geomagnetism,

Navi Mumbai. The accuracy of measurements was checked by GBW-07401 Geochemical Standard Reference Soil Sample. The duplicates of several samples showed that precision of measurement for major elements was better than 2%, while it was better than 5% for trace elements.

4.2.2 Spatial Distribution of Major and Trace Elements

The major elements Aluminum (Al), Titanium (Ti) and Iron (Fe) are considered to be indicators of detrital flux and are stable during sedimentary processes in most environments (Engstrom and Wright, 1984; Benson et al., 1996; Lisitzin, 1996; Young and Nesbitt, 1998; Juyal et al., 2009). The spatial distribution of these major elements namely Al, Fe and Ti along the entire Gulf of Kachchh coastline is shown in Table 4.2.

Table 4.2: Spatial distribution of major elements in intertidal sediments of the Gulf of Kachchh coast.

Locations	**Al_2O_3**	**Fe_2O_3**	**TiO_2**
a	16.86	7.56	1.04
b	2.94	6.38	7.65
c	3.27	4.18	5.43
d	8.41	14.83	10.93
e	8.19	15.52	12.44
f	8.86	19.73	12.14
g	11.97	12.6	3.44
h	9.60	14.01	8.55
i	6.08	2.19	0.42

j	12	6.51	1.49
k	14.78	7.40	1.05
l	13.18	5.98	0.92
m	13.41	6.69	1.08
o	13.62	6.88	1.02
p	14.42	7.97	1.04
r	11.74	5.46	1.06
s	12.03	5.89	1.16
t	14.47	8.95	1.40
u	14.16	9.24	1.59
v	12.64	9.58	0.95
w	14.42	8.63	1.12
x	15.09	7.38	0.90
y	12	5.11	0.85

The concentration of Al is highest at Jakhau (a) and reduces in northern sandy segment of Gulf of Kachchh upto the location ---- (f). It again increases and dominates in the inner gulf mudflat with values near to 15 % (i.e. from h to u). The spatial distribution of Al-concentration suggests its affinity to clay minerals (i.e. enriched in mudflats). Whereas Fe concentration is highest in sandy segment of northern coast (~19 %), it reduces eventually in the inner gulf mudflats (~5 %) and increases again along the southern coast (~12 %), indicating magnetic minerals being its major contributors. The Deccan Trap basalts present in the landmasses of Kachchh and Saurashtra are believed to be major contributors of these magnetic minerals. The Ti

concentration is highest in sandy segment of the northern coast of the Gulf of Kachchh, but is negligible in the mudflats of inner gulf and southern coast of the Gulf of Kachchh, indicating its source could mostly be the Kachchh mainland fluvial system.

The concentrations of Rb and ratios of Rb/Ga have been used by several workers previously to elucidate the provenance in the Arabian Sea, as Rb concentrations are higher in the potassium-rich illite-dominated sediments of the Indus River compared to the smectite-rich Deccan Trap material (Ramaswamy et al., 2007). Staubwasser and Sirocko, (2001) have also used Rb/Ga as an indicator for Indus derived sediments. Table 4.3 shows values of Rb/Ga in intertidal sediments of the Gulf of Kachchh coast and some previously published values from offshore suspended sediments. The western part of Kachchh coast shows similar values as reported by Ahmad et al. (1998) from river bed sediments of the River Indus. The northern sandy coast of Gulf of Kachchh shows very low Rb values and low Rb/Ga ratio indicating their source being Kachchh mainland fluvial systems, which contains fewer concentrations of Rb and Rb/Ga. The inner Gulf of Kachchh mudflats show enrichment in Rb and Rb/Ga values (128, 6.28), which is even more enriched in mouth of southern coast of Gulf of Kachchh (148, 7.14). This is again supplementary to fact that River Indus is a major end-member contributing to this coastline in suspended sediment fraction.

Table 4.3: Average elemental concentrations of Rb and Rb/Ga along major segments of Gulf of Kachchh coast and previous works.

Location	**Rb (ppm)**	**Rb/Ga**	**Reference**
Western part of Kachchh coast (Proximal to River Indus) (n = 2)	140	6.87	This study
Northern sandy segment (n = 7)	31	2.17	This study

Mudflats of central and inner GoK (n = 14)	128	6.28	This study
Mouth of southern coast of GoK (n = 2)	148	7.14	This study
Western Gulf of Kachchh (near the mouth) (n = 13)	130	7.15	Ramaswamy *et al.* 2007
Central Gulf of Kachchh (n = 6)	115	6.74	Ramaswamy *et al.* 2007
Eastern Gulf of Kachchh (near head) (n = 6)	57	6.52	Ramaswamy *et al.* 2007
Indus River sediments (n = 9)	137	9.15	Ahmad *et al.* 1998

Chapter 5

Sediment Dispersal System

5.1 General

As evidenced by grain size studies, mineral magnetic studies, clay mineral studies and sediment geochemistry of coastal sediments, the hinterland ~ the Kachchh mainland and Saurashtra peninsula, is an important and significant contributor of >63 micron fraction of sediment load to the coastal sediment dispersal system. Hence, the author studied the fluvial systems draining from these landmasses to document the sediment contribution from these end-members. Several ephemeral coastal rivers like Kankawati, Rukmavati, Nagwati, Bhukhi, Aji, Macchu, Demi and Adhoi drain from Kachchh mainland and Saurashtra into the Gulf of Kachchh (Figure 5.1).

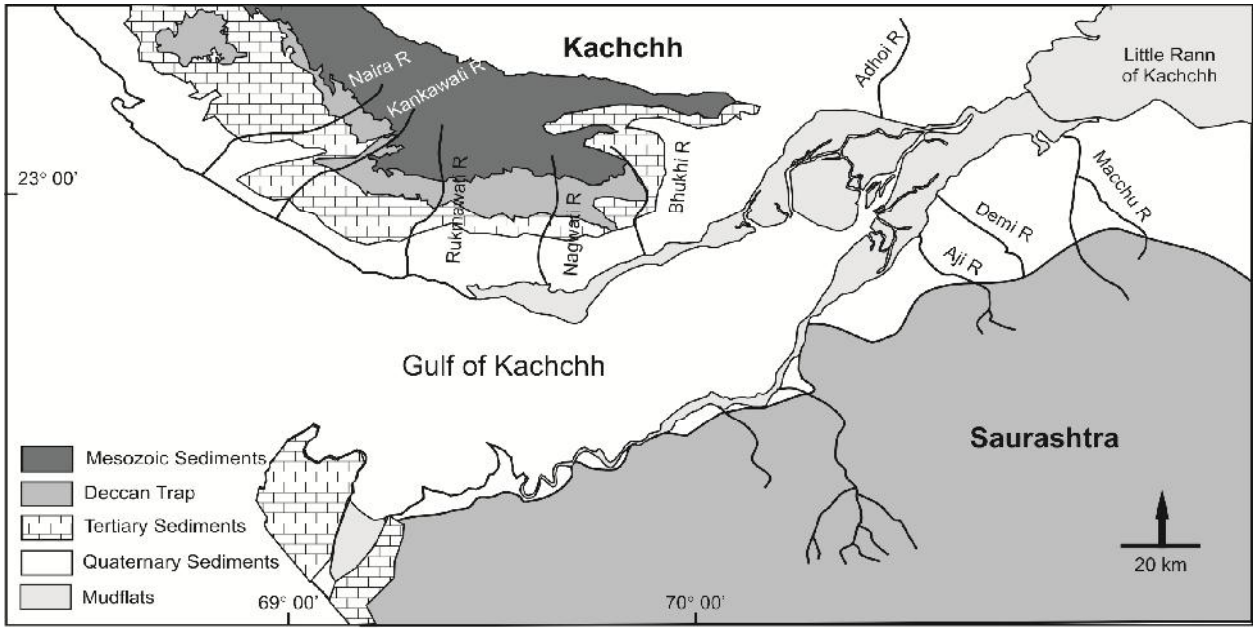

Figure 5.1: Hinterland coastal rivers draining into the Gulf of Kachchh.

The fluvial systems of Kachchh mainland mostly originate from the Mesozoic rocks comprising sandstones and shale outcropping at Katrol hill range forming geomorphic highs. The Deccan Trap basalts cover a large part of the pediment zone and have the Tertiary rocks constituted by limestone, shale and sandstone fringing the hill ranges. The Quaternary deposits constitute the coastal alluvial plains which are the reworked sediments derived from the uplands. Similarly the coastal fluvial systems of Saurashtra peninsula rise from the Barda hills composed of basalt, granophyre, trachyte and similar rocks belonging to the Deccan Trap Formation and traverse predominantly through the basalt and laterites Tertiary limestones and clay beds are present near the coastline where these fluvial systems debouch into the Gulf of Kachchh. The geological setup of Kachchh basin is well documented (Biswas, 1987, 1993); however there is a lack of literature regarding the detailed mineralogical studies of these sediments (Dubey and Chatterjee, 1997; Mishra and Tiwari, 2005). Mineralogical studies in the Gulf of Kachchh have been restricted to suspended sediment samples collected from the offshore and hence, interpretations drawn out of it symbolize only the provenance of suspended load brought from the Indus source (Chauhan et al., 2006; Ramaswamy et al., 2007). The textural and compositional characteristics of the sediments being delivered by the coastal streams in to the Gulf of Kachchh needs to be ascertain using all proxies studied for the coastal sediments to better unravel the input mechanism and strength of the aforesaid sources. Therefore, a special study was done on one of the very prominent coastal river basin in the Kachchh that drains through all possible lithological variants that constitute the hinterland areas of Kachchh and Saurashtra. This is the Rukmawati river basin whose sediment dispersion is described in the following section.

5.2 Rukmawati River basin

The author selected Rukmawati River basin for detailed sediment dispersal study as it is one of the major rivers of Kachchh district, western India. It is an ephemeral river originating from the Katrol hill range and debouching into the Gulf of Kachchh. The major strike of the geological formations in Kachchh mainland is east-west and the direction of flow of this river is from north to south hence, it drains through all these geological units. The uplands of the river has sedimentary rock outcrops in its catchment mostly comprising of sandstones and shales of Juran and Bhuj Formations of Jurassic-Cretaceous age (Biswas, 1987; 1993). The middle reaches of the river is composed of basalts of the Deccan Trap Formation of Late Cretaceous age overlain by the Tertiary outcrops comprising of friable sandstones and shales belonging to the Kankawati Series (Biswas, 1987; 1993). The lower reaches hold the Quaternary record which occurs in the form of Miliolite Formation (friable grainstone with allochems) and coastal alluvium. Rukmawati river exhibits first order topography in its upland regions, but shows remarkably deeply incised channel and entrenched meanders in its middle and lower reaches.

Ten locations were sampled within Rukmawati River basin (Figure 5.2), from wherein three samples were collected from each location and were packed in air tight plastic bags (total 30 samples from the entire catchment representing all major geological formations). Also two additional locations toward east off the mouth of Rukmawati River were sampled (n = 6) from the intertidal zone, to study the transport of sediments derived from Rukmawati basin by the longshore currents. Figure 5.2 shows major geological formations, physiographic divisions and major sampling sites (i.e. R1, R2,..., RP, NN) along the Rukmawati River. Sampling was restricted to channel bed only, as in a dryland regime it is susceptible to rapid transportation of large amount of sediments downstream during flash flood events.

Grain size analysis was carried out using mechanical sieving following standard procedure (Folk, 1974), and different statistical parameters calculated at the M.S. University of Baroda (Vadodara). Different size fractions were separated from the bulk samples for further analysis, viz, very coarse sand (>1.0 mm), coarse sand (1.0-0.5 mm), medium sand (0.5-0.25 mm), fine-very fine sand (0.25-0.063 mm) and silt + clay (<0.063 mm).

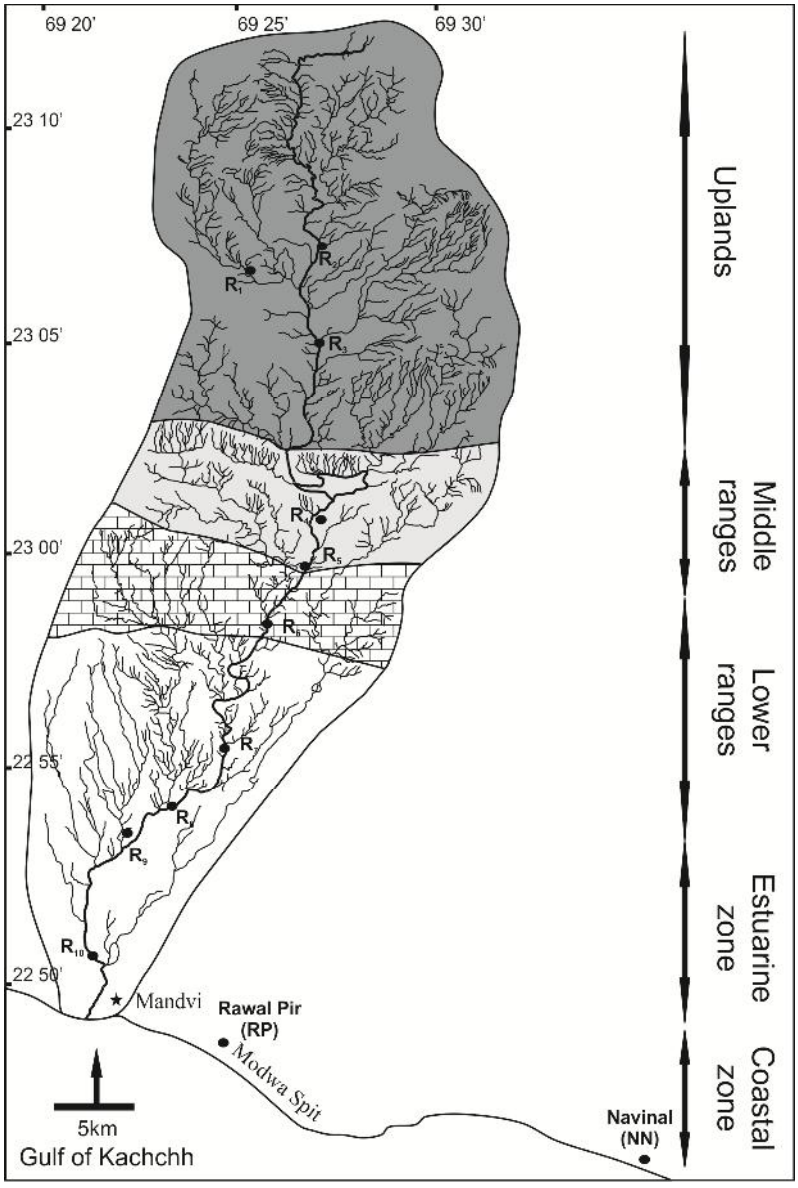

Figure 5.2: Geological map of Rukmawati River basin showing sampling sites and major physiographic divisions.

5.2.1 Granulometric Analysis

The granulometric analysis and different computed statistical parameters are shown in Table 5.1**.** The grain size distribution shows considerable downstream-ward fining of sediments as fine-very fine sand and medium sand size becomes dominant in lower reaches (i.e. R6, R8, R10) compared to coarse and very coarse sediments dominant in upper reaches (i.e. R1, R2, R3). Increase in coarse sediments is also observed at R7 and R9 due to a presence of incised cliffs of unconsolidated sediments which on account of erosion gives rise to a large amount of coarse grained sediments. The locations RP and NN along the coast show an absence of very coarse sand and an overwhelming dominance of fine-very fine sand. However, the concentration of <63 μ fraction (silt + clay) could not be observed at RP and NN because, both these locations are sandy landform dominating coast.

Table 5.1: Granulometric analysis and statistical parameters for Rukmawati river basin.

Location	**Concentration**					**Statistical parameters**			
	Very Coarse sand	**Coarse sand**	**Medium sand**	**Fine sand**	**Silt + Clay**	**Mean**	**Standard Deviation**	**Skewness**	**Kurtosis**
R1	21.04	33.01	19.74	23.92	2.28	0.17	1.43	0.29	0.93
R2	8.35	13.13	45.58	30.83	2.1	0.63	1.04	-0.03	1.37
R3	0.01	63.28	35.84	0.02	0.01	-0.14	0.52	0.23	0.98
R4	32.14	20.27	11.02	25.05	11.53	0.3	1.86	0.35	0.72
R5	10.9	10.9	45	21.93	11.26	0.75	1.42	0.16	1.66
R6	3.34	11.52	22.92	53.53	8.69	1.23	1.2	-0.05	1.28

R7	27.8	36.45	6.83	23.69	5.22	-0.94	1.78	0.53	0.92
R8	22.84	9.48	13.39	46.69	7.59	0.77	1.74	-0.26	0.71
R9	18.13	51.08	22.58	7.36	0.84	-0.31	0.86	0.16	1.24
R10	7.61	9.13	28.7	49.13	5.43	1.06	1.2	-0.11	1.3
RP	0.02	21.1	17.5	59.0	2.1	1.89	0.91	-0.27	0.66
NN	0	0.09	5.71	93.8	0.39	2.47	0.46	-0.03	1.43

5.2.2 Mineral Magnetic Measurements

Mineral magnetic measurements were carried out on sub-fraction of all 36 samples (n=144). The sub-fractions were of coarse sand (C), medium sand (M), fine-very fine sand (F) and silt + clay (SC). The very coarse fraction was avoided as it contained lithoclats and were not suitable for mineral magnetic studies. The magnetic concentration dependant parameters of χ, χ_{arm} and SIRM depict that R4 and R5 middle stations contain the higher concentration of magnetic minerals with χ values ranging up to 140 x 10^{-7} m^3kg^{-1} (Figure 5.3). The magnetic mineral concentration decreases further in lower reaches as χ ranges up to 20 x 10^{-7} m^3kg^{-1} and then shows enhanced χ values of about 80 x $10^{-7}m^3kg^{-1}$ in estuarine and coastal zones. SIRM shows an identical trend. Similarly χ_{arm} is highest at middle stations R4 and R5 with values of 3.5 x $10^{-5}m^3kg^{-1}$ and again peaks at estuarine zone with values of 2.0 x $10^{-5}m^3kg^{-1}$ at station R10 but, drops again to about 0.5 x $10^{-5}m^3kg^{-1}$ at coastal zone stations RP and NN. The dominant magnetic signal carriers were in fine-very fine sand and <63 μ fraction (silt + clay). The magnetic mineralogical parameters like Soft IRM, Hard IRM and S-ratio showed that ferrimagnetic mineral phases dominated most of the catchment in all size fractions.

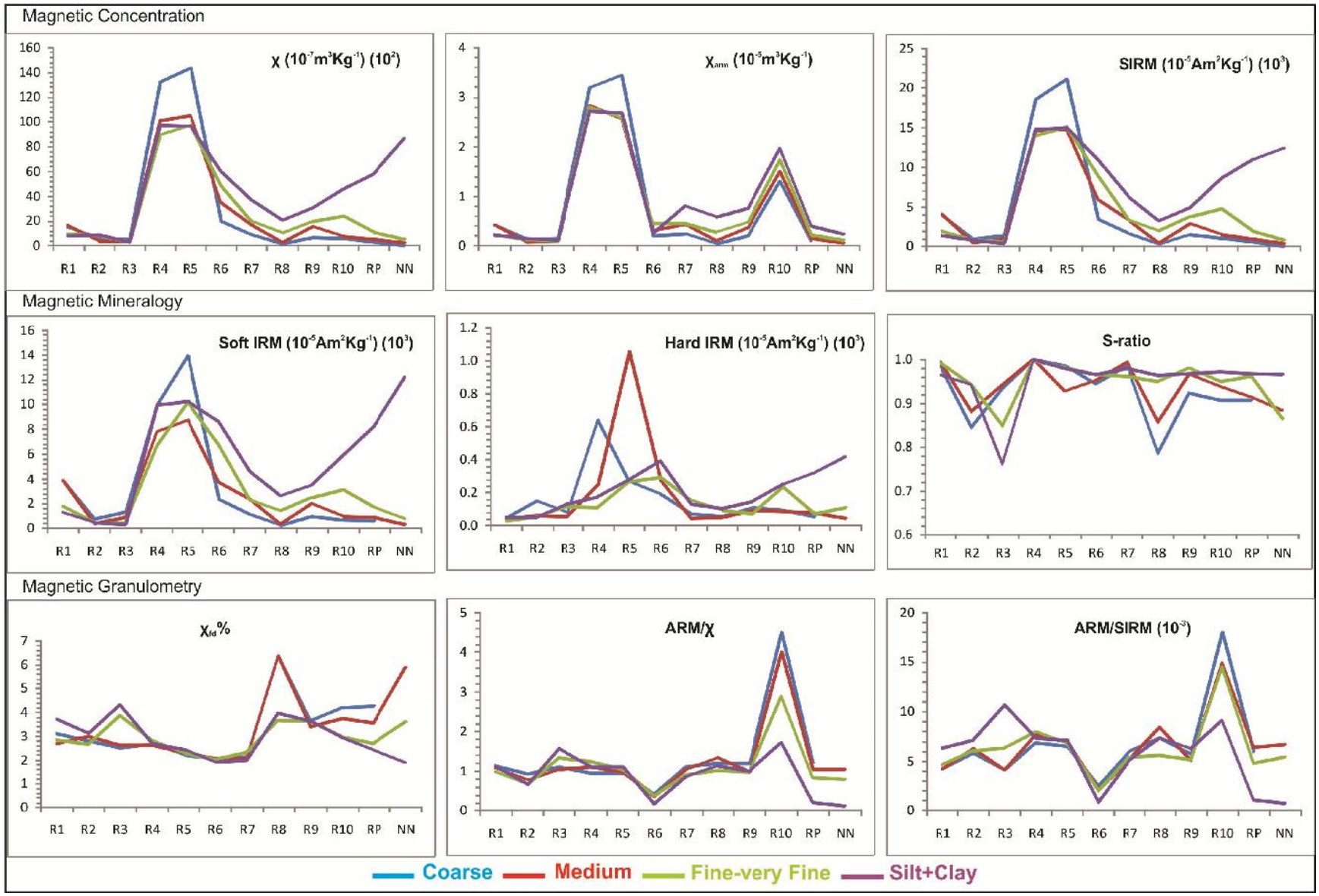
Magnetic Concentration
χ (10⁻⁷m³Kg⁻¹) (10²)
χarm (10⁻⁵m³Kg⁻¹)
SIRM (10⁻⁵Am²Kg⁻¹) (10³)
Magnetic Mineralogy
Soft IRM (10⁻⁵Am²Kg⁻¹) (10³)
Hard IRM (10⁻⁵Am²Kg⁻¹) (10³)
S-ratio
Magnetic Granulometry
χfd%
ARM/χ
ARM/SIRM (10⁻³)
R1 R2 R3 R4 R5 R6 R7 R8 R9 R10 RP NN
Coarse
Medium
Fine-very Fine
Silt+Clay

Figure 5.3: Mass specific mineral magnetic parameters surface samples of the Rukmawati River basin illustrating magnetic concentration, granulometry and composition.

The uplands are characterised by both, ferrimagnetic as well as anti-ferromagnetic mineral assemblages (Figure 5.3). The coarse and medium size fractions were carrying hard coercivity mineral phases in lower reaches. The coarse and medium size fractions were carrying hard coercivity mineral phases in lower reaches. The S-ratio mostly being >0.95 in middle, lower, estuarine reaches and coastal zone, can be attributed to reflect the presence of Ti-rich magnetite as dominant mineral assemblage. Figure 5.4 shows plot of DC demagnetization for <63 μ fraction, where it is clear that uplands (U) have hard coercivity mineral assemblage (values greater than 40 mT), whereas rest of zones have dominantly soft coercivity mineral assemblage (values less than 30 mT). The magnetic granulometry as indicated by χ_{fd}%, ARM/SIRM and ARM/χ shows that the magnetic minerals are dominantly of multidomain (MD) size range with stable single domain (SSD) size range only in the estuarine zone and in finer fraction in uplands (i.e. R3).

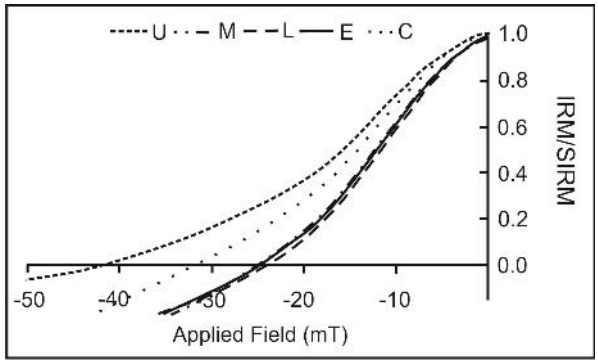

Figure 5.4: plot of DC demagnetization for <63 μ fraction. Note the value of U-uplands >40 mT.

5.2.3 Heavy Mineral Analysis

The heavy mineral analysis was carried out on the medium and fine-very fine sand size fraction, where the heavy mineral concentration ranges from 3% to 39% (Table 5.2). The upland region was characterized by intermediate amount of heavy minerals, namely garnet, tourmaline, staurolite, zircon and opaques which are mostly magnetic minerals. The middle reaches hosted the basaltic rocks and yielded the highest concentration of heavy minerals (i.e. 39%), which were dominantly opaques followed by diopside. The garnet, tourmaline, staurolite, etc. were also present in negligible amount. The lower reaches had intermediate amount of heavy minerals with dominance of opaques followed by diopside, garnet, tourmaline, staurolite and zircon. The estuarine region R10 and R9 shows increase in heavy mineral amount with dominance of opaques followed by diopside, muscovite, biotite, zircon and staurolite. Whereas the coastal zone has higher concentration of opaques (i.e. magnetic minerals) followed by diopside and mica minerals (muscovite and biotite), trace amounts of tourmaline can be noticed at RP.

Table 5.2: Results of Heavy mineral analysis in medium and fine grain sand fraction. HMC-heavy mineral concentration, G-garnet, T-tourmaline, St-staurolite, Z-zircon, D-diopside, B-biotite, M-muscovite and Op-opaques.

Location	HMC		Heavy Mineral Type							
	Mean	± SD	G	T	St	Z	D	B	M	Op
R1	14	6	20	18	16	10	0	0	0	36
R2	9.2	3.15	22	16	15	12	0	0	0	35
R3	3.2	3.5	21	17	14	9	0	0	0	39
R4	9	4.1	2	1	1	1	15	0	0	80

R5	39.1	2.2	1	1	1	2	10	0	0	85
R6	23.8	5.4	4	2	3	3	18	0	0	70
R7	7.5	3.8	2	3	3	2	22	0	0	68
R8	9	4	1	1	2	1	33	0	0	62
R9	8	6.6	0	0	1	1	29	9	8	52
R10	14	5.7	0	0	0	2	26	8	12	52
RP	16	4	0	2	0	0	21	10	9	58
NN	5	2.5	0	0	0	0	6	6	8	80

5.2.4 Clay Mineralogy

The clay mineral analysis was performed on 12 samples from each site following the method described in chapter 4. The results obtained show that the uplands have the characteristic presence of kaolinite, smectite and little amount of illite (Table 5.3). The middle reaches showed pronounce presence of smectite and kaolinite, the dominance of which masked other clay minerals. The lower reaches on the other end had presence of kaolinite, smectite and illite. Whereas the estuarine region shows the presence of characteristic clay minerals viz, illite, chlorite, kaolinite and smectite, where illite and chlorite are dominant clay minerals. We have used the S/K and I+Ch/S+K ratios to illustrate and better understand the provenance shifts within Rukmawati river basin. The low values of S/K ratio in uplands ranging from 0.26 to 0.49, followed by high values in the middle reaches peaking up to 4.92 are indicative of source shift

(i.e. change in provenance). The I+Ch/S+K values are used to illustrate the characteristic River Indus influence in the estuarine zone and coastal zone with values ranging from 1.8 to 4.5.

Table 5.3: Major clay mineral assemblages and their ratios. S-smectite, K-kaolinite, Ch-chlorite, I-illite.

Locations	**Smectite (%)**	**Illite (%)**	**Chlorite (%)**	**Kaolinite (%)**	**S/K**	**I+Ch/S+K**
R1	28.5	0	0	71.3	0.40	-
R2	25.2	2.1	0	72.6	0.35	-
R3	20.1	4.1	0	75.9	0.26	-
R4	83.12	0	0	16.88	4.92	-
R5	74.87	0	0	25.13	2.98	-
R6	51.7	4.5	0	43.7	1.18	-
R7	49.1	8.2	0	42.5	1.16	-
R8	48.4	12.5	0	38.9	1.24	-
R9	23.2	39.2	25.4	12.2	1.90	1.82
R10	15.6	40.4	36	8	1.95	3.24
RP	13.4	37.5	42	7.1	1.89	3.88
NN	12	40	42	6	2	4.56

5.2.5 Geochemistry

Selective samples were studied for major element concentrations viz., Mg, Ti, Fe and Al (Table 5.4). The concentration of Al is highest at uplands of about 17.1% and it is reduced consistently downstream with minimum value of 9.17% at the coastal zone. Whereas, the Fe shows highest concentration at middle reaches of about 13.94%, it remains as low as 8.9% in uplands and 9.05% in lower reaches (i.e. downstream) but, eventually it increases in estuarine zone and coastal zone to about 12.6%. However, Ti remained nearly constant in entire main channel to about 1.5%, then peaks to 3.4% in estuarine zone and 6.7% in coastal zone. Mg on the other shows a similar trend like Fe with peak values in middle reaches (5.5%), lower values up to 2.8% in uplands (2.4%) and lower reaches, and again higher values (4.0-4.5%) in estuarine and coastal zones.

Table 5.4: Concentration of major elements in the Rukmawati River basin and its adjoining coastal zone.

Major Domains	Mg (%)	Ti (%)	Fe (%)	Al (%)
Uplands	2.456	1.612	8.969	17.1
Middle Reaches	5.512	1.68	13.94	13.89
Lower Reaches	2.806	1.578	9.05	10.87
Estuarine zone	4.089	3.447	12.6	11.97
Coastal zone	4.55	6.781	12.225	9.174

5.2.6 Nature of Sediment Contribution from Rukmawati river

Downstream fining is a common process observed in worldwide basins (Amos et al., 2004; Radoane et al., 2007; Frings, 2008). However due to lateral addition of different new sediment sources in the pathway of the fluvial system, it is not always the case. Our study also shows downstream fining of sediments, but few locations have coarser sediments due to incised unconsolidated cliffs in the lower reaches, which tend to get easily eroded during flashy discharge (in turn acting as sources of sediments)**.** Medium and fine-grain size sediment class is dominant class throughout the basin. Studies have shown that during peak discharges in dryland regimes, the medium-fine grain sand, which typically is transported as bedload, is carried as suspension load (Amos et al 2004). Silt + Clay (<63 μ) fraction is highest at R4 and R5, indicating highly weathered form of Deccan Trap basalt which is yielding high amount of fine sediments as well as coarse lithoclasts. The grain size distribution of the coastal zone, which shows that the fine sand and medium sand size class is dominant size class and due to the longshore currents it gets entrained and has longer residence time before it moves eastwards along the coast.

Similarly magnetic mineral concentrations are comparatively low in the uplands, whereas there is an immediate increase at the Deccan basalt middle reaches. It gets reduced downstream in the lower reaches, and gets enriched again in the estuarine and coastal zones. As the Deccan basalts are one of the major sources of magnetic minerals (Basavaiah and Khadkikar, 2004), the middle reaches are testimony to this fact. The increase in magnetic mineral concentration in the estuarine and coastal zones is due to enrichment of magnetic minerals carried along the coast by longshore currents delivered by Kankawati and Kharod Rivers located west of Rukmawati River (Figure 5.1). The enhanced distribution of magnetic minerals in all size fractions in Deccan Trap

region is indicative of its being source of magnetic minerals in all size ranges. Magnetic mineral granulometry observed suggests that coarser MD grain size is dominant in the entire catchment and the finer SSD size range is present only in estuarine and coastal zones and to some extent in uplands (i.e. R3). Superparamagnetic grains are not considerably contributing to the magnetic component of entire catchment as χ_{fd}% is <5% throughout the catchment.

The magnetic mineralogy of uplands is characterized by both, soft as well as hard magnetic components as evidenced by S-ratio between 0.76 and 0.99 and coercivity plot (Figure 5.3 & 5.4). In the middle reaches, the Deccan basalts are overwhelmingly contributing to the soft (i.e. ferrimagnetic) components in all size ranges. Downstream locations also show dominance of soft (i.e. ferrimagnetic) components, but at location R8 coarse and medium sand fraction shows presence of hard (anti-ferromagnetic) components also, which must have been derived from the uplands. The estuarine zone (R9 and R10) is characteristic and important 'sub-sink' in the transit of sediments, showing presence of ferrimagnetic component in magnetic minerals having its source in both the hinterland Deccan basalts and through longshore currents redistributing the sediments delivered from Kankawati and Kharod River mouths (Figure 5.1). These could also be observed at coastal zone locations of RP and NN, where mixture of ferrimagnetic as well as anti-ferromagnetic mineral fluxes is present. In all locations ferrimagnetic mineral assemblages are found to dominate the magnetic mineral assemblages, which again confirm the Deccan basalt being the major source of magnetic minerals in the region.

Provenance characterization and discrimination in sand fraction has been evaluated using several methods, of which heavy mineral analysis is considered to be a robust method and strong indicator of sediment source (Garzanti et al., 2005; Yang et al., 2009). The upland region, which hosts Mesozoic sedimentary sequence of sandstone and shale, shows strong signature of medium

grade metamorphic and acid/basic igneous source, with minerals like garnet, tourmaline, staurolite, zircon and opaque's (i.e. magnetic minerals etc). Here it is considered to be originally derived from the Nagarparker hills in the north (mostly bearing granite-syenite suite) and the Aravallis in the east (consisting of low-medium grade metamorphic), which were sources to these sedimentary sequences. Other studies (e.g. Mishra and Tiwari, 2005; Fursich et al., 2005) in Kachchh mainland and island belt regions have also pointed out similar interpretations employing different methods like paleoecological, stable isotopic studies and clay mineralogy. The middle region of the basin, which is covered by the Deccan basalt has highest concentration of heavy minerals in channel sediments and shows dominance of opaques (namely magnetic minerals), followed by diopside and minor amount of garnet, tourmaline, staurolite and zircon. As evidenced by mineral magnetic parameters, the Deccan Trap Formation is rich source of ferrimagnetic minerals (e.g. magnetite), which is also seen in terms of heavy minerals. Due to the profound dominance of opaques, the concentration of other minerals being derived from uplands is suppressed. Second in dominance of diopside is derived from highly weathered Deccan basalts. It is found to get enriched in downstream course. In the lower reaches, the heavy minerals show dominance of opaques followed by Deccan basalt derivatives and minor amount of upland reworked sedimentary mineral assemblages. The estuarine region shows characteristic muscovite and biotite, which are fed by longshore currents and redistributed inlands by estuarine currents, as they are not found in any of hinterland rocks, but occur in large amount in River Indus load (Prizomwala et al., 2012). The presence of zircon and minor amount of staurolite can be attributed to hinterland input from uplands and/or redistributed by estuarine currents brought from longshore currents off the mouth of the River Indus, which drains through high–medium grade metamorphic and granitic-gneissic sources.

Clay mineralogy is an established proxy in the Arabian Sea along the western margin of India due to characteristic different lithology found in the hinterland (Kolla et al., 1981; Chauhan, 1994; Rao and Rao, 1995). The upland region with dominance of kaolinite was indicative of its primary source of metamorphics to those sediments, which is supportive to interpretations drawn out of heavy mineral analysis. The low values on S/K ratio are supplementary to this fact. Thamban et al., (2002) reported presence of high kaolinite in sediments offshore of southern India which were derived from hinterland of gneissic geology. The dominance of smectite distribution in middle reaches was due to its Deccan basalt origin, which was characterized by high S/K ratio (>2.5). Deccan Trap being source and predominant contributor of smectite group of minerals is also evidenced by S/K ratio being >2.5 at middle reaches and >1.0 for rest of its transit downstream. However, the estuarine region shows increased amounts of illite (40%) and chlorite (36%), which are characteristically derived from the River Indus (see Kolla et al., 1981; Thamban et al., 2002; Chauhan et al., 2006). These are characteristic clay minerals derived due to physical and mechanical weathering in the cold and arid climate. The major catchment of River Indus is being the Himalayas, its sediments are rich in these type of clay minerals (Kolla et al., 1981; Thamban et al., 2002; Chauhan et al., 2006).

The concentration of different major elements in the sediments is due to the variety of mineral assemblages. Hence, the geochemical analysis of selective major elements provides supplementary information to the heavy mineral, mineral magnetic and clay mineralogical analysis. Figure 5.5 shows the variation of selective major elements in the catchment major domains. Bivariant plot shows a strong correlation between Mg and Fe indicating that these could be carried by the same mineral phase.

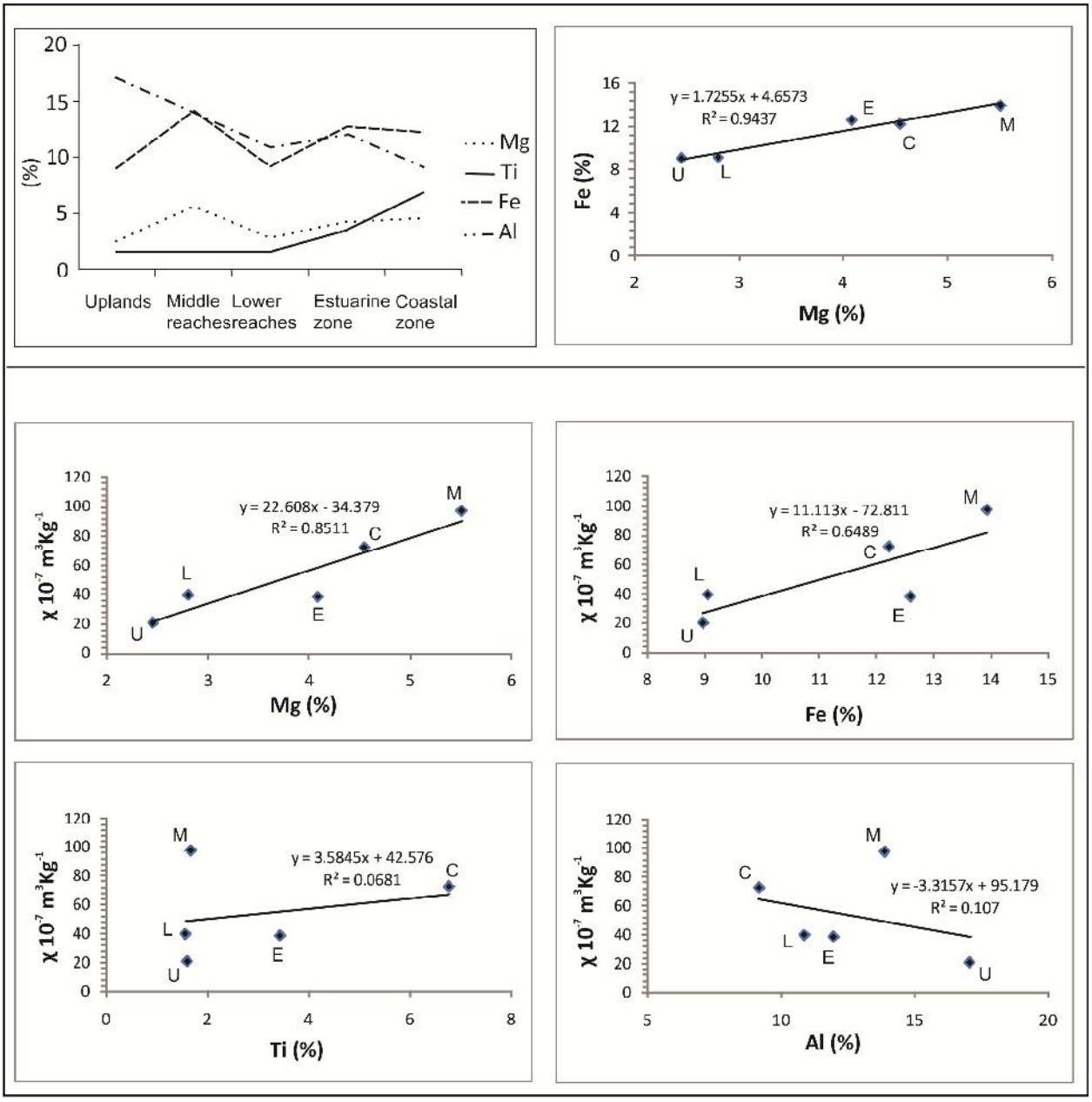

Figure 5.5: Variations in major elements along the Rukmawati River basin and their correlation with magnetic susceptibility (χ).

Figure 5.5 shows a good correlation between Mg vs χ and Fe vs χ, indicating that these could be carried predominantly by the magnetic mineral phases. The increase in Ti in the estuarine and coastal zone with S-ratio values peaking 0.95 is indicative of Ti-rich magnetite as dominant magnetic mineral assemblage. Whereas the increase in Al in uplands can be

manifestation of dominance of kaolinite ($Al_2Si_2O_5(OH)_4$) in clay mineralogy, subsequently dominance of illite and chlorite in estuarine and coastal zones, with magnetic minerals, seems major controlling factor for increase in concentration of Fe and Mg in <63 μ fraction. The weak correlation values for Ti and Al with χ is indicative of these are not being present in dominance in magnetic minerals throughout the basin.

Employing various modern as well as conventional techniques like, environmental magnetism, heavy mineral analysis, clay mineralogy and major elemental analysis of provenance discrimination, the author has documented various catchment scale sources and their discriminating signatures form Rukmawati River basin. The study demonstrates the role of lithology, climatic regimes and relief changes in effecting provenance signatures in a dryland fluvial regime. The study also serves as primary database of sediments being derived from one end member (i.e. Kachchh mainland), which gets mixed with River Indus sources derived sediments along the Partial sink (i.e. Gulf of Kachchh in this case) and being ultimately delivered off the continental shelf off the mouth of Gulf of Kachchh into the Arabian Sea (i.e. sink). Following are brief concluding points to be noted,

1. It is showed that how different regimes/lithologies control the concentration and type of sediment delivery from a catchment bearing different signatures in different modes of sediment transport.
2. The 'uplands' and 'Deccan basalts' are two characteristically different sources of sediments within the Rukmawati River basin well discriminated by several parameters like χ and S/K ratios.

3. The estuarine zone which is a sub-sink within the Rukmawati River basin, typically shows mixing of landward and offshore distributed sediments, which are getting transported eastwards into the inner Gulf of Kachchh through longshore currents as depicted by trends of χ and S/K ratio.

5.3 Coastal Sediment Dispersal System

Integrating the present understanding of the current dynamics (Nair et al., 1982; Chauhan, 1994; Kunte et al., 2003; Chauhan et al., 2006; Prizomwala et al., 2012) the sediments should enter the gulf mouth from northwestern part and travelling along the Gulf of Kachchh coastline they should exit from southwestern part. In this scenario the concentration of River Indus provenance (within sand and heavy mineral content) should be highest at northwestern end (proximal to River Indus) and should subsequently reduce along the rest of the pathway. On the other hand, the clay fraction should show predominant signatures of River Indus provenance along the entire route owing to the magnitude of sediment flux being released from the River Indus. However in contrast our results on grain size analysis, heavy mineral analysis, clay mineralogy, mineral magnetic studies (on both size fractions) and geochemistry of intertidal sediments do not reflect this, but showed three major provenance signatures along the GoK coastline (Figure 5.6). Three major end-members which have been identified are (a) River Indus, (b) Kachchh mainland and (c) Saurashtra peninsula, which exhibit distinct clay mineral, geochemical and magnetic properties.

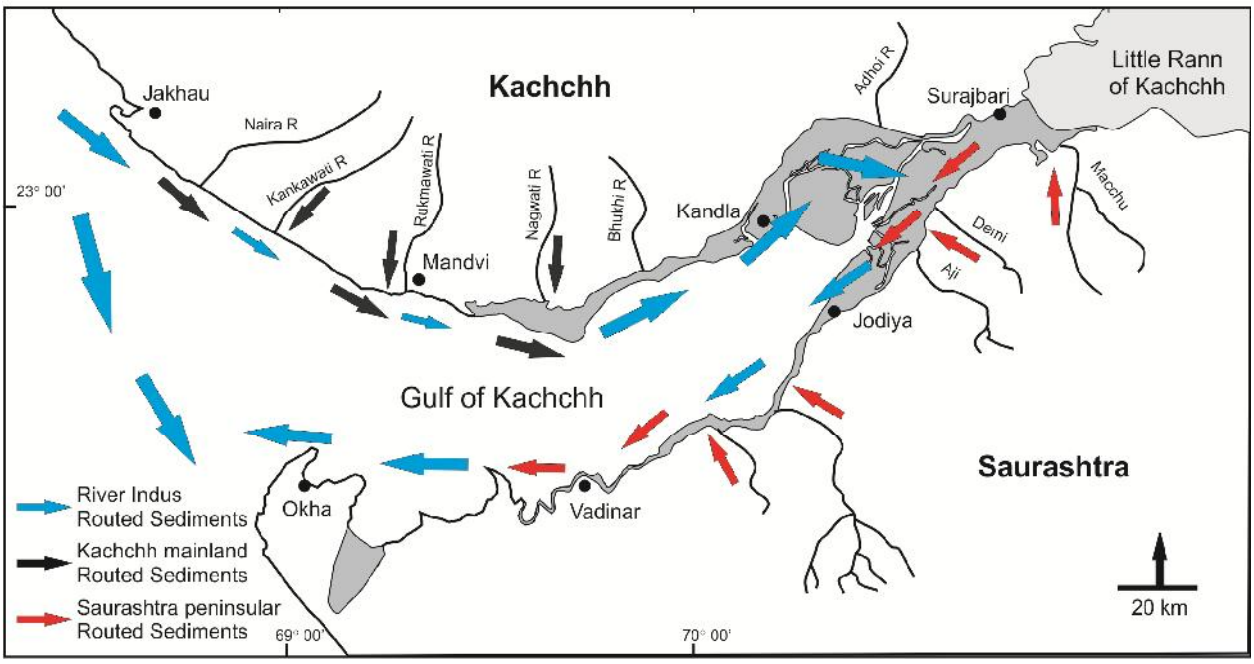

Figure 5.6: Schematic diagram of sediment dispersal system along the Gulf of Kachchh coast.

(a) River Indus provenance

The River Indus is major contributor of < 63 micron fraction, transported in suspension as evidenced by clay mineralogy (dominant illite-chlorite assemblage), Al (Figure 5.7) and Rb concentration and Rb/Ga ratio. The suspended sediments advecting from River Indus enter the Gulf of Kachchh along the mouth of northern coast and travels all along the northern coast via long-shore currents (Kunte et al., 2003; Prizomwala et al., 2012). As it reaches central Gulf of Kachchh the currents are deflected towards northeastern direction and it travels all along mudflats of the inner Gulf of Kachchh, where most of the suspended sediments are deposited. In other words the residence time of suspended sediments in Gulf of Kachchh is more in the mudflats of inner Gulf of Kachchh, which is also evidenced by clear water patch (low suspended sediment concentration) reported by Ramaswamy et al. (2007) along the southern coast of Gulf of Kachchh. The currents then get reversed at the head of inner Gulf of Kachchh and continue to

travel along the southern coast of Gulf of Kachchh (Kunte et al., 2003; Prizomwala et al., 2012). The suspended sediment concentration near the southern coast of Gulf of Kachchh is fairly less compared to the suspended sediment concentration along central and northern coast (Ramaswamy et al., 2007). Some part of River Indus borne suspended sediments also travel directly southwards and it can be evidenced by I+Ch / S+K ratio being >2 at mouth of southern coast of Gulf of Kachchh in clay mineralogy (Figure 5.8), enrichment in Rb and Rb/Ga ratio in geochemistry (Table 5.5).

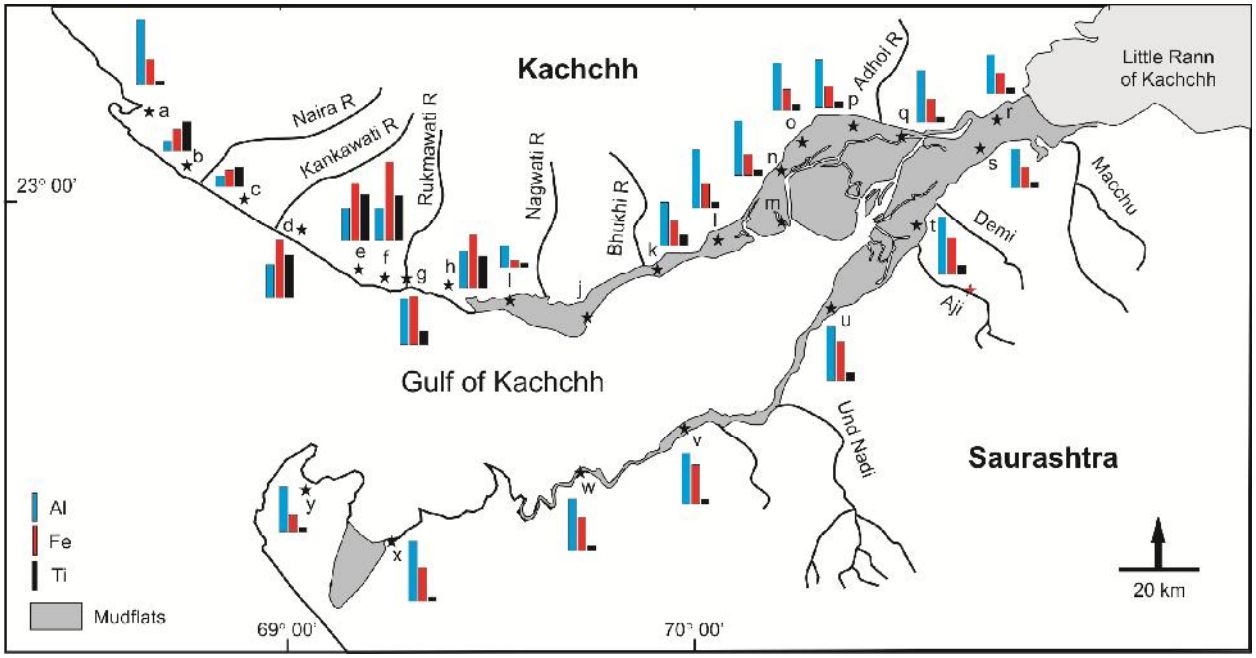

Figure 5.7: Spatial distribution of concentration of Al, Ti and Fe in intertidal sediments of Gulf of Kachchh coast.

(b) The Kachchh mainland provenance

The Kachchh mainland provenance can be observed in the > 63 micron fraction along the northern sandy coast of GoK in heavy mineral studies and mineral magnetic studies (Prizomwala et al., in press). Coastal rivers of Kachchh mainland namely, Kankawati, Rukmawati and Kharod acts as suppliers of the hinterland derived sediments along the coastline which was evidenced by

increase in concentration and type of heavy minerals, concentration of Ti – Fe (Figure 5.7) and magnetic minerals at these river mouths (Prizomwala et al., in press).

(c) The Saurashtra peninsular provenance

The Saurashtra peninsular provenance is characterized by I+Ch / S+K ratio that range between 0.5 and 1 in clay mineralogy owing to the dominance of smectite-kaolinite assemblage and enrichment in mineral magnetic concentration along the southern coast of inner Gulf of Kachchh (Figure 5.8). The inner mudflats although gains major part of the clay fraction from River Indus sediment flux, the southern part of inner gulf mudflats exhibits dominance of Deccan Trap derived clay minerals (i.e. smectite). This is contradictory to the understanding that the coastal rivers within Gulf of Kachchh do not contribute sediments owing to their ephemeral nature. It has been noted from other studies around the globe that 'dryland' rivers also supply considerable amount of sediments to world oceans annually (Tooth 2000).

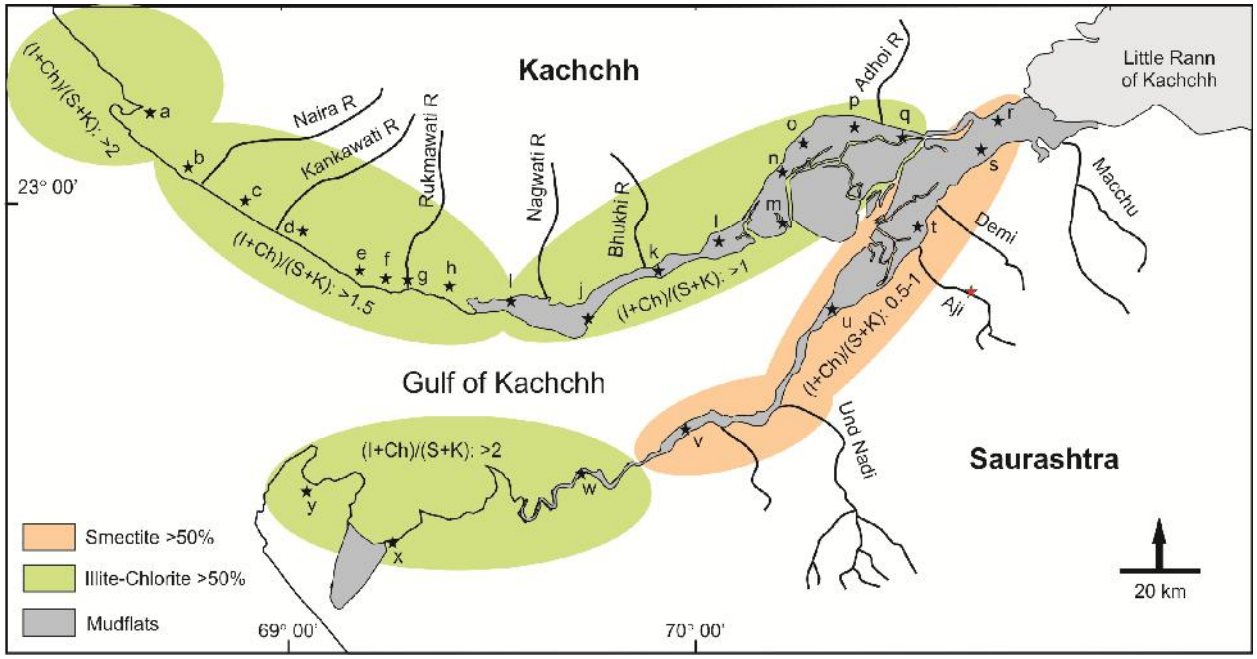

Figure 5.8: Spatial distribution of clay mineral assemblage in the intertidal sediments of the Gulf of Kachchh coast.

Based on robust earlier mentioned various proxies, we have listed distinct provenance discriminating signatures of the proximal (i.e. Kachchh / Saurashtra) and the distal (i.e. Indus) end members, which would be helpful in elucidating the source-to-sink component in the region (Table 5.5).

Table 5.5: Major provenance discriminating signatures of distal (i.e. River Indus) and Proximal (i.e. Kachchh mainland / Saurashtra peninsula) end member in various proxies.

Proxies	**River Indus**	**Kachchh Mainland / Saurashtra Peninsula**	**Discriminating Parameter**
Clay mineralogy	Illite-Chlorite (>50%)	Smectite (>40%) and Kaolinite (Chlorite abscent)	I+Ch/S+K ratio
Sediment Geochemistry	Al > Fe > Mg >Ti	Fe > Mg > Al > Ti	Concentration of Al
Heavy Mineral Assemblages	Mica minerals	Opaques and Epidote	Mica minerals
Mineral Magnetic Properties	Concentration: Low Grain size: stable single domain Mineralogy antiferromagnetic	Concentration: Moderate to High Grain size: multidomain Mineralogy ferrimagnetic	Magnetic susceptibility and mineralogy

Till date all the approaches employed so far in the Gulf of Kachchh have been taking into account the mineral assemblages and their concentrations; however there exists no study on single grain probe analysis and isotopic fingerprinting for provenance discrimination, which has been employed recently quite successfully in different parts of world (Clift et al., 2001; Weldeab

et al., 2002; Kessarkar et al., 2003). Genetic mineralogy and isotopic studies would prove more fruitful in better tracking the sediment transit mechanism as well as ascertaining the provenance of these coastal sediments.

Chapter 6

Sink Potential of the inner Gulf of Kachchh

6.1 Rationale

Vast muddy flat lands fringing the coastline are called "Mudflats" (Folk, 1954). Sedimentation in a mudflat is mostly controlled by the tidal currents. Owing to its evolution in calm and sheltered environment, the processes acting in the mudflats have lack of erodibility due to low hydrodynamic regime and good near continuous preservation potential. The efforts it takes to raise a core from ocean bottom are by far too much as compared with the ones it takes to collect core from mudflat environment. Also, there is a marked difference between sediment dynamics within a mudflat environment. The mudflat deposits near high water line experiences least wave activity and low hydrodynamic energy regime; the middle part has intermediate hydrodynamic energy regime, whereas nearer to the low water line, sediments are sandier due to more proximity to wave activity and they are under higher hydrodynamic regime. Thus, mudflat deposits nearer to high water line could serve as promising high resolution archives of past climatic changes. To test this hypothesis a shallow core was raised from Mundra which is situated on mudflats of the inner Gulf of Kachchh coast.

6.2 Mundra Core

The present study site is located near Mundra, on the southern coast of the Kachchh (Figure 6.1). The reasons for selection of this site was (1) it falls in 'transition zone' as described by Prizomwala et al. (2010) and hence, is very sensitive to changes in sediment supply and energy conditions in this macrotidal regime, and (2) it hosts mudflats above the present day tidal

range and which are unaffected by anthropological activities going on and preserves the sedimentation sequence.

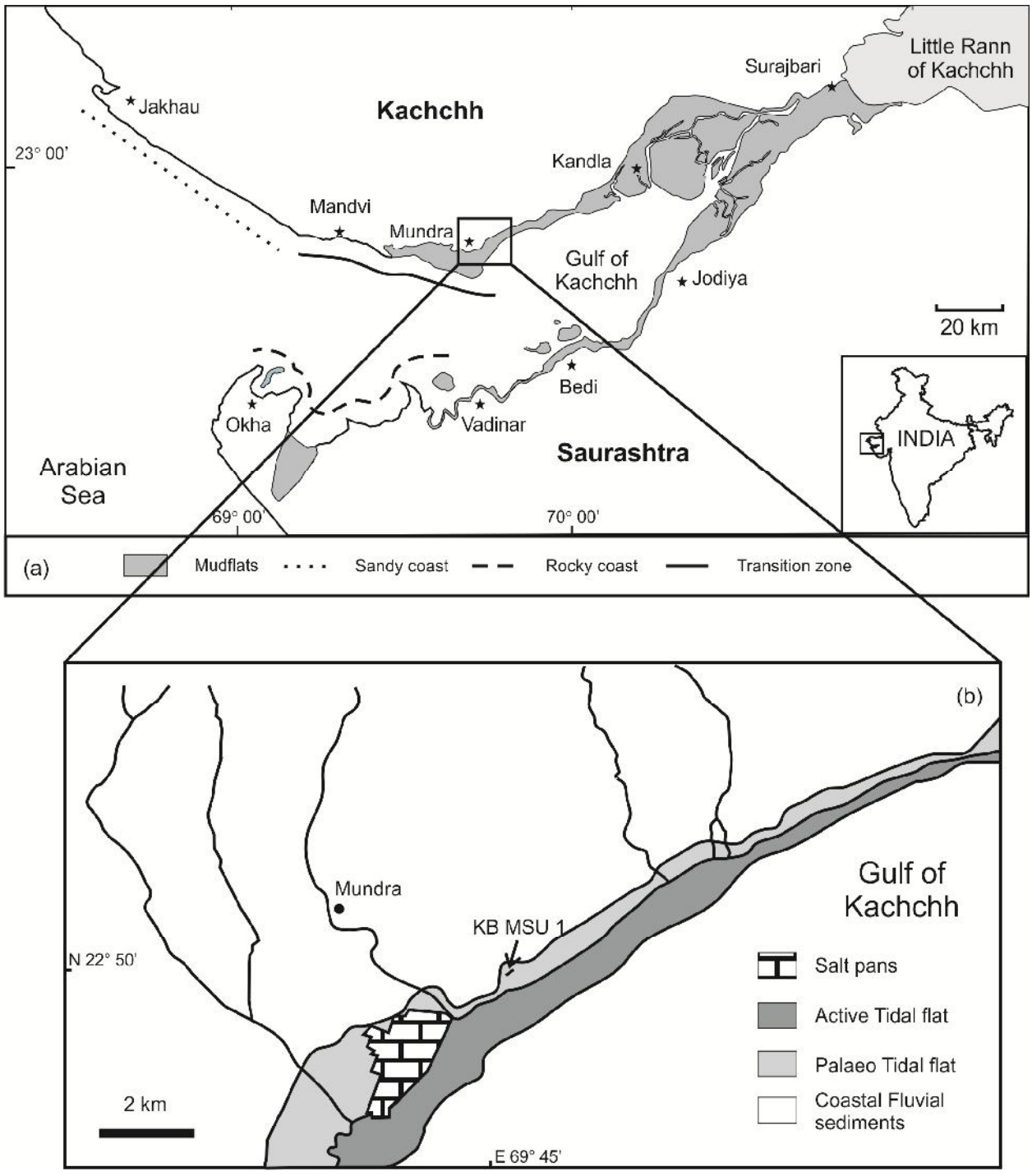

Figure 6.1: Location of the core (KB MSU-1) raised from the Gulf of Kachchh coast at Mundra.

6.2.1 Chronology:

Three ^{14}C radiocarbon dates were obtained on handpicked mollusk shells using accelerated mass spectrometry (AMS), which by extrapolation indicated that the sequence covers time period from 1300 AD up to 400 AD with an average sedimentation rate of 1.33 mm a^{-1}. Figure 2 shows the calibrated age-depth model and sedimentation rate for the sequence. The sedimentation rate varied from 1.14 mm a^{-1} (~least) during the 410 AD to 680 AD and 1.35 mm a^{-1} (~highest) during the 680 AD to 1049 AD.

Optical stimulated Luminescence (OSL) provides the precise depositional age of the sediment, when during the sediment transport the day-light luminescence erases the geological luminescence to zero or near zero-value (Singhvi et al., 2001). In present study two OSL ages were obtained from two sand layers which gave an age of 1.3 ± 0.15 ka (at 35 cm depth) and 2.5 ± 0.2 ka (at 102 cm depth) from the PRL, Ahmedabad, India. However as they show older ages than the shells present below, pointing to an incomplete zeroing of the luminescence age (bleaching) of these sand layers. Hence these two ages were not used in age model.

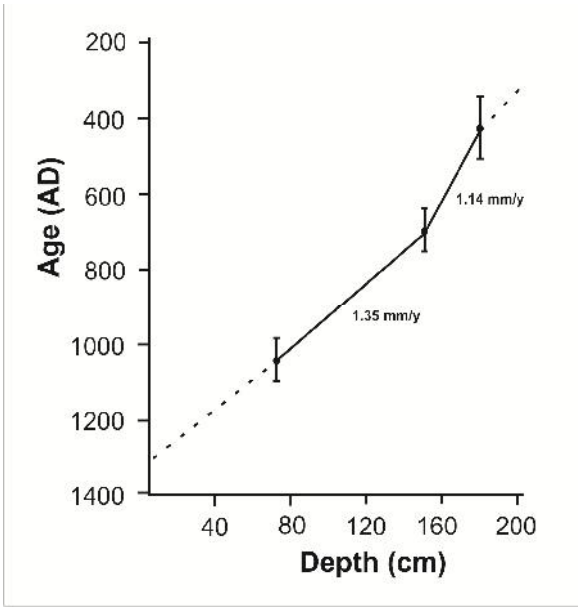

Figure 6.2: Depth versus calibrated ^{14}C AMS dates showing sedimentation rate of the sequence.

6.2.3 Sedimentary Sequence

At Mundra coastline, just above the high tide line a shallow trench about 202 cm deep was dug parallel to the coastline. The sequence showed three sand dominant and alternating clayey silt dominant units (Figure 6.2).

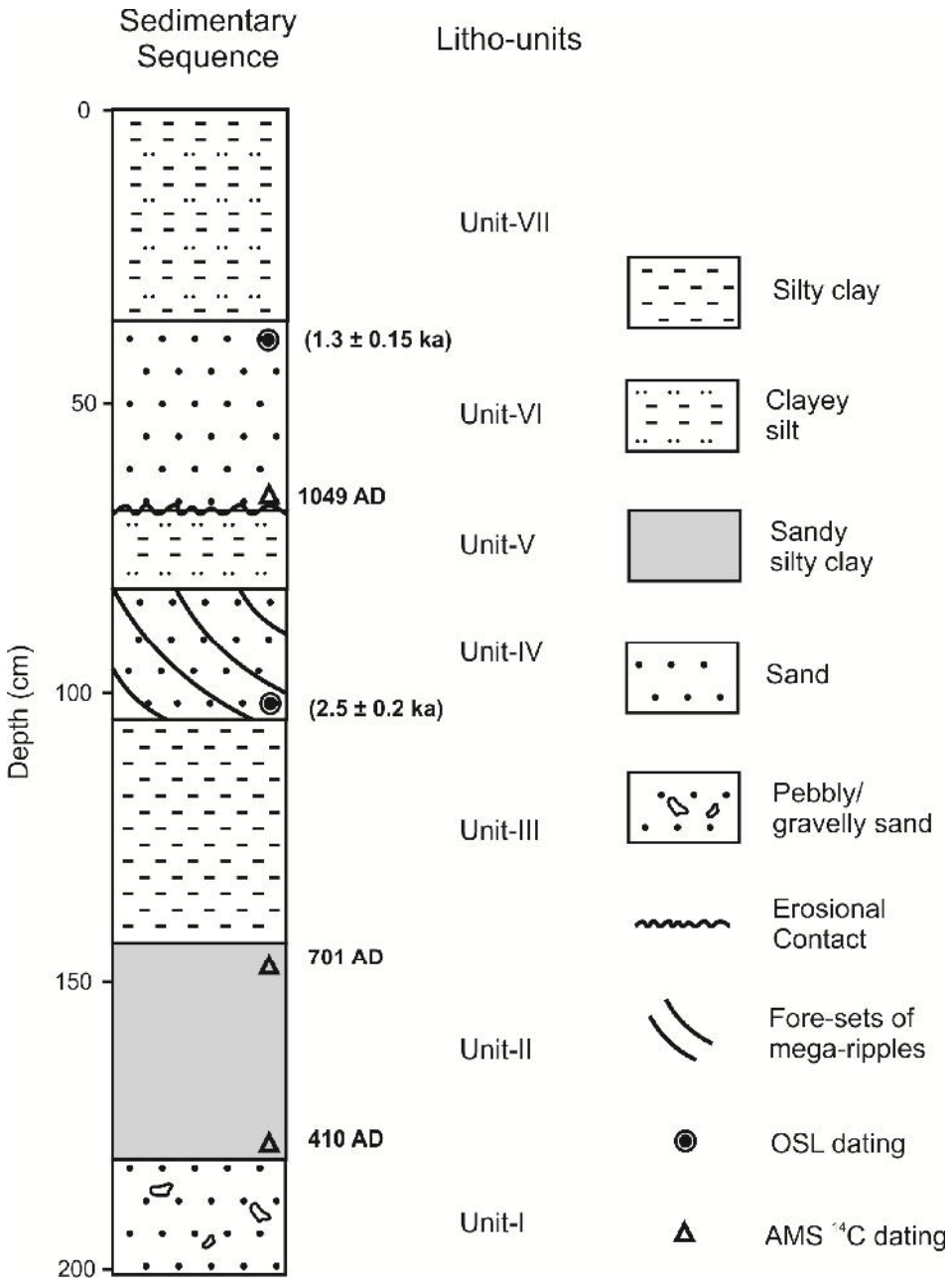

Figure 6.3: Litholog of the Mundra core exhibiting various litho units and it's geochronology.

Unit-I

The bottom most unit in this core is a pebbly/gravelly sand unit (Unit-1) which is 22 cm thick, with pebbles up to 2 - 3 cm in length admixed with a significant amount of gravels. The presence of pebbly/gravely sand is indicative of high flux of sediment deposited in a strong hydrodynamic energy condition.

Unit-II

Overlain the pebbly/gravelly sand unit is a 32 cm thick sandy clayey silt (Unit-2) layer. Grain size analysis of this unit showed that it has dominant silt (50-70 %), followed by very fine sand (25 – 40 %) and small amounts of clay (5 – 20 %). The gradational change in grain size from coarse grained sediment at bottom to relatively finer grain size in overlying unit is indicative of change in past energy condition i.e. gradual reduction in energy condition in this case.

Unit-III

On top of Unit-2 is resting a bluish grey colored laminated silty clay (Unit-3) of about 44 cm thickness which had dominant clay (60 – 80 %) followed by silt (16 – 35 %) and negligible amount of sand (4 - 8 %). Deposition of clayey unit with laminations in a coastal environment is indicative of calm (i.e. low) energy condition during deposition.

Unit-IV

Above that overlain the Unit-3 is a coarse grained sand layer showing mega-ripples with foresets dipping towards coastline. The base of this sandy layer is gravelly to coarse grained sand. The sediments of this sandy layer show pronounced assorted nature in sediment

distribution with presence of 1-2.5 cm long pebbles of the Deccan basalt. The seaward dipping orientation of foresets of these mega ripples and its assorted nature suggest the deposition of this unit under a high energy condition.

Unit-V

Resting above this unit is laminated clayey silt (Unit-5) layer of about 10 cm thickness, which has a sharp erosional contact with the above lying massive assorted sand layer (i.e. Unit-6). The change in grain size from coarse sand to clayey silt, is indication of regaining normal tidal regime after short spell/s of high flux that has deposited the unit 4.

Unit-VI

Unit-6 has several clasts (1 - 2 cm diameter) of the Deccan trap basalt embedded in it and also shows mud intraclasts and few mud lamilae. Interestingly Unit-6 (assorted sand) is seen sandwiched between the two clayey silt units (Unit-5 and Unit-7). Unit 5 has a sharp contact with overlying 'assorted, medium to coarse grained' sand layer i.e. unit 6, which again has a sharp contact with above lying clayey silt unit 7. The stratigraphic position of this sand layer is ambiguous, owing to (1) its sandwiched nature with above and below lying clayey silt units, (2) sharp contact with both over and below lying units, (3) absence of any physical or biological structure, as usually observed along the coastal environments, (4) assorted nature of grain size distribution, (5) occurrence of abraded nature of foraminifers and abundant broken older shell fragments and (6) presence of mud intraclasts and mud lamilae. All these observations point towards the deposition of this sand layer by action of a high energy marine event such as Tsunami that might have occurred around 1050 AD.

According to Morton et al. (2007), Kortekass and Dawson, (2007) and Shanmugam (2011) tsunami sand layers show a variety of characteristics and differ from storm deposits few of which are (1) presence of mud interclasts and mud lamilae, (2) in a muddy environment the tsunami sand layer is sandwiched with a sharp contact with overlying and underlying mud layers, (3) absence of any primary physical or biological structure and (4) lack of sorting in grain size distribution within sand layer. The Gulf of Kachchh coast has in past experienced historical tsunami events, one of the famous and recent one being 28th November, 1945 Makran tsunami which supposedly had run up height of 11m in the Gulf of Kachchh (Pararas-Carayannis et al., 2006). Several other historical tsunami events have been summarized by Shukla et al (2010).

Unit-VII

Unit-6 is capped by a 38 cm thick clayey silt (Unit-7) layer awhich shows thin laminations, typical of tidal flat sedimentation indicating the regaining of the system after the high energy event.

6.2.3 Geochemistry

Geochemistry is often used as a proxy for sediment flux as well as to ascertain provenance of sediments (Young and Nesbitt, 1998; Staubwasser and Sirocko, 2001; Singh, 2010; Tyagi et al*.,* 2012). A total of 101 samples at 2-cm interval were analyzed for major and trace elements and organic carbon estimation. The analysis for major oxides and trace elements was done by making glass pills with mixture of lithum tetraborate/metaborate and these pills were analyzed using X-ray fluorescence Spectrometry (Axios from PANalytical Limited) at the Institute of Geochemistry at ETH Zurich. The analytical precision for major oxides and trace elements was better than 5% and 10% respectively. The total inorganic carbon (TIC) content was

measured with a coulometric device (5012 Coulometer, UIC Inc. Coulometrics). Additionally $CaCO_3$ % was also calculated using the empirical formula ($CaCO_3$ % = ((TIC x 100)/12)). The precision of analysis was better than 2 % for $CaCO_3$.

Ratios of several major oxides namely TiO_2/Al_2O_3, and Fe_2O_3/Al_2O_3 are used as detrital proxies, as they are most resistant to diagenetic changes during transportation and partial storage (Von rad et al., 1999; Tyagi et al., 2012). Variation in input of Aluminum, Titanium and Iron has also been used to reflect changes in terrigenous flux from local watershed (Peterson et al., 2000). The concentration of $CaCO_3$ in marine sediments reflects variations in the biogenic productivity. It is also known that the nearby hinterland regions are rich in magnetic minerals largely derived form the Deccan trap basalts (Prizomwala et al., 2012, in press). Hence, variations in TiO_2/Al_2O_3 and Fe_2O_3/Al_2O_3 are very much controlled by local influx, whereas variations in Al_2O_3 are result of clay minerals derived dominantly from the River Indus. Other discriminating tools are Rb enriched in suspensions carried by the River Indus and the high contents in Sr in the Deccan Traps (Shukla et al., 2001; Ramaswamy et al., 2007).

The bottom most part of the sequence dates back to 410 AD and older (Figure 6.4). The period between 410 AD and 540 AD shows an increase in major and trace element concentrations, indicating enhanced erosion in the catchment (Figure 6.4). The period from 0 AD to 500 AD is characterized by warmer climatic conditions in Europe affiliated to the Roman Warm Period (Lamb, 1985; Bianchi and McCave, 1999). As the dates from this part of the sequence spans from 410 AD to 540 AD, it could be correlated with the later part of the Roman Warm Period. This time span was followed by a cooling spell with glacier advances in Europe called Cold Dark Ages (CDA) (Lamb, 1985; Bianchi and McCave, 1999).

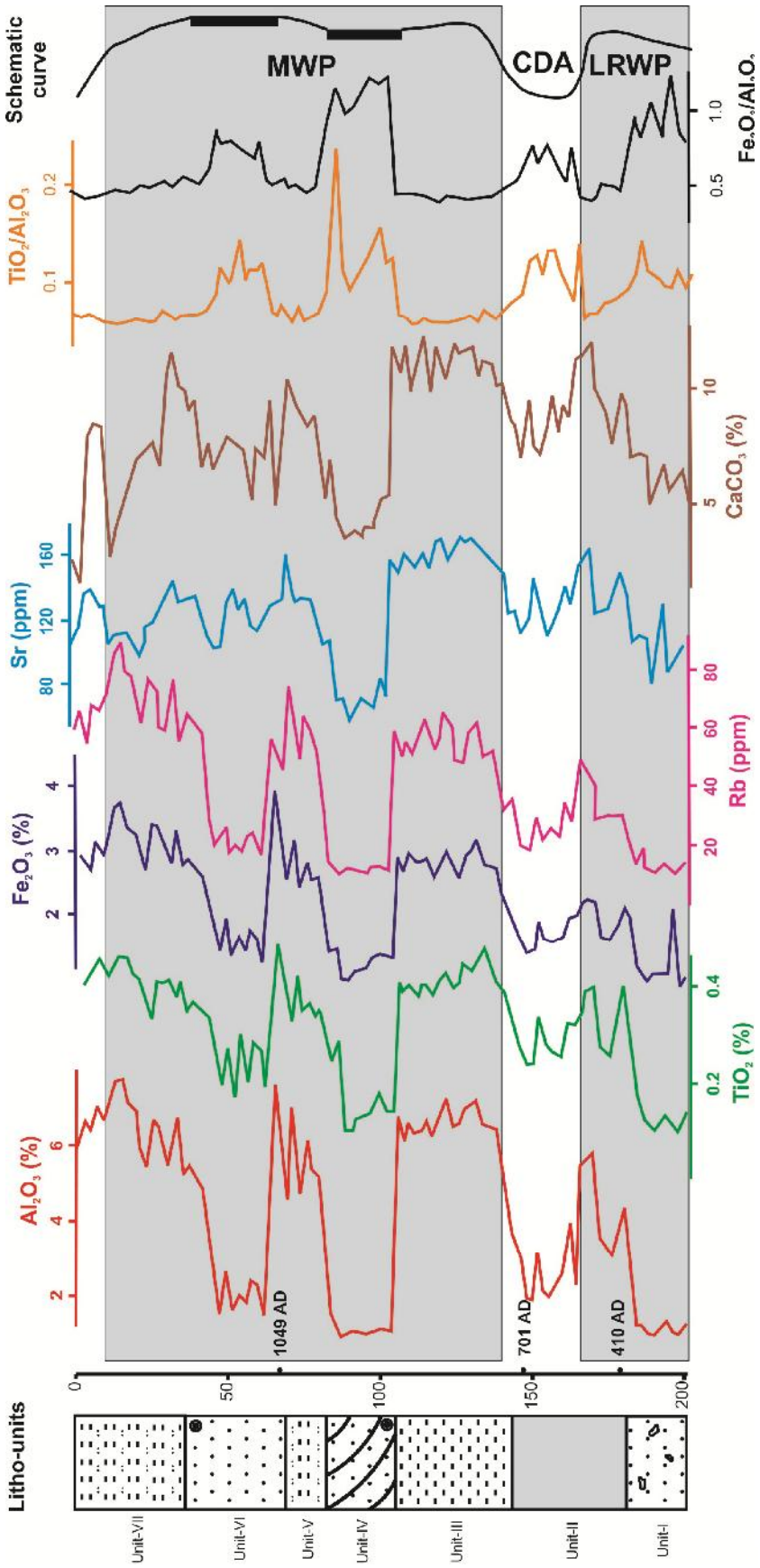

Figure 6.4: Temporal variations in geochemical parameters. Thick black vertical bars on the schematic curve indicates depositional ages of those units is negligible in geological time scale (i.e. few hours).

In our data the period between 540 AD to 750 AD is characterized by weakening in strength of the ISM as documented by decrease in Indus derived detrital flux (Figure 6.3: Al_2O_3 and Rb) and relative increase in local detrital flux (Figure 6.4: TiO_2/Al_2O_3, Fe_2O_3/Al_2O_3 and Sr), which reflects the cooler and drier period in the NAR. Furthermore, since 750 AD up to 1250 AD, there is a significant abrupt increase in strength of ISM, which is denoted by enhanced weathering in the catchments as evidenced by increase in weathering proxies (Al_2O_3, TiO_2, Fe_2O_3, Rb and Sr). The two phases of decrease in concentration of major and trace element concentrations during this period coincides with sand layers (Unit-IV and Unit-VI). As the analysis was carried out on bulk fraction these anomalous decrease pertaining to the sand layers are attributed to the grain size dependency of geochemical parameters (Nesbitt and Young, 1996). The schematic curve illustrates the scenario of ISM variability after de-coupling the grain size effect owing to the sand layers. The period between 750 AD and 1250 AD is recorded in NAR as having SST 1ºC warmer than present and overall warmer and humid climate (Lamb, 1985; Keigwin, 1996; Mann, 2002; Cronin et al., 2010).

6.2.4 Environmental Magnetism

Environmental magnetism has been used as a palaeoclimatic proxy in several marine (Oldfield et al., 2003; Kumar et al., 2005; Thamban et al., 2007; Rao et al., 2008) and continental records (Heller and Liu, 1986; Maher et al., 1994; Hirt et al., 2003; Shankar et al., 2006; Juyal et al., 2009; Warrier and Shankar, 2009). The major boon to use this proxy is its non-destructive nature, fast, robust and efficiency in measuring several samples in short period of time. A total of 202 samples (i.e. 1 cm interval) were analyzed for various magnetic parameters as mentioned earlier (Chapter 5) at the Institute of Geophysics, ETH Zurich, Switzerland.

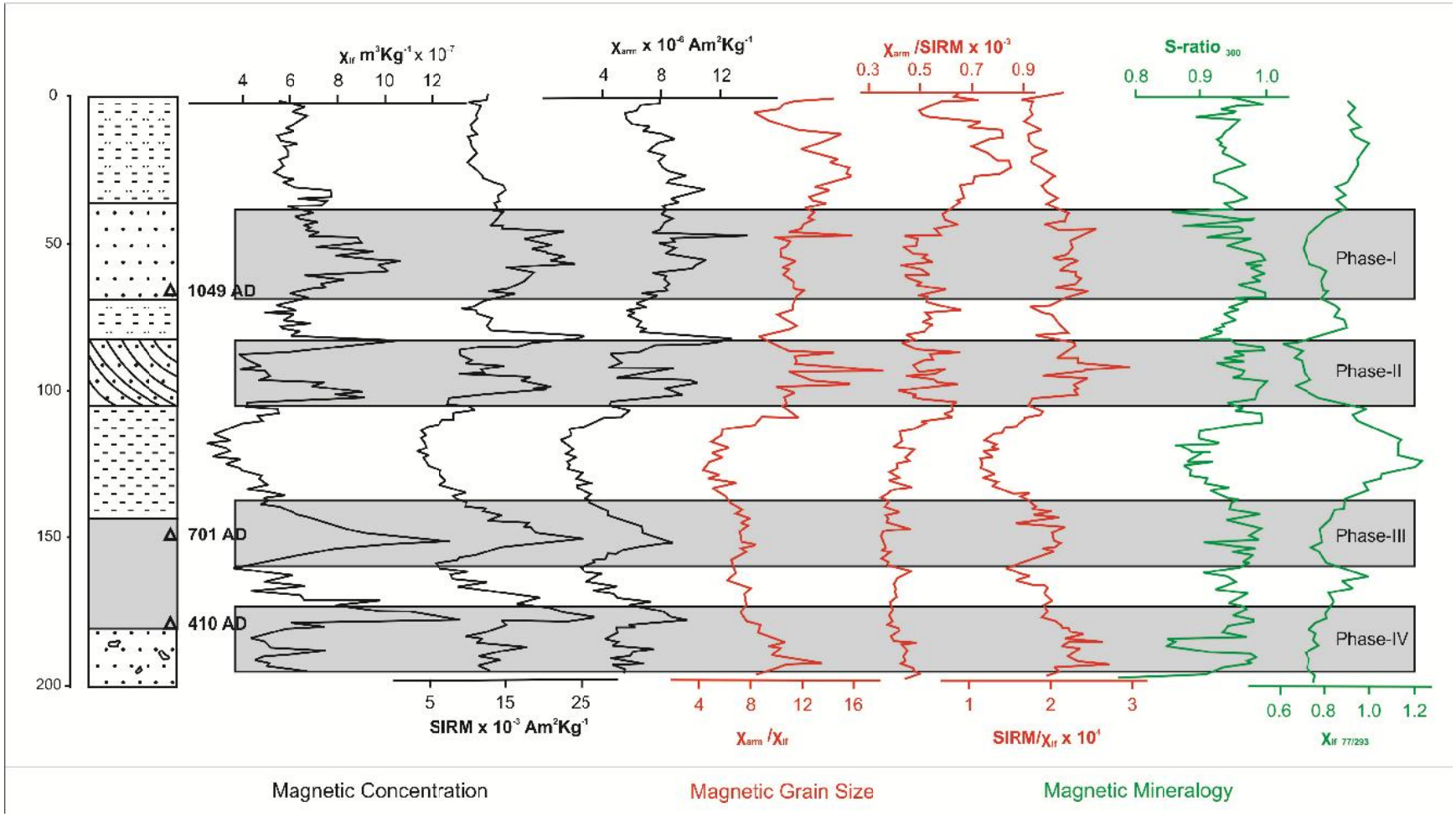

Figure 6.5: Mass specific mineral magnetic parameters illustrating magnetic concentration, grain size and composition..

Figure 6.5 shows various mineral magnetic parameters used to illustrate magnetic concentration, magnetic granulometry and magnetic mineralogy. It is known from the previous works and also from the present day sediment dispersal system that the major contributors of the magnetic minerals into the Gulf of Kachchh are the local fluvial sources draining from Kachchh mainland (Prizomwala et al., in press). Figure 6.5 shows four major phases which mark increase in magnetic mineral concentrations (χ_{lf}, χ_{arm} and SIRM). Phase-I and Phase-II correspond to the sand layers, whereas the Phase-III correspond to the CDA (540 – 750 AD) and the phase-IV correspond to the bottom part of unit-II. The sand layers were deposited on account of high energy marine inundations as revealed by the sedimentological analysis. The source of sand for the high energy tidal current / tsunami is the sandy segment of southwestern Kachchh coast. The sands from this coastal segment periodically get reworked and get redistributed in the offshore, which hosts several sand shoals. Hence, these sands are rich in magnetic minerals which are originally derived from the Kachchh mainland (Prizomwala et al., in press). The increase of magnetic mineral concentration observed in phase-III correlates with relatively drier phase as evidenced by the geochemical parameters (Figure 6.4). However, as like increase in TiO_2/Al_2O_3 and Fe_2O_3/Al_2O_3 corresponds to relative increase in flux from hinterland due to the 'dryland' nature of Kachchh mainland fluvial system, the increase in concentration of magnetic mineral concentration is also projection of the same. Similarly the increase in magnetic mineral concentration in phase-IV corresponds to bottom part of unit-II which is sandy silty clay. The sedimentological analysis of unit-II revealed that the sand content at bottom part gradually increases, which is evident here in the form of increase in magnetic mineral concentration (Figure 6.5).

The magnetic granulometry as suggested by χ_{arm}/χ_{lf}, χ_{arm}/SIRM and SIRM/ χ_{lf}, shows that most part of the sequence has multidomain magnetic minerals showing higher values and only the part of unit-III upto 750 AD shows stable single domain / pseudo single domain magnetic grain size as illustrated by lower values. Similarly the magnetic mineralogy as indicated by the S-ratio$_{300}$ and $\chi_{77/293}$ shows that entire sequence is dominated by ferrimagnetic mineral assemblage with values of S-ratio > 0.9, and only the part of unit-II upto 750 AD shows significant paramagnetic contribution with S-ratio values approaching near 0.9 and $\chi_{77/293}$ values > 1.0. The environmental magnetic parameters corroborate the geochemical parameters in highlighting the presence of MCA, CDA and LRWP in the sequence.

6.2.5 Clay Mineralogy

Clay mineral composition basically indicates the intensity of weathering at its source region which can be used as palaeoclimatic indicator (Chamley, 1989). So far, the clay mineralogy has been used by several workers for studying palaeoclimatic fluctuations at time scale of > 10^6 years (Sirocko and Lange, 1991; Thamban et al., 2002; Thamban and Rao, 2005; Boulay et al., 2007; Colin et al., 2010). However, few studies have pointed out that the clay minerals are not good palaeoclimatic indicators at time scales < 10^3 years, owing to uncertainty in transport and time of residence (Thiry, 2000; Alizai et al., 2012). The author has studied approximately 40 samples at 4 cm interval from the sequence. The two sand layers (Unit-IV and unit-VI) were the 'Clay Barren Zone' with clay content < 1 % as shows in figure 6.6 and 6.7. Figure 6.6 shows the variations in content of major clay minerals namely illite, chlorite, smectite and kaolinite in addition to the illite chemistry and crystalinity. Illites are mostly Fe-Mg rich with values < 0.35 and with low to intermediate crystalinity as depicted by values ranging between 0.2 – 0.6.

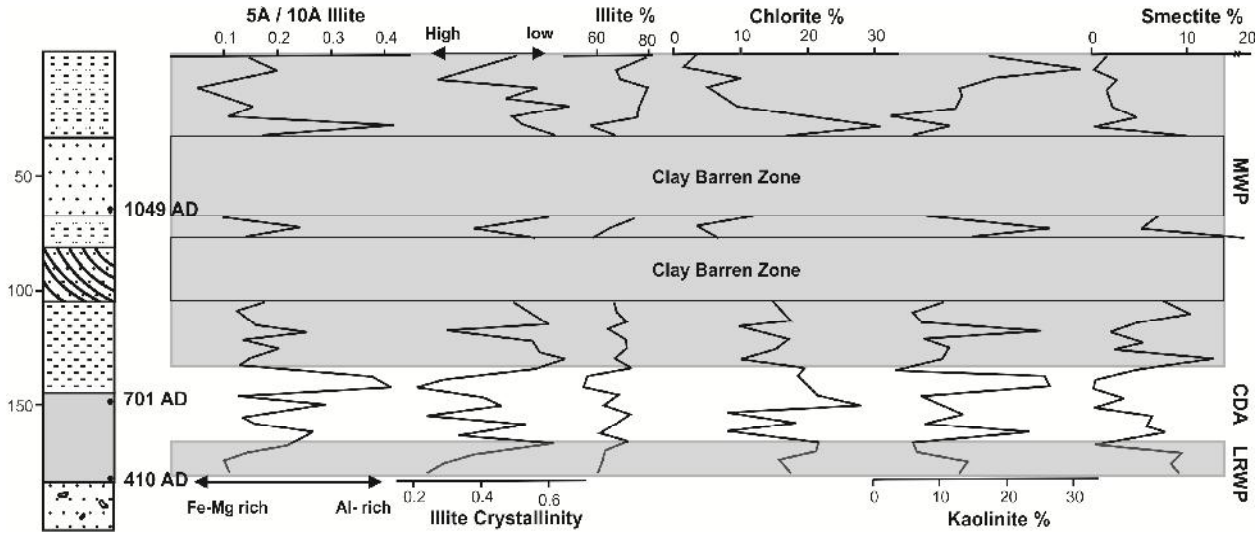

Figure 6.6 shows the variations in content of major clay minerals namely illite, chlorite, smectite and kaolinite in addition to the illite chemistry and crystalinity.

Illite is the dominant clay mineral (60 – 80 %) followed by Chlorite (2 – 32 %), Kaolinite (4 – 30 %) and Smectite (0 – 22 %). None of the major clay minerals follow any trend during the MCA, CDA and LRWP events.

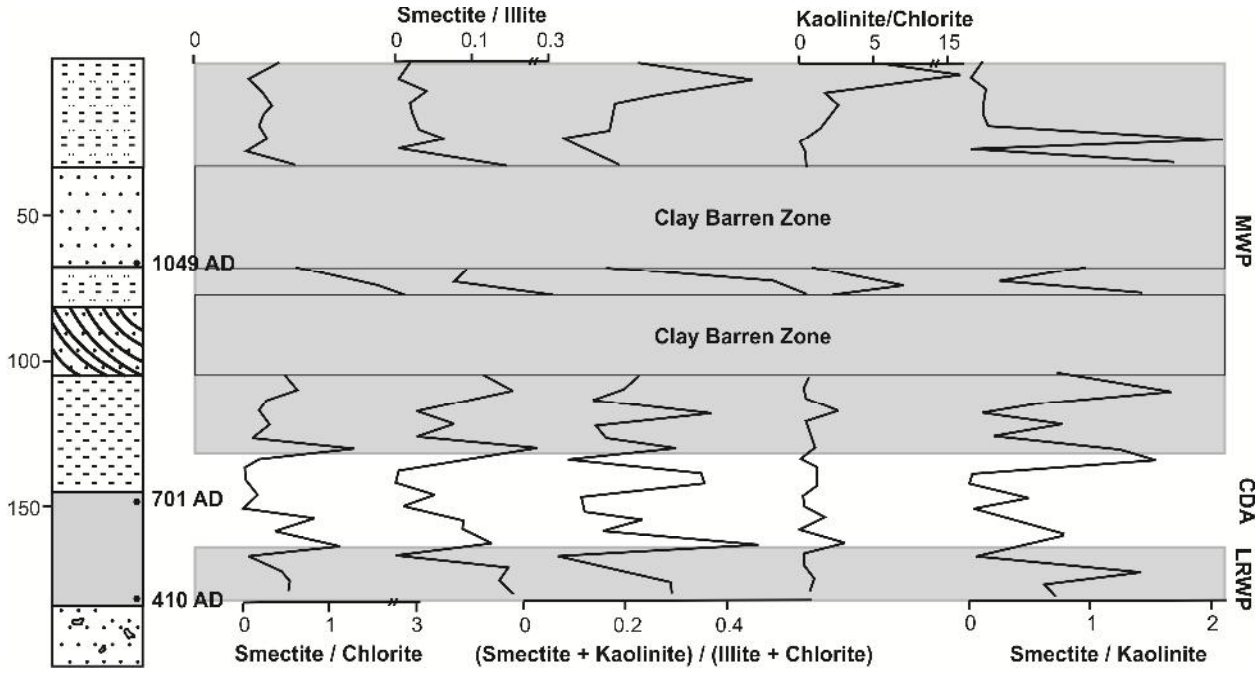

Figure 6.7 shows ratios of various clay minerals used to decipher palaeoclimatic signatures.

Ratio of Kaolinite / Chlorite is used as proxy for humidity (Thamban et al., 2002; Thamban and Rao, 2005). Whereas Smectite / Kaolinite is used as proxy for deciphering drier / wetter climatic conditions. The ratios of (Smectite + Kaolinite) / (Illite + Chlorite) is used to depict variations in weathering intensity of local source (Kachchh mainland) and distal source (Indus River). However, as shown in figure 6.7 none of the clay mineral ratios show any particular trend with respect to the MCA, CDA and LRWP events. MCA spans for about 500 years (750 – 1250 AD), CDA (750 – 540 AD) about 200 years and LRWAP (540 – 0 AD) for about 500 years. The present study supports the conclusions of Alizai et al. (2012) that clay minerals are not good indicators of weathering / palaeoclimate when time scales of $< 10^3$ years are concerned.

Chapter 7

Summary

7.1 Rationale

The Gulf of Kachchh has attracted many workers to study its offshore dynamics (current dynamics, suspended sediment transport, sediment character of sea floor and various sedimentation processes) in this complex macrotidal regime (Hashimi et al., 1978; Nair et al., 1982; Vora et al., 1987; Chauhan, 1994; Shetye, 1999; Kunte et al., 2003; Chauhan et al., 2004; Babu et al., 2005; Vethamony et al., 2005; Chauhan et al., 2006; Ramaswamy et al., 2007; Vethamony et al., 2007). However, till date there is no published literature regarding the compositional attributes of the coastal sediments, their sources and probable pathways in the Gulf of Kachchh. With the presence of marine national park and rapidly industrializing coastline, it is indeed necessary to generate a comprehensive understanding of processes acting in and along the Gulf of Kachchh coast. Hence the main aim of the present work was to achieve following objectives,

1. To delineate the major sources of sediments contributing to the Gulf of Kachchh basin.
2. To study the pathways of these coastal sediments as a sediment dispersal system in this macrotidal regime.
3. To study the sink potential of these mudflats as an archive for studying climate change / sediment supply history at a high resolution.

In order to do so the approach we followed was to firstly identify probable end-members contributing to the Gulf of Kachchh basin on the basis of literature survey and document the provenance signatures of these end-members using various provenance discriminating proxies namely, textural analysis, mineral magnetic analysis, clay mineralogy and sediment geochemistry. Secondly study the entire coastline of the Gulf of Kachchh coast using the above mentioned provenance discriminating proxies. Thirdly to integrate the data set to reconstruct a sediment dispersal model for the Gulf of Kachchh coastline and lastly to study a shallow core from the inner Gulf of Kachchh coast in order to appreciate the sink potential of these coast.

7.2 Granulometric Analysis

In general, the grain size distribution along the Gulf of Kachchh coastline showed significant role of energy of tidal currents and coastal fluvial systems, which controls the sediment transport pathways and geomorphic assemblages along the gulf coastline (Prizomwala et al., 2010). The characteristic grain size distribution pattern of the western and eastern segments of gulf also corroborated the wave dominated and tide dominated landforms along the Gulf of Kachchh coastline.

7.3 Mineral Magnetic Analysis

The characteristic difference in the concentration, grain size distribution and composition of magnetic minerals proved to be useful in delineating the provenance of the Gulf of Kachchh coastal sediments. The concentration of magnetic minerals evidenced by 'χ_{lf}' and the composition of magnetic minerals evidenced by 's-ratio' are the two distinct parameters which characteristically discriminates the respective end-members contributing to the Gulf of Kachchh basin. The provenance shifts within both coarse (i.e. > 63 micron) and fine fraction (i.e. < 63 micron) of the coastal sediments is well documented in the present study. The Deccan trap

lithology hosted in Kachchh mainland and Saurashtra mainland is are major source of high χ_{lf} and ferromagnetic minerals (s-ratio > 0.9) in the coastal sediments whereas the low χ_{lf} and antiferromagnetic minerals assemblage is manifestation of River Indus source.

Environmental Magnetism proves to be a fast, robust and efficient modern technique in sediment pathways and provenance analysis, primarily owing to its non-destructive nature.

7.4 Clay Mineralogy and Sediment Geochemistry

The Clay mineralogy showed dominance of illite-chlorite mineral assemblage, which is mainly representative of physical weathering product of cold and arid climatic regime, most likely River Indus Source. The southern coast of inner gulf showed dominance of smectite-kaolinite mineral assemblage due to predominant weathering of Deccan trap from Saurashtra landmass. The spatial distribution of clay minerals very well corroborates the offshore current dynamics in the Gulf of Kachchh. The spatial distribution of major and trace elements showed that the River Indus is major contributor of fine (< 63 micron) fraction, transported in suspension as evidenced by Al and Rb concentration and Rb/Ga ratio. Whereas the increase in Fe and Ti in the coarse (>63 micron) fraction of northern sandy segment is manifestation of the dominant contribution by Deccan trap source from Kachchh mainland via coastal fluvial system.

The study shows grain size dependency of proxies like sediment geochemistry in provenance analysis.

7.5 Characterization of Kachchh Mainland end-member

Employing various modern as well as conventional techniques like, mineral magnetic analysis, heavy mineral analysis, clay mineralogy and major elemental analysis for provenance discrimination, the study successfully documented various catchment scale sources and their

discriminating signatures from Rukmawati River basin. The study demonstrates the role of lithology, climatic regimes and relief changes in effecting provenance signatures in a dryland fluvial regime. The study also serves as primary database of sediments being derived from one end member (i.e. Kachchh mainland), which gets mixed with River Indus sources derived sediments along the Partial sink (i.e. Gulf of Kachchh in this case) and being ultimately delivered off the continental shelf off the mouth of Gulf of Kachchh into the Arabian Sea (i.e. sink). Following are brief concluding points to be noted,

1. It is showed that how different regimes/lithologies control the concentration and type of sediment delivery from a catchment bearing different signatures in different modes of sediment transport.
2. The 'uplands' and 'Deccan basalts' are two characteristically different sources of sediments within the Rukmawati River basin well discriminated by several parameters like χ and S/K ratios.
3. The estuarine zone which is a sub-sink within the Rukmawati River basin, typically shows mixing of landward and offshore distributed sediments, which are getting transported eastwards into the inner Gulf of Kachchh through longshore currents as depicted by trends of χ and S/K ratio.

7.6 Coastal Sediment Dispersal

Based on results of above mentioned proxies viz. grain size analysis, heavy mineral analysis, clay mineralogy, mineral magnetic studies and geochemistry of intertidal sediments three major end-members have been identified namely, (1) River Indus, (2) Kachchh mainland and (3) Saurashtra peninsula (Figure 7.1). The results indicate River Indus is major contributor of < 63 micron fraction, transported in suspension as evidenced by clay mineralogy, Al and Rb

concentration and Rb/Ga ratio. The suspended sediments advecting from River Indus enter the GoK along the mouth of northern coast and travels all along the northern coast via longshore currents. As it reaches central GoK the currents are deflected towards northeastern direction and it travels all along mudflats of the inner GoK, where most of the suspended sediments are deposited. In other words the residence time of suspended sediments in GoK is more in the mudflats of inner GoK, which is also evidenced by clear water patch reported by Ramaswamy et al. (2007) along the southern coast of GoK. The currents then get reversed at the head of inner GoK and continue to travel along the southern coast of GoK. The suspended sediment concentration near the southern coast of GoK is fairly less compared to the suspended sediment concentration along central and northern coast (Ramaswamy et al., 2007). Some part of River Indus born suspended sediments also travel directly southwards and it can be evidenced by I+Ch / S+K ratio being >2 at mouth of southern coast of GoK in clay mineralogy, enrichment in Rb and Rb/Ga ratio in geochemistry, magnetic concentration and magnetic mineralogy in mineral magnetic studies. The Kachchh mainland provenance can be observed in the >63 micron fraction along the northern sandy coast of GoK in heavy mineral studies and mineral magnetic studies (Prizomwala et al., in press-a). The Saurashtra peninsula provenance is characterized by I+Ch / S+K ratio that range between 0.5 and 1 in clay mineralogy owing to the dominance of Smectite-Kaolinite assemblage and enrichment in mineral magnetic concentration. It is mostly observed along the inner gulf mudflats of southern coast of GoK. Kunte et al. (2003) noted the northwestward and northward seasonal current circulation near the southern mouth of GoK, which could be seen as an alternative explanation for increase in I+Ch / S+K ratio to >2 as well as enrichment in Rb and Rb/Ga ratio at mouth of southern GoK coast (i.e. Okha and Pindara).

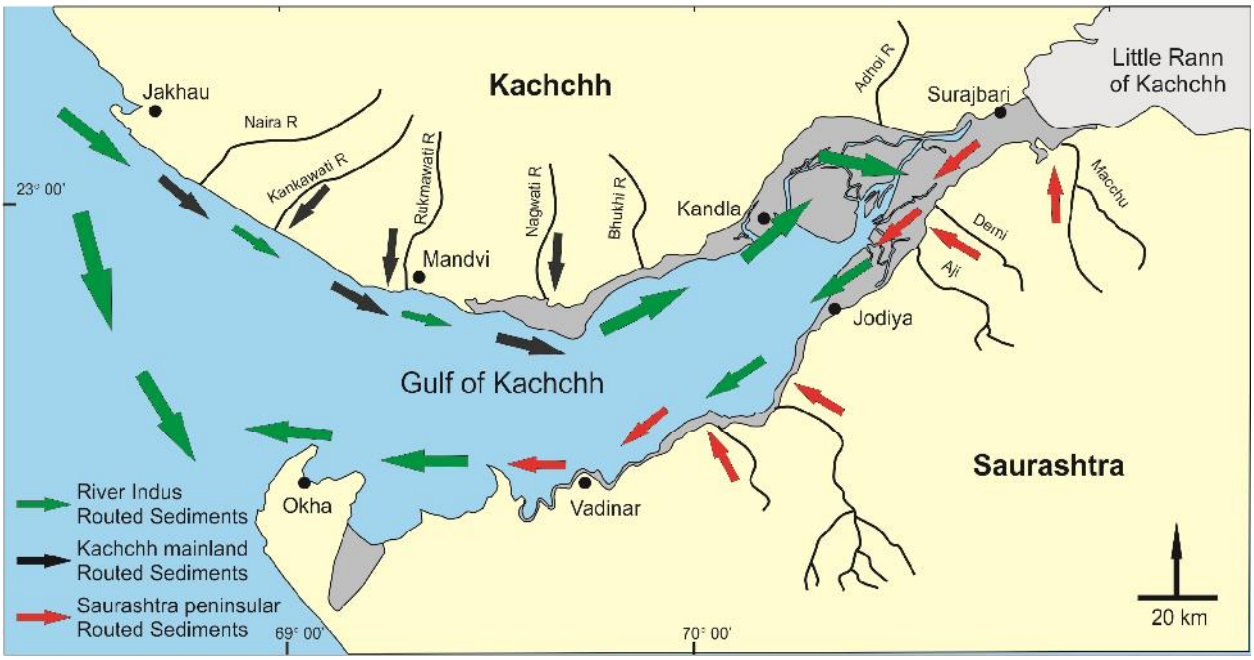

Figure 7.1: Schematic diagram of sediment dispersal system along the Gulf of Kachchh coast

7.7 Sink potential of the inner Gulf of Kachchh

A 202 cm thick sedimentary sequence from mudflats of inner Gulf of Kachchh coast was studied using various palaeoclimatic proxies like geochemical, mineral magnetic and clay mineral analysis to study the palaeo-climatic fluctuations. Three AMS ^{14}C dates obtained fomr mollusk shells indicated the sequence to range from 1300 AD to 400 AD. The sedimentological, geochemical and mineral magnetic proxies successfully documented the presence of a relatively humid phase during the 750 – 1250 AD and 540 - 410 AD and a relatively drier phase between 750 – 540 AD. Similar events have been documented in the North Atlantic Region as Medieval Warm Period (MWP ~ 750 AD – 1250 AD), Cold Dark Ages (CDA ~ 500 AD to 750 AD) and Roman Warm Period (RWP ~ 0 AD to 500 AD). The Synchronicity of these ISM events with the NAR events indicates that as like the millennial scale links, there also exists a centennial scale teleconnection between the Indian summer monsoon and the North Atlantic Region climate.

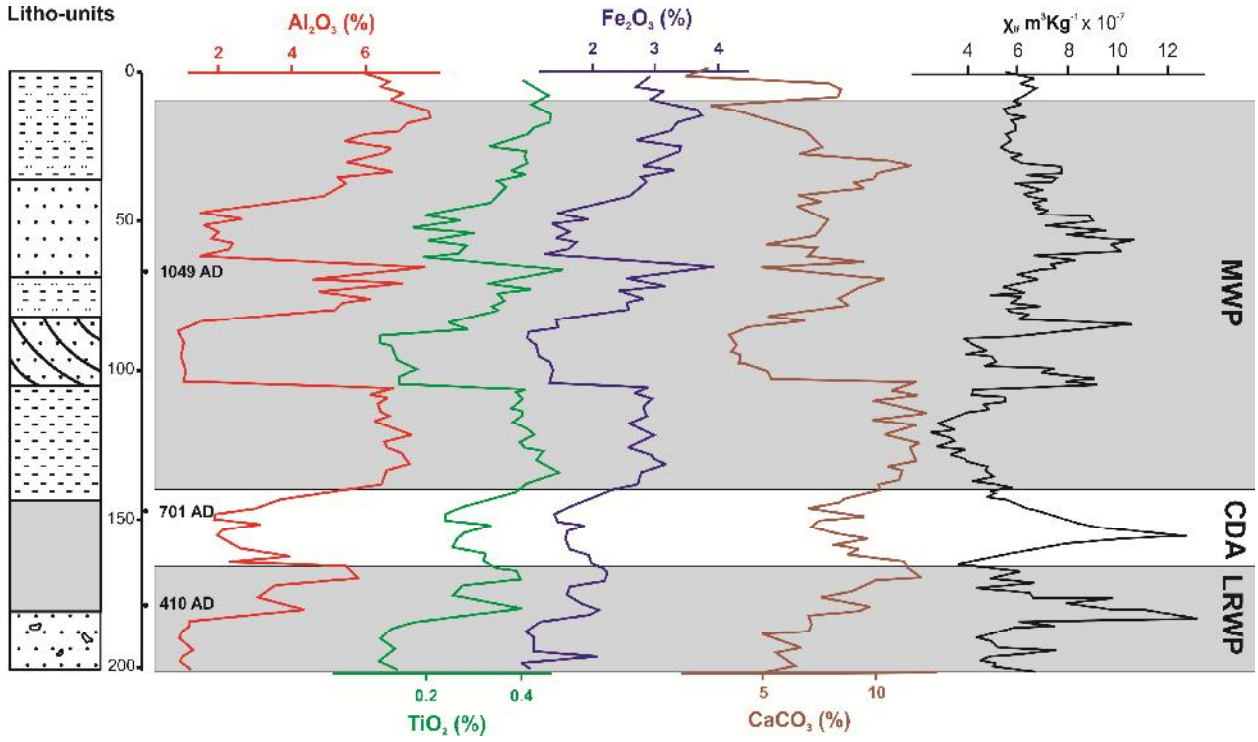

Figure 7.2: Temporal variations of geochemical parameters and magnetic susceptibility in the sequence.

The successful documentation of MCA (spanning for 500 years), CDA (spanning for 200 years) and LRWP (spanning for 500 years), exhibits the sink potential (i.e. sediment entrapping capacity) of the mudflats of the inner Gulf of Kachchh coast. The study points out that the mudflats of inner Gulf of Kachchh coast have strong potential for serving as high resolution archives to palaeo-climatic changes.

On the other hand clay mineral variations in the sequence do not corroborate the palaeoclimatic signals evidenced by the geochemical and mineral magnetic proxies. We believe that clay mineral formation is a direct response to climatic conditions and the time required to respond to changes in climate is shorter than the time interval being examined (i.e. centennial scale) in the present study. Also the sediment transport / residence time is another variable influencing this scenario. Hence the present study supports the conclusions of Alizai et al. (2012)

that clay minerals are not good indicators of weathering / palaeoclimate when time scales of < 10^3 years are being examined.

References

1. Agnihotri R, Dutta K, Bhushan R, Somayajulu B. L. K. (2002). Evidence for solar forcing on the Indian monsoon during the last millennium. Earth and Planetary Science Letters 198, 521–527.

2. Ahmad, T., Khanna, P. P., Chakrapani, G. J., Balakrishnan, S., (1998). Geochemical characteristics of water and sediment of the Indus River, Trans-Himalaya, India: constraints on weathering and erosion. Journal of Asian Earth Sciences 16, 333–346.

3. Allen, P. A. (2008). From landscapes into geological history. Nature, 451, 274-276.

4. Aloupi, M., Angelidis, M. O., (2001). Geochemistry of Natural and anthropogenic metals in the coastal sediment of the island of Lesvos, Aegean Sea. Environmental Pollution 113, 211–219.

5. Alizai, A., Hillier, S., Clift, P. D., Goisan, L., Hurst, A., VanLaningam, S., Macklin, M., (2012). Clay mineral variations in Holocene terrestrial sediments from the Indus basin. Quaternary Research 77 (3), 368 – 381.

6. Amos, K. J., Alexander, J., Horn, A., Pocock, G. D. and Fielding, C. R. (2004). Supply limited sediment transport in a high-discharge event of the tropical Burdekin River, NorthvQueensland, Australia. Sedimentology 51, 145–162.

7. Babu, M. T., Vethamony, P. and Desa, E. (2005). Modelling tide-driven currents and residual eddies in the Gulf of Kachchh and their seasonal variability: A marine environmental planning perspective. Ecological modeling 184, 299-312.

8. Banerjee, S. K., King, J., Marvin, J., (1981). A rapid method for magnetic granulometry with applications to environmental studies. Geophysical Research Letters 8, 333–336.

9. Basavaiah, N., (2011). Geomagnetism: Solid Earth and Upper Atmosphere Perspectives, Springer, Dordrecht, The Netherlands, pp. 410.

10. Basavaiah N. and Khadkikar A. S., (2004). Environmental magnetism and its application towards palaeomonsoon reconstruction. Journal Indian Geophysical Union 8 (1), 1-14.

11. Beloussov, V. V., (1962) *Basic Problems of Geotectonics*, McGraw Hill, London, p. 816.

12. Benson, L. V., Burdett, J. W., Kashgarian, M., Lund, S. P., Phillips, F. M., Rye, R. O., (1996). Climate and hydrologic oscillations in the Owens Lake Basin and adjacent Sierra Nevada, California. Science 274, 746–749.

13. Bhatia, M. R., Cook, K. A. W., (1986). Trace element characteristics of graywackes and tectonic setting discrimination of sedimentary basins. Contribution of Mineralogy and Petrology 92, 181–193.

14. Bhatt N., (2000). Lithostratigraphy of Neogene-Quaternary deposits of Dwarka-Okha area, Gujarat. Journal of Geological society of India 55, 139-148.

15. Bianchi, G. G. and McCave, I. N., (1999). Holocene periodicity in North Atlantic climate and deep ocean flow south of Iceland. Nature 397, 515-517.

16. Biscaye, P. E., (1965). Mineralogy and sedimentation of recent deep sea clay in Atlantic ocean and adjacent seas and oceans. Geological society of America Bulletin 76, 803-832.

17. Biswas, S. K. (1974). Landscape of Kutch – A morphotectonic analysis. Indian Journal of Earth Science 1 (2), 177-190.

18. Biswas, S. K. (1977) Mesozoic Rock Stratigraphy of Kutch. Quarterly Journal of the Geological, Mining and Metallurgical Society of India, 49, 1-52.

19. Biswas, S. K., (1980). Structure of Kutch–Kathiawar region, Western India. Proceedings of the 3rd Indian Geological Congress, Pune, pp. 255–272.

20. Biswas, S. K., (1982). Rift basins in western margin of India with special reference to hydrocarbon prospects. Bulletin of American Association of Petroleum Geologist, 66, 1497–1513.

21. Biswas, S. K., (1987). Regional tectonic framework, structure and evolution of western marginal basins of India. Tectonophysics 135, 307-327.

22. Biswas, S. K., (1993). Geology of Kutch. K.D. Malaviya institute of petroleum exploration, Dehradun. pp. 450.

23. Biswas, S. K., and Khattri, K. N., (2002). A geological study of earthquakes in Kachchh, Gujarat, India. Journal of Geology Society of India 60, 131-142.

24. Biswas, S. K. (2005). A review of structure and tectonics of Kutch basin, western India, with special reference to earthquakes. Current science 88, 1592-1600.

25. Bond G, Kromer B, Beer J, Muscheler R, Evans M. N, Showers W, Hoffmann S, Lotti-Bond R, Hajdas I, Bonani G. (2001). Persistent solar influence on North Atlantic climate during the Holocene. Science 294, 2130–2136.

26. Booth, C. A., (2002). Sediment-Source-Linkages in the Gwendraeth Estuary, South Wales, based on mineral magnetic analyses. Unpublished PhD thesis. University of Wolverhampton.

27. Booth, C. A., Walden, J., Neal, A., Smith, J. P., (2005). Use of mineral magnetic concentration data as a particle size proxy: A case study using marine, estuarine and fluvial sediments in the Carmarthen Bay area, South Wales, U.K. Science of The Total Environment 347, 241-253.

28. Boulay, S., Colin, C., Trentesaux, A., Clain, S., Liu, Z., Lauer-Leredde, C., (2007). Sedimentary responses to the Pleistocene climatic variations recorded in the South China Sea. Quaternary Research 68, 162–172.

29. Castelltort S., and Van Den Driessche J., (2003). How plausible are high-frequency sediment supply-driven cycles in the stratigraphic record? Sedimentary Geology 157, 3-13.

30. Chamley, H., (1989). Clay Sedimentology. Springer-Verlag, Berlin. 267 pp.

31. Chamyal, L. S., Maurya, D. M. and Raj, R., (2003). Fluvial systems of the drylands of western India: a synthesis of Late Quaternary environments and tectonic changes. Quaternary International 104, 69-86.

32. Chauhan, O. S., (1994). Influence of macrotidal environment on shelf sedimentation, Gulf of Kachchh, India. Continental Shelf Research 14, 1477–1493.

33. Chauhan, O. S., Almeida, F., Suneetha, J., (2000). Influence of sedimentation on geomorphology of the northwestern continental margin on India. Marine Geology 23, 259-265.

34. Chauhan, O. S., Jayakumar, S., Menezes, A. A., Suneethi, J., Shradha, N., Rajawat, A. S., Nayak, S. R., Ramanamurthy, M. V., Subramanian, B. R., (2004). Tidal currents as feeders of the river Indus flux into the macrotidal Gulf of Kachchh, India. - 3rd Indian National Conference on Harbour and ocean engineering, NIO, Goa, 174-183.

35. Chauhan, O. S., Jayakumar, S., Menezes, A. A., Rajawat, A. S., Nayak, S. R., (2006). Anomalous inland influx of River Indus, Gulf of Kachchh, India. - Marine Geology 229, 91-100.

36. Cho, Y. G., Lee, C. B., Choi, M. S., (1999). Geochemistry of surface sediments off the southern and western coasts of Korea. Marine Geology 159, 111–129.

37. Clift, P. D., Shimizu, N., Layne, G. D., Blusztajn, J., (2001). Tracing patterns of erosion and drainage in the Paleogene Himalaya through ion probe Pb isotope analysis of detrital K-feldspars in the Indus Molasse, India. Earth and Planetary Science Letters 188, 475-491.

38. Colin, C., Siani, G., Sicre, M. A., Liu, Z., (2010). Impact of the East Asian monsoon rainfall changes on the erosion of the Mekong River basin over the past 25,000 yr. Marine Geology 271 (1–2), 84–92. doi:10.1016/j.margeo.2010.01.013.

39. Cronin, T. M., Hayo, K., Thunell, R. C., Dwyer, G. S., Saenger, C., Willard D. A., (2010). The Medieval Climate Anomaly and Little Ice Age in Chesapeake Bay and the North Atlantic Ocean. Paleoclimatology, paleogeography, paleoecology 297, 299-310.

40. De Martini P. M., Barbano, M. S., Smedile, A., Gerardi, F., Pantosti, D., Del Carlo, P., Pirrotta C., (2010). A Unique 4000 yrs long geological record of multiple tsunami indundations in the Augusta Bay (eastern Sicily, Italy). Marine Geology 276, 42-57.

41. Dubey, N., and Chatterjee, B. K., (1997). Sandstone of Mesozoic Kachchh basin: Their provenance and basinal evolution. Indian Journal of Petroleum Geology 6, 55-68.

42. Ellwood, B. B., Balsam, W. L., and Roberts, H. H., (2006). Gulf of Mexico sediment sources and sediment transport trends from magnetic susceptibility measurements of surface samples. Marine Geology 230, 237-248.

43. Engstrom, D. R., Wright Jr., H. E., (1984). Chemical stratigraphy of lake sediment as a record of environmental change. In: Haworth, E.Y., Lund, J.W.G. (Eds.), Lake Sediment and environmental History. Leicester University press, pp. 11–67.

44. Fleitmann D, Burns S. J, Mudelsee M, Neff U, Kramers J, Mangini A, Matter A. (2003). Holocene forcing of the Indian monsoon recorded in a stalagmite from southern Oman, Science 300, 1737 – 1739.

45. Folk, R. L., (1954). The distinction between grain size and mineral composition in sedimentary-rock nomenclature. Journal of Geology 62, 344-359.

46. Folk, R. L., (1974): Petrology of sedimentary rocks. Hemphill Publishing Co. Texas 184 pp.

47. Fralick, P. W., Kronberg, B. I., (1997). Geochemical discrimination of clastic sedimentary rock sources. Sedimentary Geology 113, 111–124.

48. Frings, R. M., (2008). Downstream fining in large sand bed-rivers. Earth Science Reviews, 87, 39-60.

49. Fursich, F. T., Singh, I. B., Joachimski, M., Krumm, S., Schlirf, M., Schlirf, S., (2005). Paleoclimate reconstruction of the Middle Jurassic of Kachchh (western India): An integrated approach based on paleoecological, oxygen isotopic and clay mineralogical data. Palaeogeography, Palaeoclimatology, Palaeoecology 217, 289-309.

50. Gao, S., Collins, M. B., (1994). Analysis of grain-size trends for defining sediment transport pathways in marine environments. - Journal of Coastal Research 10, 70-78.

51. Garzanti, E., Vezzoli, G., Andó, S., Paparella, P., Clift, P., (2005). Petrology of Indus River sands: a key to interpret erosion history of the Western Himalayan Syntaxis. Earth Planetary Science Letters 229, 287–302.

52. Glennie, K. W. and G. Evans (1976). A reconnaissance of the recent sediments of the Ranns of Kutch, India. Sedimentology 23, 625-647

53. Goodbred, S. L., (2003). Response of Ganga dispersal system to climate change: a source-to-sink view since the last interstade. Sedimentary Geology 162, 83-104.

54. Gupta A. K, Anderson D. M, Overpeck J. T. (2003). Abrupt changes in the Asian southwest monsoon during the Holocene and their links to the North Atlantic Ocean. Nature 421, 354–357.

55. Hashimi, N. H., Nair, R. R., Kidwai. R. M., (1978). Sediments of Gulf of Kachchh- A high energy tide dominated environment. - Indian Journal of Marine Sciences 7, 1-7.

56. Heller F. and Liu T. S. (1986). Paleoclimatic and sedimentary history from magnetic susceptibility of loess in China. Geophysical Research Letters 13, 1169–1172.

57. Hequette, A., Hemdane, Y. and Anthony, E. J. (2008). Determination of sediment transport paths in macrotidal shoreface environments: a comparison of grain-size trend analysis with near-bed current measurements. Journal of Coastal Research 24, 695-707.

58. Hirt, A. M., Lanci, L., and Koinig, K., (2003). Mineral magnetic record of Holocene environmental changes in Sägistalsee, Switzerland. Journal of Paleolimnology 30, 321–331.

59. Horng, C. S., Huh, C. A., (2011). Magnetic properties as tracers for source-to-sink dispersal of sediments: A case study in the Taiwan Strait, Earth Planetary Science Letters, doi:10.1016/j.epsl.2011.07.002

60. Jenkins P. A., Duck, R. W., Rowan, J. S., and Walden J., (2002). Fingerprinting of bed sediment in Tay estuary, Scotland: an environmental magnetism approach. Hydrology and Earth System Sciences 6 (6), 1007-1016.

61. Jiang, F., Li, A., Li, T., (2011). Sediment pathway of East China Sea inferred from an R-mode factor analysis of surface sediments in Okinawa trough. Quaternary International. 230 (1-2), 13-20.

62. Juyal N, Pant R. K, Basavaiah N, Bhusan R, Jain M, Saini N. K, Yadava M. G, Singhvi A. K. (2009). Reconstruction of Last Glacial to early Holocene monsoon variability from relict lake sediments of the Higher central Himalaya, Uttrakhand, India. Journal of Asian Earth Sciences 34, 437–449.

63. Kar, A. (1993). Neotectonic influence on morphological variations along coastline of Kachchh, India. Geomorphology 8, 199-219.

64. Keigwin, L. D. (1996). The Little Ica Age and the Medieval Warm Period in the Sargasso Sea. Science 274, 1504-1508.

65. Kessarkar, P. M., Rao, V. P., Ahmad, S. M. and Badu, B. A., (2003). Clay minerals and Sr-Nd isotopes of the sediments along the western margin of India and their implication for sediment provenance. Marine Geology 202, 55-69.

66. Kim, G., Yang, H., Church, T. M., (1999). Geochemistry of alkaline earth elements (Mg, Ca,Sr, Ba) in the surface sediments of the Yellow Sea. Chemical Geology 153, 1–10.

67. Kortekaas, S., Dawson, A. G., (2007). Distinguishing tsunami and storm deposits: an example from Martinhal, SW Portugal. Sedimentary Geology 200, 208–221.

68. Kolla, V., Henderson, L., Biscaye, P. E. (1976). Clay mineralogy and sedimentation in the western Indian ocean. Deep-Sea Research 23, 949–961.

69. Kolla, V., Kostecki, J. E., Robinson, F., Biscaye, P. E. (1981). Distribution and origin of clay minerals and quartz in surface sediments of the Arabian Sea. Journal of Sedimentary Petrology 51, 563-569.

70. Konta, J. (1985). Mineralogy and chemical maturity of suspended matter in major rivers sampled under SCOPE/UNEP project. Mitt. Geol.-paleontol. Inst. Univ. Hamburg, 58, 557-568.

71. Kuehl, S. A., Brunskill, G. J., Burns, K. A., Fugate, D. C., Kniskern, T., Meneghini, L., (2004). Nature of sediment dispersal off the Sepik River, Papua New Guinea: preliminary

sediment budget and implications for margin processes. Continental Shelf Research 24 (19), 2417–2429.

72. Kumar, A. A., Rao, V. P., Patil, S. K., Kessarkar, P. M., Thamban, M., (2005). Rock magnetic records of the sediments of the eastern Arabian Sea: evidence for late Quaternary climatic change. Marine Geology 220, 59–82.

73. Kunte P. D, Wagle B. G and Sugimori Y (2003). Sediment transport and depth variation study of the Gulf of Kutch using remote sensing; Int. J. Remote Sensing 24, 2253-2263.

74. Lamb, H. H. (1985) Climatic History and the Future, Princeton Univ. Press,.

75. Lepland A, Stevens R. L., (1996). Mineral magnetic and textural interpretations of sedimentation in the Skagerrak, eastern North Sea. Marine Geology 135, 51–64.

76. Lisitzin, A. P., (1996). The age of terrigenous material as an indicator of its origins (Age and Isotopic Measurements). Oceanic Sedimentation, Lithology and Geochemistry American Geophysical Union Publication. pp. 192–230.

77. Liquete, C., Canals, M., Lastras, G., Amblas, D., Urgeles, R., Mol De, B., Batist De, M., Hughes-Clarke, J. E., (2007). Long-term development and current status of the Barcelone continental shelf: A source-to-sink approach. Continental shelf research 27, 1779-1800.

78. Liu, S., Zhang, W., He, Q., Li, D., Liu, H., Yu, L., (2010). Magnetic properties of East China sea shelf sediments off Yangtze estuary: Influence of provenance and particle size. Geomorphology 119, 212-220.

79. Maher, B. A., (1988). Magnetic properties of some synthetic submicron magnetites. Geophysical Journal 94, 83–96.

80. Maher B., Thompson R. and Zhou L. P. (1994). Spatial and temporal reconstructions of changes in the Asian palaeomonsoon: a new mineral magnetic approach. Earth Planetary Science Letters 125, 461– 471.

81. Maher, B. A., Watkins, S. J., Brunskill, G., Alexander, J., and Fielding, C. R. (2009). Sediment provenance in a tropical fluvial and marine context by magnetic ‘fingerprinting’ of transportable sand fractions. Sedimentology 56, 841-861.

82. Mann, M. E. (2002). Medieval Climatic Optimum. In *Encyclopedia of Global environmental change,* edited by M. C. MacCracken and J. S. Perry, John Wiley, Chichester, U. K. pp. 514– 516,

83. Mathur U. B. and Mehra, S., (1975). Report on Quaternary deposit of Porabandar area, Junagadh dist. Gujarat. Progress repost, Geological Survey of India 1974-1975.

84. Maurya, D. M., Thakkar, M. G., Patidar, A. K., Bhandari, S., Goyal, B., and Chamyal, L. S., (2008). Late quaternary geomorphic evolution of coastal zone of Kachchh, Western India. Journal of Coastal Research 24, 746-758.

85. Milliman, J.D., Qin, Y. S.; Ren, M. E.; and Saito, Y., (1987), Man's influence on the erosion and transport of sediment by Asian rivers: the Yellow River (Huanghe) example: Jour. Geology 95, 751-762.

86. Mishra, D., and Tiwari, R. N., (2005). Provenance study of silliciclastic sediments, Jhura dome, Kachchh, Gujarat. Journal of Geological society of India 65, 703-714.

87. Morton, R. A., Gelfenbaum, G., Jaffe, B. E., (2007). Physical criteria for distinguishing sandy tsunami and storm deposits using modern examples. Sedimentary Geology 200, 184–207.

88. Nair, R. R., Hashimi, N. H., Rao, V. P. (1982). On the possibility of high velocity tidal streams as dynamic barrier to longshore sediment transport: evidence from continental shelf off the Gulf of Kachchh, India. Marine Geology 47, 77-86.

89. Oldfield, F., Maher, B. A., Donoghue, J., Pierce, J., (1985). Particle size related, mineral magnetic source sediment linkages in the Rhode River catchment, Maryland, USA. Journal of the Geological Society of London 142, 1035–1046.

90. Oldfield, F., (1994). Toward the discrimination of fine-grained ferrimagnets by magnetic measurements in lake and near-shore marine sediments. Journal of Geophysical Research 99(5), 9045.

91. Oldfield, F., Yu, L., (1994). The influence of particle size variations on the magnetic properties of sediments from the north-eastern Irish Sea. Sedimentology 41, 1093–1108.

92. Oldfield, F., Asioli, A., Accorsi, C. A., Mercuri, A. M., Juggins, S., Langone, L., Rolph, T., Trincardi, F., Wolff, G., Gibbs, Z., Vigliotti, L., Frignani, M., van der Post, K., Branch, N., (2003). A high resolution Late Holocene palaeo environmental record from the central Adriatic Sea. Quaternary Science Reviews 22, 319 – 342.

93. Overpeck, J. T., Anderson, D. M., Trumbore, S. & Prell, W. L. (1996). The Southwest Monsoon over the last 18,000 years. Climate Dynamics 12, 213–225.

94. Pararas-Carayannis G, (2006). The potential of tsunami generation along the Makran subducation zone in the Northern Arabian Sea case study: the earthquake and tsunami of November 28, 1945, (paper presented at 3rd tsunami symposium of the tsunami society, East-West Center, University of Hawaii, Honolulu, Hawaii) May 23–25, 24(5), 358–383.

95. Pedreros, R., Howa, H. L., and Michel, D., (1996). Application of grain size trend analysis for the determination of sediment transport pathways in intertidal areas. – Marine Geology 135, 35-49.

96. Peterson, L. C., Haug, G. H., Hughen, K. A., and Rohl, U., (2000). Rapid changes in the hydrologic cycle pf the tropical Atlantic during the Last Glacial. Science 290, 1947 – 1951.

97. Pethick, J., (2000): An introduction to coastal geomorphology. Oxford University press Inc. 260 pp.

98. Petschick, R., Kuhn, G., and Gingele, F., (1996). Clay mineral distribution in surface sediments of south Atlantic: sources, transport and relation to oceanography. Marine Geology 130, 203-229.

99. Pettijohn, F. J., Potter, P. E., Siever, R., (1987). Sand And Sandstones, second version. Springer-Verlag, New York, pp. 553.

100. Prasad S., and Enzel Y., (2006). Holocene paleoclimates of India. Quaternary Research, 66, 442–453.

101. Prell W. L, Kutzbach J. E. (1992). Sensitivity of the Indian monsoon to forcing parameters and implications for its evolution. Nature 360, 647–652.

102. Prizomwala S. P., Shukla S. B. and Bhatt Nilesh., (2010). Geomorphic assemblage of the Gulf of Kachchh coast, Western India: Implication in understanding the pathways of coastal sediments. Zeitschrift fur Geomorphologie 54 (1), 31-46.

103. Prizomwala S. P., Shukla S. B. and Bhatt N., (2012). Distribution of Indus born mica along Gulf of Kachchh coast: Implications in understanding offshore dynamics. Journal of Geological Society of India 79, 557-562.

104. Prizomwala S. P., Shukla S. B., Basavaiah, N., and Bhatt N., (in press) Provenance discrimination studies on sediments of SW Kachchh coast, western India: Insights from heavy mineral and mineral magnetic analysis. Journal of Coastal Research. DOI: 10.2112/JCOASTRES-D-11-00048.1

105. Ramaswamy, V., Nagender, N. B., Vethamony, P., Illangovan, D., (2007). Source and dispersal of suspended sediment in macro-tidal Gulf of Kachchh. Marine Pollution Bulletin 54, 708-719.

106. Radoane, M., Radoane, N., Dumitnu, D., Miclaus, C., (2007). Downstream variation in bed sediment size along the East Carpathian rivers: evidence of the role of sediment sources. Earth Surface Processes and Landforms 33 (5), 674-694.

107. Rao, V. P., and Rao, B. R., (1995). Provenance and distribution of clay minerals sediments in sediments of the western continental shelf and slope of India. Continental Shelf Research, 15 (14), 1757-1771.

108. Rao, V. P., Kessarkar, P. M., Patil, S. K. and Ahmad, S. M., (2008). Rock magnetic and geochemical record in a core from the eastern Arabian Sea: diagenetic and environmental implications during the late Quaternary. Palaeogeo. Palaeoclimat. Palaeoecol. 270, 46–52.

109. Rao V. P., Kessarkar, P. M., Thamban, M., and Patil S. K., (2010). Paleoclimatic and Diagenetic History of the Late Quaternary Sediments in a Core from the Southeastern Arabian Sea: Geochemical and Magnetic Signals. Journal of Oceanography 66, 133-146.

110. Reimer P. J, Baillie M. G. L, Bard E, Bayliss A, Beck J. W, Blackwell P.G, Bronk Ramsey C, Buck C. E, Burr G. S, Edwards R. L, Friedrich M, Grootes P. M, Guilderson T. P, Hajdas I, Heaton T. J, Hogg A. G, Hughen K. A, Kaiser K. F, Kromer B, McCormac F. G, Manning S. W, Reimer R. W, Richards D. A, Southon J. R, Talamo S, Turney C .S.

M, van der Plicht J, Weyhenmeyer C. E. (2009). IntCal09 and Marine09 radiocarbon age calibration curves, 0–50,000 years cal BP. Radiocarbon 51(4), 1111–1150.

111. Schmidt A M, Von Dobeneck T, Bleil U. (1999). Magnetic characterization of Holocene sedimentation in the South Atlantic. Palaeoceanography 14, 465–481.

112. Shankar, R., Prabhu, C. N., Warrier, A. K., Vijaya Kumar, G. T., Sekar, B., (2006). A multidecadal rock magnetic record of monsoonal variations during the past 3700 years from a tropical Indian tank. Journal of the Geological Society of India 68, 447–459.

113. Shanmugam, G., (2011). Process-sedimentological challenges in distinguishing paleo-tsunami deposits. Natural Hazards, DOI 10.1007/s11069-011-9766-z

114. Shetye, S. R., (1999). Tides in the Gulf of Kachchh, India. Continental Shelf Research, 19, 1771–1782.

115. Shrivastava, P. K. (1963). Geology of Saurashtra. Unpublished ONGC report.

116. Shukla, A. D., Bhandari, N., Kusumgar, S., Shukla, P. N., Ghevariya, Z..G., Gopalan, K., Balaram, V., (2001). Geochemistry and magnetostratigraphy of Deccan flows at Anjar Kutch. Proc. Indian Academy of Science - Earth Planetary Science 110, 111–132.

117. Shukla, S. B., Patidar, A. K., Bhatt, N., (2008) Application of GPR in study of shallow subsurface sedimentary architecture of Modwa spit, Gulf of Kachchh. Journal of Earth System Science 117 (1), 33-40.

118. Shukla, S. B., Prizomwala, S. P., Ukey, V., Bhatt, N. P., and Chamyal, L. S., (2010). Coastal geomorphology and Tsunami hazard scenario along the Kachchh coast, Western India. Indian Journal of Marine Science 39 (4), 549-556.

119. Shumilin, E., Paez-Osuna, F., Green-Ruiz, C., Sapozhnikov, D., Rodriguez-Meza, G., Godinez-Orta, L., (2001). Arsenic, antimony, selenium and other trace elements in sediments of the La Paz Lagoon, Peninsula of Baja California, Mexico. Marine Pollution Bulletin 42, 174–178.

120. Singh P., (2010). Geochemistry and provenance of stream sediments of the Ganga river and its major tributaries in the Himalayan region, India. Chemical Geology 269, 220-236.

121. Singhvi A K, Bluszcz A, Bateman M. D, Rao S. (2001). Luminescence dating of loess–palaeosol sequences and coversands: methodological aspects and palaeoclimatic implications. Earth Science Reviews 54: 193–211.

122. Singer, A. (1984). The paleoclimatic interpretation of clay minerals in sediments- a review. Earth science review 21, 251-293.

123. Singhvi A. K, Bluszcz A, Bateman M. D, Rao S. (2001). Luminescence dating of loess–palaeosol sequences and coversands: methodological aspects and palaeoclimatic implications. Earth Science Reviews 54, 193–211.

124. Singhvi, A. K., Williams, M. A. J, Rajaguru, S. N., Misra, V. N., Chawla, S., Stokes, S., Chauhan, N., Francis, T., Ganjoo, R. K., Humphreys, G. S., (2010). A ~ 200 ka record of climatic change and dune activity in the Thar Desert, India. Quaternary Science Reviews 29, 3095-3105.

125. Sinha A, Cannariato K. G, Stott L. D, Cheng H, Edwards R. L, Yadava M. G, Ramesh R, Singh I, B., (2007). A 900-year (600 to 1500 AD) record of the Indian summer monsoon precipitation from the core monsoon zone of India. Geophysical Research Letters 34, L16707.

126. Sirocko F, GarbeSchonberg D, Mclntyre A, Molfino B. (1996). Teleconnections between the subtropical monsoons and high-latitude climates during the last deglaciation. Science 272, 526–529.

127. Sionneau, T., Bout-Roumazeilles, V., Biscape, P. S., Van Vliet-Lanoe, B., Bory, A., (2008). Clay mineral distribution in and around the Mississippi river watershed and Northern Gulf of Mexico: sources and transport pattern, Quaternary Science Reviews 27, 1740-1751.

128. Spagnoli, F., Bartholini, G., Dinelli, E., Giordano, P., (2008). Geochemistry and particle size of surface sediments of Gulf of Manfredonia (Southern Adriatic Sea). Estuarine, Coastal and Shelf Science 80, 21-30.

129. Staubwasser, M., Sirocko, F., (2001). On the formation of laminated sediments on the continental margin o□ Pakistan: the e□ects of sediment provenance and sediment redistribution. Marine Geology 172, 43–56.

130. Swift D. J. P. (1982). Tidal sand ridges and shoal retreat massif. Marine Geology 18, 105-134.

131. Syvitski, J. P. M., Kettner, A. J., Correggian, A., and Nelson, B. W., (2005). Distributary channels and their impact on sediment dispersal. Marine Geology 222-223, 75-94.

132. Thamban, M., Rao, V. P., (2005). Clay minerals as palaeomonsoon proxies: evaluation and relevance to the late Quaternary record from SE Arabian Sea. In: Rajan, S., Pandey, P.C. (Eds.), Antarctic Geoscience: Ocean-atmosphere Interaction and Paleoclimatology. National Centre for Antarctic & Ocean Research, Goa, India, pp. 198–215.

133. Thamban, M., Rao, V. P., Schneider, R. R., (2002). Reconstruction of late Quaternary monsoon oscillations based on clay mineral proxies using sediment cores from the western margin of India. Marine Geology 186, 527–539.

134. Thamban, M., Kawahata, H., Rao, V. P., (2007). Indian Summer monsoon variablility during the Holocene as recorded in sediments of the Arabian Sea: timing and implications. Journal of Oceanography 63, 1009–1020.

135. Thompson, R., J. Bloemendal, J. A. Dearing, F. Oldfield, T. A. Rummery, J. C. Stober, and G. M. Turner, (1980). Environmental applications of magnetic measurements, Science 207, 481-486.

136. Thompson, R., and F. Oldfield, (1986). Environmental Magnetism, Allen and Unwin, Winchester, Mass.,.

137. Tooth, S., (2000). Process, form and change in dryland rivers: a review of recent research. Earth Science Reviews 51, 67-107.

138. Tyagi, A. K., Shukla, A. D., Bhushan, R., Thakker, P. S., Thakkar, M. G., and Juyal, N., (2012). Mid-Holocene sedimentation and landscape evolution in the western Great Rann of Kachchh, India. Geomorphology 151-152, 89-98.

139. Van lancker, V., Lanckneus, J., Hearn, S., Hoekstra, P., Levoy, F., Miles, J., Moerkerke, G., Monfort, O., Whitehouse, R., (2004): Coastal and nearshore morphology, bedforms and sediment transport pathways at teignmouth (UK). – Continental Shelf Research 24, 1171-1202.

140. Vethamony, P., Reddy, G. S., Babu, M. T., Desa, E., Sudheesh, K., (2005). Tidal eddies in a semi-enclosed basin: a model study. Marine Environmental Research 59, 519–532.

141. Vethamony, P., Babu, M. T., Ramanamurty, M. V., Saran, A. K., Joseph, A., Sudheesh, K., Padgaonkar, R. S., Jayakumar, S., (2007). Thermohaline structure of an Inverse Estuary – the Gulf of Kachchh: measurements and model simulations. Marine Pollution Bulletin, 54(6), 697-707.

142. Von Rad, U., Schulz, H., Riech, V., den Dulk, M., Berner, U., Sirocko, F., (1999). Multiple monsoon-controlled breakdown of oxygen-minimum conditions during the past 30,000 years documented in laminated sediments off Pakistan. Palaeogeography, Palaeoclimatology, Palaeoecology 152, 129–161.

143. Vora, K. H., Chauhan O. S. and Rao, B. R., (1987). Some geological processes in the macro-tidal regime of Gulf of Kachchh, Northwest coast of India. Indian Journal of Marine Science 16, 230-234.

144. Wagle, B.G., (1979). Geomorhology of the Gulf of Kutch. Indian Journal of Marine Science 8, 123–126.

145. Warrier, A.K., and Shanker, R., (2009). Geochemical evidences for the use of magnetic susceptibility as a palaeorainfall proxy in the tropics. Chemical Geology 265, 553 – 562.

146. Walden, J., Slattery, M. C., Burt, T. P., (1997). Use of mineral magnetic measurements to fingerprint suspended sediment sources: approaches and techniques for data analysis. Journal of Hydrology 202, 353–372.

147. Wang, Y., Dong, H., Li, G., Zhang, W., Oguchi, T., Bap, M., Jiang, H., and Bishiop, M., (2010). Magnetic properties of muddy sediments on the northeastern continental shelves of China: Implication for provenance and transportation. Marine Geology 274, 107-119.

148. Wasson, R.J., (2003). A sediment budget for the Ganga-Brahmaputra catchment. Current science 84 (8), 1041-1047.

149. Weadeab, S., Emeis, K. C., Hemleben, C., and Siebel, W., (2002). Provenance of lithogenic surface sediments and pathways of riverine suspended matter in the Eastern Mediterranean Sea: evidence from $^{143}Nd/^{144}Nd$ and $^{87}Sr/^{86}Sr$ ratios. Chemical Geology 186, 139– 149.

150. Wynne, A. B., (1872). Geology of Kutch. Mere. GeoL Surv. India, 9(1):81,113.

151. Yang, S. Y., Jung, H. S., Lim, D. I., Li, C. X., (2003). A review on provenance discrimination of sediments in Yellow sea. Earth Science Reviews 63, 93-120.

152. Yang, S., Wang, Z., Guo Y., Li, C., Cai, J., (2009). Heavy mineral composition of Changjiang (Tangtze river) sediments and their provenance tracing implication. Journal of Asian Earth Science 35, 56-65.

153. Young, G. M., and Nesbitt, H. W., (1998). Processes controlling the distribution of ti and al in weathering profiles, Siliciclastic sediments and sedimentary rocks. Journal of Sedimentary Research 68 (3), 448-455.

List of full Length Papers of Siddharth Prizomwala from PhD thesis

1. **"Clay minerals as palaeoclimatic proxy for centennial scale events?" Prizomwala, S. P.**, Bhatt, Nilesh, and Winkler, W., (Under Preparation)

2. **"A 900 year sedimentation record from the Gulf of Kachchh, western India coast: Centennial scale teleconnection between the ISM and the NAR events?" Prizomwala, S. P.**, Bhatt, Nilesh, Hajdas, I, Hirt, A. M., and Winkler, W., *(Under Review)*

3. "**Understanding the sediment routing system along the Gulf of Kachchh coast, western India: Provenance and sediment pathways**" **Prizomwala, S.P.,** Nilesh Bhatt and Basavaiah N., *Journal of Earth System Science (In Press)*

4. **"Sediment fluxes from small dryland fluvial catchment, Kachchh, Western India: Provenance discrimination and insights into source-to-sink studies in a macrotidal environment". Prizomwala S.P.,** Nilesh Bhatt and Basavaiah, N., *International Journal of Sediment Research (In Press)*.

5. **"Provenance Discrimination Studies on Sediments of the SW Kachchh Coast, Western India: Insights from Heavy Mineral and Mineral Magnetic Analysis". Prizomwala S.P.,** Shukla S.B., Basavaiah, N., and Bhatt Nilesh, *Journal of Coastal Research* 2013, Vol 29 (1), 52–60.

6. **"Distribution of Indus born mica along Gulf of Kachchh coast: Implications in understanding offshore dynamics". Prizomwala, S.P**., Shukla, S.B., and Nilesh Bhatt, *Journal of Geological society of India* 2012, Vol 79, 557-562.

7. "**Geomorphic assemblage of coastline of Gulf of Kachchh, western India: Implications in understanding the pathways of coastal sediments**". **Prizomwala, S. P**., Shukla, S.B., and Bhatt, N.P., *Zeistcrift fur geomorphologiea* 2010 Vol. 54 (1), 31-46.

List of full Length Papers of Siddharth Prizomwala outside PhD thesis

1. **"Tectonic geomorphology and neotectonic signatures from the south Saurashtra, Western India: A multidisciplinary approach" Prizomwala, S. P.**, Ukey, V., Joshi, P., Bhatt, Nilesh, Maurya, D. M., and Chamyal, L. S., *(Under Review)*

2. **"Internal Sedimentary Architecture and Coastal Dynamics as Revealed by Ground Penetrating Radar, Kachchh coast, Western India".** Shukla, S.B., Chowksey, V., **Prizomwala, S.P.,** Ukey, V., Nilesh Bhatt and Maurya, D.M., *Acta Geophysica (In Press)*.

3. **"Coastal geomorphology and Tsunami hazard scenario along the Kachchh coast, Western India".** Shukla, S.B., **Prizomwala, S.P**., Ukey, V., Bhatt, N.P., and Chamyal, L.S., *Indian Journal of Marine Science* 2010 Vol. 39 (4), 549-556.

Presentations at various National and International Conferences

1. **"Was the Medieval Warm Period Global?: Evidenced from the Gulf of Kachchh coast, western India"** to be presented at 4th OSM meeting of PAGES at Goa, during 13th to 16th Feb 2013.

2. **"High resolution Mid to Late Holocene paleoclimatic reconstruction from the mudflats of the Gulf of Kachchh, western India"** presented at *EGU General Assembly meeting*, at Vienna, Austria during 22-27th April 2012.

3. **"Application of environmental magnetism in source-to-sink studies: an example from Kachchh, western India"** presented at *20th SwissSed meeting* at Fribourg, Switzerland on 25th February, 2012.

4. **"Source-to-Sink studies of dryland tropical fluvial system : A case study from Rukmavati river, Kachchh, Western India"** presented at the *IGCP 582 meeting and conference on TROPICAL RIVERS: HYDRO-PHYSICAL PROCESSES, IMPACTS, HAZARDS AND MANAGEMENT* held at IIT Kanpur, India during 5-7 January 2012.

5. **"Mudflats of Gulf of Kachchh coast: Archives of sea level fluctuations and palaeo-environmental changes since mid-Holocene"** presented at *9th Swizz Geoscience Meeting* at Zurich, Switzerland during 11-13th November 2011.

6. **"Provenance discrimination and Sediment dispersal in a macrotidal regime, Gulf of Kachchh, Western India: Implications in source to sink studies"** presented at the *XVIII INQUA congress* held at Bern, Switzerland during 21-27th July 2011.

7. **"Sediment flux from a dryland fluvial regime in Kachchh, Western India: Insights in provenance discrimination and source-to-sink studies"** Presented at 28th *International Association of Sedimentologists'* meeting held at Zaragoza, Spain, during 5-8th July 2011.

8. **"Coastal geomorphic setup of Kachchh coast, Western India: Implications in 'Hunting' sites for Palaeo-tsunami deposits"** Presented at *International conference on Geomorphology and Hazard* held at Kanyakumari, during 21-23 July, 2010.

9. **"Mudflats from the Gulf of Kachchh coast: Implications in studies on climate change"** Presented at *XXIV Gujarat Science Congress* 2010, held at Gujarat University, Ahmedabad on 21st March, 2010.

10. "**Textural and mineralogical characteristics of sediments of Gulf of Kachchh coast, Western India: Implications in understanding provenance and sediment pathways**" Presented at *National conference on Quaternary geological processes: Natural hazards & climate change* held at Lucknow University, in Lucknow during 25-26th February, 2009.

11. "**Sediment characteristics of the tidal flats of Gulf of Kachchh coast, Western India : Implications in understanding the coastal dynamics**" Presented in XXV convection of

Indian Association of Sedimentologists & National seminar on sedimentary basins of India – Their Geological significance and economic prospects, held at M.S. University of Baroda during 26-28 December, 2008.

Provenance discrimination and Source-to-Sink studies from a dryland fluvial regime: an example from Kachchh, western India

S.P. Prizomwala[1], Nilesh Bhatt[1]* and N. Basavaiah[2]

[1]The Department of Geology, The M. S. University of Baroda, Vadodara, India

[2]Indian Institute of Geomagnetism, Kalamboli , New Panvel, Navi Mumbai, India

Email: nilesh_geol@yahoo.com

Abstract:

Tracing the sediment delivery from its source terrain to its ultimate sink envisage multiple factors that play a vital role in understanding present day erosional engine. To accomplish this, it is significant to distinguish the variable end-members contributing to the basin. The findings from the study of dryland coastal fluvial regime in Kachchh (Western India), which is one of the end members contributing to the Gulf of Kachchh coast (partial sink) and finally to the Arabian Sea (ultimate sink) have been presented here. A multi-proxy sediment provenance such as grain-size, clay minerals, geochemistry and magnetic minerals has been employed to evaluate the provenance discriminating characteristics of the Kachchh dryland fluvial system and factors influencing them. The results of different proxies indicate that the provenance signatures of uplands are quite characteristic with magnetic susceptibility (χ) values of $<20 \times 10^{-7}$ m^3kg^{-1} and smectite (S)/kaolinite (K) ratio between 0.26 and 0.49. The middle reaches of Deccan basalt show marked increase in magnetic mineral concentration with χ values (140×10^{-7} m^3kg^{-1}) and S/K ratio (4.92), while the estuarine tract shows χ values ($80 \times 10^{-7} m^3kg^{-1}$), S/K ratio (1.90) and, characteristic heavy minerals (i.e. mica minerals), probably reflect the interplay between land and sea oscillations. Major sources to sediments within catchment scale were identified, viz., upland sedimentaries and middle reaches (i.e. Deccan basalt derived sediments). The present study draw cautions in provenance of sediment discrimination in areas influenced by Deccan basalt that has the overwhelming sediment delivery and a comparatively subdued effects of other provenance signatures. The studied proxies of mineralogy of clays, magnetic minerals and geochemistry of heavy and major elements serve as the potential for fingerprint of sediment source regions and hence behold a strong position in source to sink studies globally.

Journal of Earth System Science (In Press)

Understanding the Sediment Routing System along the Gulf of Kachchh coast, Western India: Provenance and Sediment Pathways

S.P. Prizomwala[1], Nilesh Bhatt[1]* and N. Basavaiah[2]

[1]The Department of Geology, The M. S. University of Baroda, Vadodara, India

[2]Indian Institute of Geomagnetism, Kalamboli , New Panvel, Navi Mumbai, India

Email: nilesh_geol@yahoo.com

Abstract:

Studies on sediment routing system have remained a hot topic among researchers since last decade, especially in macrotidal environments where exists a complex sediment transit mechanism. Here we examine the Gulf of Kachchh - the largest macrotidal regime in northern Arabian Sea, for sediment pathways and provenance to better understand the sediment dispersal system. We employed various established provenance discrimination techniques namely heavy mineral analysis, clay mineralogy, mineral magnetic properties, and sediment geochemistry to elucidate major end-members contributing to the Gulf of Kachchh basin and documenting their provenance discriminating signatures. For example, the variations in the clay mineralogy, (Illite+Chlorite)/(Smectite+Kaolinite) ratios, the geochemical property (Al concentration), mica minerals (i.e. Muscovite, Biotite) concentration and mineral magnetic parameters, e.g. magnetic susceptibility and S-ratio, are used to identify sources of sediment in response to three main dispersal processes around the region. The results suggest (1) River Indus, (2) Kachchh mainland fluvial system and (3) Saurashtra peninsular coastal rivers are the three major provenances contributing to the Gulf of Kachchh basin. The northern coast of the Gulf of Kachchh has dominant signatures of Kachchh mainland provenance due to its proximity and similarly the southern coast has dominance of Saurashtra peninsular provenance. However, the River Indus, comparatively more distant source has dominant provenance signatures in the inner gulf mudflats.

(Under Review)

A 900 year Record of Sedimentation from the Gulf of Kachchh, western coast of India: Centennial scale teleconnection between the ISM and the NAR events?

S. P. Prizomwala[1,2], Nilesh Bhatt[2]*, I. Hajdas[3], A. M. Hirt[4], W. Winkler[5]

[1]Institute of Seismological Research, Raisan, Gandhinagar - 389002, India

[2]Department of Geology, The M. S. University of Baroda, Vadodara – 390002, India

[3]PSI/ETH, AMS ^{14}C labratory, Honggerberg HPK 8093, Zurich, Switzerland

[4]Institut für Geophysik, ETH-Zentrum, CH-8092 Zürich, Switzerland

[5]Geologisches Institut, ETH-Zentrum, CH-8092 Zürich, Switzerland

Abstract:

The last two millennia showed to have had periods with sea surface temperature (SST) ~1 ºC warmer and cooler than present in Europe and surrounding regions (i.e. North Atlantic Region, NAR), which are well known as "Medieval Climatic Anomaly (MCA)". Several studies have also discussed the millennial scale synchronization between the strength of the Indian summer Monsoon (ISM) and the NAR events. Whereas there is little attempt to study the short term climatic variations in the ISM due to the paucity of high resolution archives and more commonly chronological uncertainties. The question, how synchronous the short term (century scale) climatic perturbations of the NAR events with the ISM are, has not been addressed adequately until now. Here we document a century scale relationship between the NAR events and the ISM using a 900 year long high resolution ISM regulated archive from the Gulf of Kachchh coast spanning from 1300 – 400 AD. Our data show evidence of the Medieval Warm Period (MWP), Cold Dark Ages (CDA) and Late section of Roman Warm Period (LRWP), which exhibits that as like the millennial scale links, the ISM also exhibits centennial scale correlation with the NAR events.